DOI:
10.7554/eLife.59142

Document Version
Peer reviewed version

Citation for published version (APA):
Russell, J. P., Lim, X., Santambrogio, A., Yianni, V., Kemkem, Y., Wang, B., Fish, M., Haston, S., Grabek, A., Hallang, S., Lodge, E. J., Patist, A. L., Schedl, A., Mollard, P., Nusse, R., & Andoniadou, C. L. (2021). Pituitary stem cells produce paracrine WNT signals to control the expansion of their descendant progenitor cells. *eLife*, *10*, 1-23. Article e59142. https://doi.org/10.7554/eLife.59142

24 Hills Road, **P** 01223 855346
Cambridge **W** elifesciences.org
CB2 1JP **T** @elife_sciences

Pituitary stem cells produce paracrine WNT signals to control the expansion of their descendant progenitor cells

Tracking no: 20-05-2020-RA-eLife-59142R1

Impact statement: Stem cells of the pituitary gland contribute to organ growth cell non-autonomously by promoting proliferation of committed progenitors through WNT ligand secretion.

Competing interests: Roel Nusse: Reviewing editor, *eLife*

Author contributions:
John Russell: Conceptualization; Formal analysis; Investigation; Methodology; Writing - original draft; Writing - review and editing Xinhong Lim: Resources; Writing - review and editing Alice Santambrogio: Formal analysis; Investigation Val Yianni: Software; Formal analysis; Investigation Yasmine Kemkem: Resources; Investigation Bruce Wang: Resources Matthew Fish: Resources; Investigation Scott Haston: Investigation Anaëlle Grabek: Resources Shirleen Hallang: Investigation Emily Lodge: Investigation Amanda Patist: Investigation Andreas Schedl: Resources; Supervision Patrice Mollard: Resources; Supervision; Funding acquisition; Methodology; Writing - review and editing Roel Nusse: Resources; Supervision; Funding acquisition; Methodology; Writing - review and editing Cynthia Andoniadou: Conceptualization; Supervision; Funding acquisition; Investigation; Methodology; Writing - original draft; Writing - review and editing

Funding:
UKRI | Medical Research Council (MRC): Cynthia Lilian Andoniadou, MR/L016729/1; UKRI | Medical Research Council (MRC): Cynthia Lilian Andoniadou, MR/T012153/1; Deutsche Forschungsgemeinschaft (DFG): Cynthia Lilian Andoniadou, 314061271 - TRR 205; Howard Hughes Medical Institute (HHMI): Roel Nusse; Agence Nationale de la Recherche (ANR): Patrice Mollard, ANR-18-CE14-0017; Fondation pour la Recherche Médicale (FRM): Patrice Mollard, DEQ20150331732; Lister Institute of Preventive Medicine: Cynthia Lilian Andoniadou The funders had no role in study design, data collection and interpretation, or the decision to submit the work for publication.

Data Availability:
Sequencing data can be accessed through the following link: https://www.ncbi.nlm.nih.gov/bioproject/PRJNA421806
Datasets Generated: Pituitary stem cells produce paracrine WNT signals to control the expansion of their descendant progenitor cells: Andoniadou CL et al, 2020, https://www.ncbi.nlm.nih.gov/bioproject/PRJNA421806, NCBI Bioproject, PRJNA421806 Reporting Standards: N/A

Ethics:
Human Subjects: No Animal Subjects: Yes Ethics Statement: This study was performed under compliance of the Animals (Scientific Procedures) Act 1986, Home Office License (P5F0A1579) and KCL Biological Safety approval for project 'Function and Regulation of Pituitary Stem Cells in Mammals'

Pituitary stem cells produce paracrine WNT signals to control the expansion of their descendant progenitor cells

John Parkin Russell[1], Xinhong Lim[2,3], Alice Santambrogio[1,4], Val Yianni[1], Yasmine Kemkem[5], Bruce Wang[6,7], Matthew Fish[6], Scott Haston[8], Anaëlle Grabek[9], Shirleen Hallang[1], Emily Jane Lodge[1], Amanda Louise Patist[1], Andreas Schedl[9], Patrice Mollard[5], Roeland Nusse[6], Cynthia Lilian Andoniadou[1,4,*]

[1] Centre for Craniofacial and Regenerative Biology, King's College London, Floor 27 Tower Wing, Guy's Campus, London, SE1 9RT, United Kingdom

[2] Skin Research Institute of Singapore, Agency for Science, Technology and Research, Singapore 308232

[3] Lee Kong Chian School of Medicine, Nanyang Technological University, Singapore 308232

[4] Department of Medicine III, University Hospital Carl Gustav Carus, Technische Universität Dresden, 01307 Dresden, Germany

[5] Institute of Functional Genomics (IGF), University of Montpellier, CNRS, INSERM, F-34094 Montpellier, France

[6] Howard Hughes Medical Institute, Stanford University School of Medicine, Stanford, CA 94305-5329; Department of Developmental Biology, Stanford University School of Medicine, Stanford, CA 94305-5329, USA

[7] Department of Medicine and Liver Center, University of California San Francisco, San Francisco, CA 94143-1346, USA

[8] Developmental Biology and Cancer, Birth Defects Research Centre, UCL GOS Institute of Child Health, London, WC1N 1EH, United Kingdom

[9] Université Côte d'Azur, Inserm, CNRS, iBV, Nice 06108, France.

* Corresponding author

E-mail: cynthia.andoniadou@kcl.ac.uk. Phone: +44 20 7188 7389. Fax: +44 20 7188 1674

ABSTRACT

In response to physiological demand, the pituitary gland generates new hormone-secreting cells from committed progenitor cells throughout life. It remains unclear to what extent pituitary stem cells (PSCs), which uniquely express SOX2, contribute to pituitary growth and renewal. Moreover, neither the signals that drive proliferation nor their sources have been elucidated. We have used genetic approaches in the mouse, showing that the WNT pathway is essential for proliferation of all lineages in the gland. We reveal that $SOX2^+$ stem cells are a key source of WNT ligands. By blocking secretion of WNTs from $SOX2^+$ PSCs *in vivo*, we demonstrate that proliferation of neighbouring committed progenitor cells declines, demonstrating that progenitor multiplication depends on the paracrine WNT secretion from $SOX2^+$ PSCs. Our results indicate that stem cells can hold additional roles in tissue expansion and homeostasis, acting as paracrine signalling centres to coordinate the proliferation of neighbouring cells.

KEY WORDS

SOX2, paracrine signal, WNT, pituitary gland, stem cell, feedforward regulation

INTRODUCTION

How stem cells interact with their surrounding tissue has been a topic of investigation since the concept of the stem cell niche was first proposed (Schofield, 1978). Secreted from supporting cells, factors such as WNTs, FGFs, SHH, EGF and cytokines, regulate the activity of stem cells (Nabhan et al., 2018; Palma et al., 2005; Tan and Barker, 2014). Furthermore, communication is known to take place in a bi-directional manner (Doupe et al., 2018; Tata and Rajagopal, 2016).

The anterior pituitary (AP) is a major primary endocrine organ that controls key physiological functions including growth, metabolism, reproduction and the stress responses and exhibits tremendous capability to remodel its constituent hormone populations throughout life, in response to physiological demand. It contains a population of *Sox2* expressing stem cells that self-renew and give rise to lineage-committed progenitors and functional endocrine cells (Andoniadou et al., 2013; Rizzoti et al., 2013). During embryonic development, $SOX2^{+}$ undifferentiated precursor cells of Rathke's pouch, the pituitary anlage (Arnold et al., 2011; Castinetti et al., 2011; Fauquier et al., 2008; Pevny and Rao, 2003), generate all committed endocrine progenitor lineages, defined by the absence of SOX2 and expression of either POU1F1 (PIT1), TBX19 (TPIT) or NR5A1 (SF1) (Bilodeau et al., 2009; Davis et al., 2011). These committed progenitors are proliferative and give rise to the hormone-secreting cells. Demand for hormone secretion rises after birth, resulting in dramatic organ growth and expansion of all populations by the second postnatal week (Carbajo-Perez and Watanabe, 1990; Taniguchi et al., 2002). $SOX2^{+}$ pituitary stem cells (PSCs) are most active during this period, but the bulk of proliferation and organ expansion during postnatal stages derives from $SOX2^{-}$ committed progenitors. The activity of $SOX2^{+}$ PSCs gradually decreases and during adulthood is minimally

activated even following physiological challenge (Andoniadou et al., 2013; Gaston-Massuet et al., 2011; Gremeaux et al., 2012; Zhu et al., 2015). By adulthood, progenitors carry out most of the homeostatic functions, yet $SOX2^+$ PSCs persist throughout life in both mice and humans (Gonzalez-Meljem et al., 2017; Xekouki et al., 2018). The signals driving proliferation of committed progenitor cells are not known, and neither is it known if $SOX2^+$ PSCs can influence this process beyond their minor contribution of new cells.

The self-renewal and proliferation of numerous stem cell populations relies upon WNT signals (Basham et al., 2019; Lim et al., 2013; Takase and Nusse, 2016; Wang et al., 2015; Yan et al., 2017). WNTs are necessary for the initial expansion of Rathke's pouch as well as for PIT1 lineage specification (Osmundsen et al., 2017; Potok et al., 2008). In the postnatal pituitary, the expression of WNT pathway components is upregulated during periods of expansion and remodelling. Gene expression comparisons between neonatal and adult pituitaries or in GH-cell ablation experiments (Gremeaux et al., 2012; Willems et al., 2016), show that the WNT pathway is upregulated during growth and regeneration.

Our previous work revealed that during disease, the paradigm of supporting cells signalling to the stem cells may be reversed; mutant stem cells expressing a degradation-resistant β-catenin in the pituitary, promote cell non-autonomous development of tumours through their paracrine actions (Andoniadou et al., 2013; Gonzalez-Meljem et al., 2017). Similarly, degradation-resistant β-catenin expression in hair follicle stem cells led to cell non-autonomous WNT activation in neighbouring cells promoting new growth (Deschene et al., 2014). In the context of normal homeostasis, stem cells have been shown to influence daughter cell fate in the mammalian airway epithelium and the *Drosophila* gut via 'forward regulation'

models, where the fate of a daughter cell is directed by a stem cell via juxtacrine Notch signalling (Ohlstein and Spradling, 2007; Pardo-Saganta et al., 2015). It remains unknown if paracrine stem cell action can also promote local proliferation in normal tissues.

Here, we used genetic approaches to determine if paracrine stem cell action takes place in the anterior pituitary and to discern the function of WNTs in pituitary growth. Our results demonstrate that postnatal pituitary expansion, largely driven by committed progenitor cells, depends on WNT activation. Importantly, we show that $SOX2^+$ PSCs are the key regulators of this process, acting through secretion of WNT ligands acting in a paracrine manner on neighbouring progenitors. Identification of this forward-regulatory model elucidates a previously unidentified function for stem cells during tissue expansion.

RESULTS

WNT-responsive cells in the pituitary include progenitors driving major postnatal expansion.

To clarify which cells respond to WNT signals in the postnatal anterior pituitary, we first characterised the anterior pituitary cell types activating the WNT pathway at P14, a peak time for organ expansion and a time point when a subpopulation of $SOX2^+$ stem cells are proliferative. The *Axin2-CreERT2* mouse line (van Amerongen et al., 2012) has been shown to efficiently label cells with activated WNT signalling in the liver, lung, breast, skin, testes and endometrium among other tissues (Lim et al., 2013; Moiseenko et al., 2017; Syed et al., 2020; van Amerongen et al., 2012; Wang et al., 2015). *Axin2* positive cells were labelled by GFP following tamoxifen induction in

Axin2$^{CreERT2/+}$;*ROSA26*$^{mTmG/+}$ mice and pituitaries were analysed 2 days post-induction. We carried out double immunofluorescence staining using antibodies against uncommitted (SOX2), lineage committed (PIT1, TPIT, SF1), and hormone-expressing endocrine cells (GH, PRL, TSH, ACTH or FSH/LH) together with antibodies against GFP labelling the WNT-activated cells. We detected WNT-responsive cells among all the different cell types of the anterior pituitary including SOX2$^+$ PSCs, the three committed populations and all hormone-secreting cells (Figure 1A, Figure 1 – figure supplement 1A).

To confirm if the three committed lineages as well as uncommitted SOX2$^+$ PSCs all expand in response to WNT, we further lineage-traced *Axin2*-expressing cells for 14 days after tamoxifen administration at P14. Double labelling revealed an increase in all four populations between 2 and 14 days (Figure 1A, B). This increase reached significance for the PIT1 (13.7% at 2 days to 30.3% at 14 days, P=0.000004) and TPIT (3.78% to 11.03%, P=0.008) populations, but not SF1 (0.5% to 4%, n.s.). As this time course ends at P28 at the commencement of puberty, we repeated the analysis for SF1 cells to P42, which spans puberty and the expansion of gonadotrophs (Figure 1 – figure supplement 1B). This reveals a significant expansion in WNT-responsive SF1$^+$ cells as a proportion of the total SF1$^+$ population (P=0.0048, n=3). Lineage tracing of the PIT1-derivates (GH$^+$ somatotrophs, PRL$^+$ lactotrophs, TSH$^+$ thyrotrophs) reveals that there is a preferential expansion of somatotrophs and thyrotrophs (Figure 1 – figure supplement 1C). Only a minority of SOX2$^+$ PSCs were WNT-responsive at 2 days (0.57%) and this population expanded to 2% at 14 days (n.s.), suggesting that these are self-renewing. GFP$^+$ cells were traced for a period of 8 weeks post-induction, which revealed that WNT-responsive descendants continued to expand at the same rate as the rest of the pituitary (n=4-8 mice per time point at P16,

P21, P28, P42, P70) (Figure 1C, D). The time period between 2 and 7 days saw the greatest increase in GFP^+ cells, during which, the labelled population nearly tripled in size (Figure 1D). The persistence of labelled cells was evident in longer-term traces using the $ROSA26^{lacZ/+}$ reporter ($Axin2^{CreERT2/+};ROSA26^{lacZ/+}$), up to a year following induction at P14 (Figure 1E, *n*=4). Clonal analysis using the Confetti reporter, demonstrated that individual *Axin2*-expressing cells ($Axin2^{CreERT2/+};ROSA26^{Confetti/+}$) gave a greater contribution after four weeks compared to lineage-tracing from *Sox2*-expressing cells ($Sox2^{CreERT2/+};ROSA26^{Confetti/+}$), in support of predominant expansion from WNT-responsive lineage-committed progenitors (Figure 1 – figure supplement 1D).

To establish if signalling mediated by β-catenin is necessary for organ expansion we carried out deletion of *Ctnnb1* in the $Axin2^+$ population from P14 during normal growth ($Axin2^{CreERT2/+};Ctnnb1^{lox(ex2-6)/lox(ex2-6)}$ hereby $Axin2^{CreERT2/+};Ctnnb1^{LOF/LOF}$). Due to morbidity, likely due to *Axin2* expression in other organs, we were limited to analysis up to 5 days post-induction. Deletion of *Ctnnb1* resulted in a significant reduction in the number of dividing cells, marked by pH-H3 (40% reduction, Figure 1 – figure supplement 2A, *P*=0.0313, *n*=3), confirming that activation of the WNT pathway is necessary for expansion of the pituitary populations. This deletion did not result in significant differences in overall numbers among the three lineages, as determined by the numbers of $PIT1^+$, $SF1^+$ or $ACTH^+$ cells among the targeted population (Figure 1 – figure supplement 2B, *n*=4 controls, 2 mutants). The number of SOX2+ stem cells and cells undergoing cell death also remained unaffected during the 5 day period (Figure 1 – figure supplement 2C and D). Taken together, these results confirm that postnatal AP expansion depends on

WNT-responsive progenitors across all lineages, in addition to SOX2^{+} PSCs (Figure 1F).

WNT/β-catenin signalling is required for long-term anterior pituitary expansion from SOX2^{+} pituitary stem cells.

We further explored the role of WNT pathway activation in postnatal SOX2^{+} stem cells. To permanently mark WNT-responsive cells and their descendants whilst simultaneously marking SOX2^{+} PSCs, we combined the tamoxifen-inducible *Axin2$^{CreERT2/+}$;ROSA26$^{tdTomato/+}$* with the *Sox2$^{Egfp/+}$* strain, where cells expressing SOX2 are labelled by EGFP (*Axin2$^{CreERT2/+}$;Sox2$^{Egfp/+}$;ROSA26$^{tdTomato/+}$*). Following tamoxifen administration from P21, tdTomato- and EGFP-labelled cells were analysed by flow sorting after 72h, by which point all induced cells robustly express tdTomato (Figure 2A, Figure 2 – figure supplement 1). Double-labelled cells comprised 23.4% of the SOX2^{+} population (*n*=5 individual pituitaries) (Figure 2A, arrowheads), with the majority of tdTomato^{+} cells found outside of the SOX2^{+} compartment. It was previously shown that only around 2.5-5% of SOX2^{+} PSCs have clonogenic potential through *in vitro* assays (Andoniadou et al., 2012; Andoniadou et al., 2013; Perez Millan et al., 2016). To determine if WNT-responsive SOX2^{+} cells are stem cells capable of forming colonies, we isolated double positive tdTomato^{+};EGFP^{+} cells (i.e. *Axin2^{+};Sox2^{+}*) as well as the single-expressing populations and plated these in equal numbers in stem cell-promoting media at clonal densities (Figure 2B). Double positive tdTomato^{+};EGFP^{+} cells showed a significant increase in the efficiency of colony formation compared to single-labelled EGFP^{+} cells (average 9% compared to 5%, *n*=5 pituitaries, *P*=0.0226, Mann-Whitney *U* test (two-tailed)), demonstrating WNT-responsive SOX2^{+} PSCs have a greater clonogenic

potential under these *in vitro* conditions, confirming *in vivo* data in Figure 1B. As expected from previous work, none of the single-labelled tdTomato^{+} cells (i.e. SOX2 negative) were able to form colonies (Andoniadou et al., 2012).

To confirm that PSCs with active WNT signalling through β-catenin have a greater propensity to form colonies *in vitro*, we analysed postnatal pituitaries from TCF/Lef:H2B-EGFP mice, reporting the activation of response to WNT signals. This response is detected through expression of an EGFP-tagged variant of histone H2B, which is incorporated into chromatin and diluted in descendants with cell division (Ferrer-Vaquer et al., 2010). Therefore, cells responding to, or having recently responded to WNT, as well as their immediate descendants will be EGFP^{+}. At P21, EGFP^{+} cells were abundant in all three lobes and particularly in the marginal zone harbouring SOX2^{+} stem cells (Figure 2 – figure supplement 2A). Through double mRNA *in situ* hybridisation against *Egfp* and *Sox2* in TCF/Lef:H2B-EGFP pituitaries, we confirmed that *Sox2*-expressing cells activate H2B-EGFP expression at this time point (Figure 2 – figure supplement 2B). Isolation by fluorescence-activated cell sorting and *in vitro* culture of the postnatal EGFP^{+} compartment revealed an enrichment of cells with clonogenic potential in the EGFP^{High} fraction compared to EGFP^{Low} or negative cells (Figure 2 – figure supplement 2C, *n*=5 pituitaries). Together these results reveal that a proportion of postnatal SOX2^{+} stem cells respond to WNTs through downstream β-catenin/TCF/LEF signalling and that these cells have greater clonogenic capacity *in vitro*.

To further address the role of the canonical WNT response in the activity of SOX2^{+} PSCs *in vivo*, we expressed a loss-of-function allele of β-catenin specifically in *Sox2*-expressing cells (*Sox2*$^{CreERT2/+}$;*Ctnnb1*$^{lox(ex2-6)/lox(ex2-6)}$ hereby *Sox2*$^{CreERT2/+}$;*Ctnnb1*$^{LOF/LOF}$) from P14. Twenty-two weeks following induction, at

P168, there was a substantial drop in the number of cycling cells in the pituitary of *Sox2*$^{CreERT2/+}$;*Ctnnb1*$^{LOF/LOF}$ mutants compared to *Sox2*$^{+/+}$;*Ctnnb1*$^{LOF/LOF}$ controls (Figure 2C, *n*=2 pituitaries per genotype). This was accompanied by anterior pituitary hypoplasia following the loss of *Ctnnb1* in SOX2^{+} PSCs (Figure 2D). Therefore, in this small sample size, the proliferative capacity of *Ctnnb1*-deficient SOX2^{+} PSCs and of their descendants was impaired long-term, leading to reduced growth. *In vivo* genetic tracing of targeted cells over the 22-week period (*Sox2*$^{CreERT2/+}$;*Ctnnb1*$^{LOF/+}$;*ROSA26*$^{mTmG/+}$ compared to *Sox2*$^{CreERT2/+}$;*Ctnnb1*$^{LOF/LOF}$;*ROSA26*$^{mTmG/+}$ pituitaries) revealed that targeted (*Ctnnb1*-deficient) SOX2^{+} PSCs were capable of giving rise to the three committed lineages PIT1, TPIT and SF1 (Figure 2 – figure supplement 2D), indicating that the loss of *Ctnnb1* does not prevent differentiation of SOX2^{+} PSCs into the three lineages. Downregulation of β-catenin was confirmed by immunofluorescence in SOX2^{+} (mGFP^{+}) derivatives (Figure 2 – figure supplement 2E). Although limited by a small sample size, we conclude that WNT/β-catenin signalling is likely required cell-autonomously in SOX2^{+} stem cells and their descendants (Figure 2E).

SOX2^{+} stem cells express WNT ligands.

Having established that WNT activation is responsible for promoting proliferation in the AP, we next focused on identifying the source of WNT ligands. *Axin2* expressing cells from *Axin2*$^{CreERT2/+}$;*ROSA26*$^{mTmG/+}$ mice were labelled at P14 by tamoxifen induction. Cells expressing *Axin2* at the time of induction are labelled by GFP expression in the membrane. Double immunofluorescence staining for GFP together with SOX2 revealed that *Axin2* expressing cells (mGFP^{+}) are frequently located in close proximity to SOX2^{+} PSCs (Figure 3A). Two-dimensional quantification of the

two cell types revealed that over 50% of $mGFP^+$ cells were in direct contact with $SOX2^+$ nuclei (*n*=3 pituitaries, >500 $SOX2^+$ cells per gland, Figure 3A). The analysis did not take into account the cellular processes of $SOX2^+$ cells. These results led us to speculate that $SOX2^+$ PSCs may be a source of key WNT ligands promoting proliferation of lineage-committed cells.

In order to determine if $SOX2^+$ PSCs express WNT ligands, we carried out gene expression profiling of $SOX2^+$ and $SOX2^-$ populations at P14, through bulk RNA-sequencing. Pure populations of *Sox2*-expressing cells excluding lineage-committed populations, were isolated from $Sox2^{Egfp/+}$ male and female pituitaries at P14 based on EGFP expression as previously shown (Andoniadou et al., 2012) (Figure 3B, Figure 3 – figure supplement 1A). Analysis of global gene expression signatures using 'Gene Set Enrichment Analysis' (GSEA) (Subramanian et al., 2005) identified a significant enrichment of molecular signatures related to EMT, adherens and tight junctions in the $EGFP^+$ fraction, characteristic of the $SOX2^+$ population (Figure 3 – figure supplement 1B). The $SOX2^+$ fraction also displayed enrichment for genes associated with several signalling pathways known to be active in these cells, including EGFR (Iwai-Liao et al., 2000), Hippo (Lodge et al., 2016; Lodge et al., 2019; Xekouki et al., 2019), MAPK (Haston et al., 2017), FGF (Higuchi et al., 2017), Ephrin (Yoshida et al., 2015; Yoshida et al., 2017) and p53 (Gonzalez-Meljem et al., 2017) (Figure 3 – figure supplement 1C, Supplementary File 1). Additionally, PI3K, TGFβ and BMP pathway genes were significantly enriched in the $SOX2^+$ population (Figure 3 – figure supplement 1C, Supplementary File 1). Query of the WNT-associated genes did not suggest a global enrichment in WNT targets (e.g. enrichment of *Myc* and *Jun*, but not of *Axin2* or *Lef1*) (Figure 3 – figure supplement 1D, Supplementary File 1). Instead, $SOX2^+$ PSCs expressed a unique transcriptomic

fingerprint of key pathway genes including *Lgr4*, *Znrf3*, *Rnf43* capable of regulating WNT signal intensity in $SOX2^+$ PSCs, as well as enriched expression of the receptors *Fzd1*, *Fzd3*, *Fzd4*, *Fzd6* and *Fzd7* (Figure 3 – figure supplement 1D). The predominant R-spondin gene expressed in the pituitary was *Rspo4*, specifically by the EGFP-negative fraction (Figure 3 – figure supplement 1D). The gene profiling revealed that *Wls* expression, encoding Gpr177/WLS, a necessary mediator of WNT ligand secretion (Carpenter et al., 2010; Takeo et al., 2013; Wang et al., 2015), is enriched in $SOX2^+$ PSCs (Figure 3C). Analysis of *Wnt* gene expression confirmed enriched expression of *Wnt2*, *Wnt5a* and *Wnt9a* in $SOX2^+$ PSCs, and the expression of multiple additional *Wnt* genes by both fractions at lower levels ($SOX2^+$ fraction: *Wnt5b*, *Wnt6*, *Wnt16*; $SOX2^-$ fraction: *Wnt2*, *Wnt2b*, *Wnt3*, *Wnt4*, *Wnt5a*, *Wnt5b*, *Wnt9a*, *Wnt10a*, *Wnt16*) (Figure 3D). These results reveal that $SOX2^+$ PSCs express the essential components to regulate activation of the WNT pathway and express *Wnt* genes as well as the necessary molecular machinery to secrete WNT ligands.

Paracrine signalling from $SOX2^+$ stem cells promotes WNT activation.

We sought to conclusively determine if WNT secretion specifically from $SOX2^+$ PSCs drives proliferation of surrounding cells in the postnatal pituitary gland. We proceeded to delete *Wls* only in the *Sox2*-expressing population ($Sox2^{CreERT2/+};Wls^{fl/fl}$) from P14 by a series of tamoxifen injections. Due to morbidity, we limited analyses to one week following induction. Pituitaries appeared mildly hypoplastic at P21 along the medio-lateral axis (Figure 4 – figure supplement 1, n=4 controls and n=5 mutants). To determine if this is a result of reduced proliferation, we carried out immunofluorescence using antibodies against Ki-67 and SOX2. This revealed significantly fewer cycling cells in the $SOX2^-$ population of $Sox2^{CreERT2/+};Wls^{fl/fl}$

mutant pituitaries compared to *Sox2*$^{+/+}$;*Wls*$^{fl/fl}$ controls (10.326% Ki-67 in control (*n*=4) compared to 3.129% in mutant (*n*=5), *P*=0.0008, unpaired *t*-test) (Figure 4A). Additionally, we observed a reduction of cycling cells within the SOX2^{+} population (5.582% Ki-67 in control compared to 2.225% in induced *Sox2*$^{CreERT2/+}$;*Wls*$^{fl/fl}$ mutant pituitaries, *P*=0.0121, unpaired *t*-test) (Figure 4A), resulting in a smaller SOX2^{+} cell pool in mutants (23.425% SOX2^{+}/total AP cells in *Sox2*$^{+/+}$;*Wls*$^{fl/fl}$ controls compared to 19.166% SOX2^{+}/total AP cells in induced *Sox2*$^{CreERT2/+}$;*Wls*$^{fl/fl}$ mutant pituitaries, *P*=0.0238, Student's *t*-test, *n*=5 mutants, 4 controls). To determine if reduced levels of WNT activation accompanied this phenotype, we carried out double mRNA *in situ* hybridisation using specific probes against *Lef1* and *Sox2*. There was an overall reduction in *Lef1* expression in mutants compared to controls (*n*=4 per genotype), in which we frequently observed robust expression of *Lef1* transcripts in close proximity to cells expressing *Sox2* (arrows, Figure 4B). Together, our data support a paracrine role for SOX2^{+} pituitary stem cells in driving the expansion of committed progeny through the secretion of WNT ligands (Figure 4C).

DISCUSSION

Emerging disparities between the archetypal stem cell model, exhibited by the haematopoietic system, and somatic stem cells of many organs, have led to the concept that stem cell function can be executed by multiple cells not fitting a typical stem cell paradigm (Clevers and Watt, 2018). In organs with persistent populations possessing typical functional stem cell properties yet contributing minimally to turnover and repair, the necessity for such classical stem cells is questioned. Here we show that WNT signalling is required for postnatal pituitary growth by both SOX2^{+} PSCs as well as SOX2^{-} committed progenitors. We identify an additional discreet

function for SOX2^{+} PSCs, where these signal in a feedforward manner by secreting WNT ligands as cues to stimulate proliferation and promote tissue growth.

Consistent with previous reports, our data support that SOX2^{+} PSCs contribute, but do not carry out the majority of tissue expansion during the postnatal period (Zhu et al., 2015); instead, new cells primarily derive from more committed progenitors, which we show to be WNT-responsive. We demonstrate that this population of lineage-restricted WNT-responsive cells rapidly expands and contributes long-lasting clones from postnatal stages. It remains to be shown if cells among the SOX2^{-} lineage-committed populations may also fall under the classical definition of a stem cell. Preventing secretion of WNT ligands from SOX2^{+} PSCs reveals that far from being dispensable, paracrine actions of the SOX2^{+} population that are inactive in their majority, are necessary for anterior lobe expansion from lineage-committed populations. In the adrenal gland, R-spondins are necessary for cortical expansion and zonation, where deletion of *Rspo3*, expressed by the capsule which contains adrenocortical stem cells, results in reduced proliferation of the underlying steroidogenic cells (Vidal et al., 2016). Corroborating a model where committed pituitary progenitors depend on the paracrine actions of SOX2^{+} PSCs, Zhu and colleagues observed that in pituitaries with reduced numbers of PSCs, proliferation among PIT1^{+} cells was significantly impaired (Zhu et al., 2015). It would be intriguing to see if there is a reduction in WNT signalling in this model, or following genetic ablation of adult SOX2^{+} PSCs (Roose et al., 2017).

We show that a sub-population of SOX2^{+} PSCs in the postnatal gland are also WNT-responsive and have greater *in vitro* colony-forming potential under defined conditions. This colony-forming potential is normally a property of a minority of SOX2^{+} PSCs at any given age and reflects their *in vivo* proliferative capacity

(Andoniadou et al., 2012; Rizzoti et al., 2013). A role for the WNT pathway in promoting $SOX2^+$ cell activity is supported by studies showing that pathogenic overexpression of β-catenin promotes their colony-forming ability (Sarkar et al., 2016), and their *in vivo* expansion (Andoniadou et al., 2012). Additionally, elevated WNT pathway activation has been described for pituitary side-population cells, enriched for $SOX2^+$ stem cells from young, compared to old pituitaries (Gremeaux et al., 2012). This is in line with our findings that the WNT pathway has an important function in promoting the activation of $SOX2^+$ PSCs. It remains to be shown if this response relies on autocrine WNT-signalling as for other stem cells (Lim et al., 2013), however our results reveal reduced proliferation among $SOX2^+$ PSCs and reduced $SOX2^+$ cell numbers when WNT secretion from these cells is abolished, supportive of either autocrine signalling, or paracrine signalling between different subsets of the $SOX2^+$ population.

The mechanism preventing the majority of $SOX2^+$ PSCs from responding to WNT signals remains elusive but points to heterogeneity among the population. Such regulation could occur at the level of receptor signalling; we have shown by bulk transcriptomic profiling that $SOX2^+$ PSCs express the receptors required to respond to the WNT pathway, but also express high levels of the frizzled inhibitor *Znrf3*, and the R-spondin receptor *Lgr4.* One conceivable scenario is that high levels of *Znrf3* inhibit frizzled receptors in the absence of R-spondin under normal physiological conditions, supressing a WNT response. In support of this, R-spondins have been shown to promote pituitary organoid formation (Cox et al., 2019). Whether the R-spondin/LGR/ZNRF3 module is active under physiological conditions needs to be determined. Furthermore, well-described factors expressed in PSCs are known to have inhibitory effects on β-catenin-mediated transcription, such as YAP/TAZ

(Azzolin et al., 2014; Gregorieff et al., 2015) and SOX2 itself (Alatzoglou et al., 2011; Kelberman et al., 2008).

In summary, we demonstrate an alternative mechanism for stem cell contribution to homeostasis, whereby these can act as paracrine signalling hubs to promote local proliferation. Applicable to other organs, this missing link between $SOX2^+$ PSCs and committed cell populations of the anterior pituitary, is key for basic physiological functions and renders stem cells integral to organ expansion.

MATERIALS AND METHODS

Mice

All procedures were performed under compliance of the Animals (Scientific Procedures) Act 1986, Home Office License (P5F0A1579). KCL Biological Services Unit staff undertook daily animal husbandry. Genotyping was performed on ear biopsies taken between P11 and P15 by standard PCR using the indicated primers. These experiments were not conducted at random and the experimenters were not blind while conducting the animal handling and assessment of tissue. Images are representative of the respective genotypes. For all studies, both male and female animals were used and results combined.

The *Sox2*$^{CreERT2/+}$ and *Sox2*$^{Egfp/+}$ strains were kept on a CD-1 background. *Axin2*$^{CreERT2/+}$animals were kept on a mixed background of C57BL/6 backcrossed onto CD-1 for 5 generations and were viable and fertile, with offspring obtained at the expected Mendelian ratios. *ROSA26*$^{mTmG/mTmG}$, *ROSA26*$^{Confetti/Confetti}$, *ROSA26*$^{tdTomato/tdTomato}$, *Wls*$^{fl/fl}$, *Ctnnb1*$^{fl(ex2-6)/\ fl(ex2-6)}$ and TCF/LEF:H2B-EGFP mice were kept on a mixed background of 129/Sv backcrossed onto CD-1 for at least 3 generations. For lineage tracing studies, male *Axin2*$^{CreERT2/+}$ or *Sox2*$^{CreERT2/+}$ mice were bred with homozygous *ROSA26*$^{mTmG/mTmG}$ or *ROSA26*$^{Confetti/Confetti}$ dams to produce the appropriate allele combinations on the reporter background. Pups were induced at P14 or P15 with a single dose of tamoxifen (resuspended to 20mg/ml in Corn Oil with 10% ethanol) by intraperitoneal injection, at a concentration of 0.15mg per gram of body weight. Pituitaries were harvested at the indicated time points post induction and processed for further analysis as described below. Mice were harvested from different litters for each time point at random. For litters in which there was a

surplus of experimental mice, multiple samples were harvested for each required time point.

For Wntless deletion studies, *Sox2*$^{CreERT2/+}$;*Wls*$^{fl/+}$;*ROSA26*$^{mTmG/mTmG}$ males were bred with *Wls*$^{fl/fl}$;*ROSA26*$^{mTmG/mTmG}$ dams, to produce *Sox2*$^{CreERT2/+}$;*Wls*$^{fl/+}$;*ROSA26*$^{mTmG/mTmG}$, *Sox2*$^{CreERT2/+}$;*Wls*$^{fl/fl}$;*ROSA26*$^{mTmG/mTmG}$ and *Wls*$^{fl/fl}$;*ROSA26*$^{mTmG/mTmG}$ offspring. Pups of the indicated genotypes received intraperitoneal injections of 0.15mg of tamoxifen/gram body weight on 4 consecutive days, beginning at P14, and harvested 3 days after the final injection.

For the β-catenin loss-of-function experiments, either *Sox2*$^{CreERT2/+}$;*Ctnnb1*$^{fl(ex2-6)/+}$;*ROSA26*$^{mTmG/mTmG}$ or *Axin2*$^{CreERT2/+}$;*Ctnnb1*$^{fl(ex2-6)/+}$;*ROSA26*$^{mTmG/mTmG}$ males were crossed with *Ctnnb1*$^{fl(ex2-6)/fl(ex2-6)}$;*ROSA26*$^{mTmG/mTmG}$ dams. *Axin2*$^{CreERT2/+}$;*Ctnnb1*$^{fl(ex2-6)/fl(ex2-6)}$;*ROSA26*$^{mTmG/mTmG}$ and *Axin2*$^{CreERT2/+}$;*Ctnnb1*$^{fl(ex2-6)/+}$;*ROSA26*$^{mTmG/mTmG}$ pups were induced with a single dose of tamoxifen, at a concentration of 0.15mg per gram of body weight and kept alive for 7 days before harvesting. *Sox2*$^{CreERT2/+}$;*Ctnnb1*$^{fl(ex2-6)/+}$;*ROSA26*$^{mTmG/mTmG}$ and *Sox2*$^{CreERT2/+}$;*Ctnnb1*$^{fl(ex2-6)/fl(ex2-6)}$;*ROSA26*$^{mTmG/mTmG}$ pups received two intraperitoneal injections of tamoxifen, at a concentration of 0.15mg/gram body weight, on two consecutive days and were kept alive for the indicated length of time before harvesting.

TCF/LEF:H2B-EGFP mice were culled and the pituitaries harvested at the indicated ages for the respective experiments. For fluorescence-activated cell sorting experiments, mice were harvested at 21 days of age. *Axin2*$^{CreERT2/+}$;*Sox2*$^{eGFP/+}$ males were crossed with *ROSA26*$^{tdTomat/tdTomato}$ dams to produce *Axin2*$^{CreERT2/+}$;*Sox2*$^{eGFP/+}$;*ROSA26*$^{tdTomato/+}$ that were induced with single doses of tamoxifen at 21 and 22 days of age and harvested three days after the first injection for fluorescence-activated cell sorting experiments.

Flow cytometry analysis of lineage traced pituitaries

For the quantification of cells by flow cytometry, anterior lobes of *Axin2*$^{CreERT2/+}$*;ROSA26*$^{mTmG/+}$ mice dissected at the indicated time points. The posterior and intermediate lobes were dissected from the anterior lobes under a dissection microscope. Untreated *ROSA26*$^{mTmG/+}$ and wild type pituitaries from age-matched litters were used as tdTomato only and negative controls, respectively. Dissected pituitaries were incubated in Enzyme Mix (0.5% w/v collagenase type 2 (Lorne Laboratories), 0.1x Trypsin (Gibco), 50µg/ml DNase I (Worthington) and 2.5µg/ml Fungizone (Gibco) in Hank's Balanced Salt Solution (HBSS)(Gibco)) in a cell culture incubator for up to 3 hours. 850ml of HBSS were added to each Eppendorf in order to quench the reaction. Pituitaries were dissociated by agitation, pipetting up and down 100x at first with a 1ml pipette, followed by 100x with a 200µl pipette. Cells were transferred to a 15ml Falcon tube and resuspended in 9ml of HBSS and spun down at 200g for 5 minutes. The supernatant was aspirated, leaving behind the cell pellet that was resuspended in PBS and spun down at 1000rpm for 5 minutes before being resuspended in a Live/Dead cell stain (Life Technologies, L34975) prepared to manufacturer's instructions, for 30 minutes in the dark. Cells were washed in PBS as above. The pellet was resuspended in FIX & PERM Cell Permeabilization Kit (Life Technologies, GAS003) prepared as per manufacturer's instructions for 10 minutes at room temperature. Cells were washed as above, and the pellet was resuspended in 500µl of FACS buffer (1% fetal calf serum (Sigma), 25mM HEPES in PBS) and filtered through 70µm filters (BD Falcon), into 5ml round bottom polypropylene tubes (BD Falcon). 1 minute prior to analysis, 1µl of Hoechst was added to the suspended cells and incubated. Samples were analysed on a BD

Fortessa, and gated according to negative and single fluorophore controls. Single cells were gated according to SSC-A and SSC-W. Dead cells were excluded according to DAPI (2ng/ml, incubated for 2 mins prior to sorting). GFP^+, $tdTomato^+$ and GFP^+;$tdTomato^+$ cells were gated according to negative controls in the PE-A and FITC-A channels.

Fluorescence Activated Cell Sorting for sequencing or colony forming assays

For fluorescence activated cell sorting, the anterior lobes from *Sox2*$^{eGFP/+}$, TCF/LEF:H2B-GFP or *Axin2*$^{CreERT2/+}$;*Sox2*$^{eGFP/+}$;*ROSA26*$^{tdTomato/+}$ and their respective controls were dissected and dissociated as above. After dissociation cells were spun down at 200g in HBSS and the pellet was resuspended in 500µl FACS buffer. Using an Aria III FACs machine (BD systems), samples were gated according to negative controls, and where applicable single fluorophore controls. Experimental samples were sorted according to their fluorescence, as indicated, into tubes containing either RNAlater (Qiagen) for RNA isolation or 1ml of Pit Complete Media for culture ((Pit Complete: 20ng/ml bFGF and 50ng/ml of cholera toxin in 'Pit Basic' media (DMEM-F12 with 5% Fetal Calf Serum,100U/ml Penicillin and 100µg/ml Streptomycin). Cells were plated in 12-well plates at clonal density, approximately 500 cells/well. Colonies were incubated for 7 days total before being fixed in 10% neutral buffered formalin (NBF) (Sigma) for 10 minutes at room temperature, washed for five minutes, three times, mins with PBS and stained with crystal violet in order for the number of colonies to be quantified.

RNA-sequencing

Total RNA was isolated from each sample and following poly-A selection, cDNA libraries were generated using TruSeq (Clontech, 634925). Barcoded libraries were then pooled at equal molar concentrations and sequenced on an Illumina Hiseq 4000 instrument in a 75 base pair, paired – end sequencing mode, at the Wellcome Trust Centre for Human Genetics (Oxford, United Kingdom). Raw sequencing reads were quality checked for nucleotide calling accuracy and trimmed accordingly to remove potential sequencing primer contaminants. Following QC, forward and reverse reads were mapped to GRCm38/mm10 using Hisat2 (Kim et al., 2015). Using a mouse transcriptome specific GTF as a guide, FeatureCounts (Liao et al., 2014) was used to generate gene count tables for every sample. These were utilised within the framework of the Deseq2 (Love et al., 2014) and FPKM values (generated by FPKM count (Wang et al., 2012)) were processed using the Cufflinks (Trapnell et al., 2012) pipelines which identified statistically significant gene expression differences between the sample groups. Following identification of differentially expressed genes (at an FDR < 0.05) we focused on identifying differentially expressed pathways using a significance threshold of FDR < 0.05 unless otherwise specified. The gene lists used for Gene Set Enrichment Analysis (GSEA) were as found on the BROAD institute GSEA MSigDBv.7 'molecular signatures database'. The deposited dataset can be accessed through the following link:
https://dataview.ncbi.nlm.nih.gov/object/PRJNA421806?reviewer=kr90aklsdtikh3gkh3tdlpv30s

Immunofluorescence and microscopy

Freshly harvested pituitaries were washed in PBS for 10 minutes before being fixed in 10% NBF for 18 hours at room temperature. In short, embryos and whole pituitaries

were washed in PBS 3 times, before being dehydrated through a series of 1 hour washes in 25%, 50%, 70%, 80%, 90%, 95% and 100% ethanol. Tissues were washed in Neo-Clear (Sigma) at room temperature for 10 minutes, then in fresh preheated Neo-Clear at 60 °C for 10 minutes. Subsequently, a mixture of 50% Neo-Clear:50% paraffin wax at 60°C for 15 minutes followed by three changes of pure wax for a minimum of 1 hour washes at 60°C, before being orientated to be sectioned in the frontal plane. Embedded samples were sectioned at 5µm and mounted on to Super Frost+ slides.

For immunofluorescence, slides were deparaffinised in Neo-Clear for three times ten minutes, washed in 100% ethanol for three times five minutes, and rehydrated in a series of five minute ethanol washes up to distilled water (95%, 90%, 80%, 70%, 50%, 25%, H2O). Heat induced epitope retrieval was performed with 1x DeClear Buffer (citrate pH 6) in a Decloaking chamber NXGEN (Menarini Diagnostics) for 3 minutes at 110°C. Slides were left to cool to room temperature before proceeding to block for 1 hour at room temperature in Blocking Buffer (0.2% BSA, 0.15% glycine, 0.1% TritonX in PBS) with 10% serum (sheep or donkey, depending on secondary antibodies). Primary antibodies were diluted in blocking buffer with 1% of the appropriate serum and incubated overnight at 4°C. Slides were washed three times for 10 minutes with PBST. Slides were incubated with secondary antibodies diluted 1:400 in blocking buffer with 1% serum for one hour at room temperature. Slides were washed three times with PBST as above. Where biotinylated secondary antibodies were used, slides were incubated with streptavidin diluted 1:400 in blocking buffer with 1% serum for one hour at room temperature. Finally, slides were washed with PBST and mounted using Vectashield Antifade Mounting Medium (Vector Laboratories, H-1000).

The following antibodies, along with their dilutions and detection technique, were used: GFP (1:400, Alexa Fluor-488 or -647 secondary), SOX2 raised in goat (1:200, Alexa Fluor-488 secondary), SOX2 raised in rabbit (1:100, biotinylated secondary), SOX9 (1:500, biotinylated secondary), PIT1 (1:500, biotinylated secondary), SF1 (1:300, biotinylated secondary), TPIT (1:200, biotinylated secondary), Ki-67 (1:100, biotinylated secondary), pH-H3 (1:500, biotinylated secondary), GH (1:1000, biotinylated secondary), TSH (1:1000, biotinylated secondary), PRL (1:1000, biotinylated secondary), ACTH (1:400, Alexa Fluor-555 secondary), LH/FSH (1:300, biotinylated secondary), ZO-1 (1:300, Alexa Fuor-488), E-Cadherin (1:300, Alexa Fluor-488). Nuclei were visualized with Hoechst (1:1000). Images were taken on a TCS SPS Confocal (Leica Microsystem) with a 20x objective for analysis.

mRNA *In Situ* Hybridisation

All mRNA *in situ* hybridisations were performed using the RNAscope singleplex or duplex chromogenic kits (Advanced Cell Diagnostics) on formalin fixed paraffin embedded sections processed as described in the above section. The protocol followed the manufacturer's instructions with slight modifications. ImmEdge Hydrophobic Barrier PAP Pen (Vector Laboratories, H-4000) was used to draw a barrier around section while air-drying following the first ethanol washes. Pretreatment followed the standard length of time for pituitaries (twelve minutes), while embryos were boiled for 10 minutes. For singleplex, the protocol proceeded to follow the instructions exactly. For duplex, Amplification 9 was extended to one hour and the dilution of the Green Detection reagent was increased to 1:30. For both protocols, sections were counterstained with Mayer's Haematoxylin (Vector Laboratories, H-3404), left to dry at 60°C for 30 minutes before mounting with

VectaMount Permanent Mounting Medium (Vector Laboratories, H-5000). Slides were scanned using a Nanozoomer-XR Digital Slide Scanner (Hamamatsu) and processed using Nanozoomer Digital Pathology View (Hamamatsu).

Quantification of cells

Cell numbers were quantified in ImageJ using the cell counter plugin (Schindelin et al., 2012). At a minimum, three sections per pituitary were quantified, spaced no less than 100µM apart in the tissue.

Statistics

All statistical analyses were performed in GraphPad Prism. Data points in graphs represent the mean values of recordings from a single biological replicate unless otherwise stated.

ACKNOWLEDGEMENTS

This study has been supported by the Medical Research Council (MR/L016729/1, MR/T012153/1) (C.L.A.), The Lister Institute of Preventive Medicine (C.L.A.), the Deutsche Forschungsgemeinschaft (DFG German Research Foundation) (Project Number 314061271 – TRR 205) (C.L.A.), the Howard Hughes Medical Institute (R.N.), the Agence Nationale de la Recherche (ANR-18-CE14-0017) and Fondation pour la Recherche Médicale (DEQ20150331732) (P.M.). J.P.R. was supported by a Dianna Trebble Endowment Fund Dental Institute Studentship, E.J.L. by the King's Bioscience Institute and the Guy's and St Thomas' Charity Prize PhD Programme in Biomedical and Translational Science, Y.K. by a Project Support Grant from the British Society for Neuroendocrinology. We thank Dr A.F. Parlow and the National

Hormone and Peptide Program (Harbor–University of California, Los Angeles Medical Center) for providing some of the antibodies used in this study and Prof. J. Drouin and Prof. S. Rhodes for TPIT and PIT1 antibodies respectively. We thank the High-Throughput Genomics Group at the Wellcome Trust Centre for Human Genetics (funded by Wellcome Trust grant reference 090532/Z/09/Z) for the generation of the Sequencing data. For flow sorting and analysis, this research was supported by the National Institute for Health Research (NIHR) Biomedical Research Centre based at Guy's and St Thomas' NHS Foundation Trust and King's College London. We thank Marie Isabelle Garcia, Juan Pedro Martinez-Barbera and Paul Le Tissier for useful discussions and critical comments on the manuscript.

REFERENCES

Alatzoglou, K.S., Andoniadou, C.L., Kelberman, D., Buchanan, C.R., Crolla, J., Arriazu, M.C., Roubicek, M., Moncet, D., Martinez-Barbera, J.P., and Dattani, M.T. (2011). SOX2 haploinsufficiency is associated with slow progressing hypothalamo-pituitary tumours. Human mutation *32*, 1376-1380.

Andoniadou, C.L., Gaston-Massuet, C., Reddy, R., Schneider, R.P., Blasco, M.A., Le Tissier, P., Jacques, T.S., Pevny, L.H., Dattani, M.T., and Martinez-Barbera, J.P. (2012). Identification of novel pathways involved in the pathogenesis of human adamantinomatous craniopharyngioma. Acta neuropathologica *124*, 259-271.

Andoniadou, Cynthia L., Matsushima, D., Mousavy Gharavy, Seyedeh N., Signore, M., Mackintosh, Albert I., Schaeffer, M., Gaston-Massuet, C., Mollard, P., Jacques, Thomas S., Le Tissier, P., *et al.* (2013). Sox2+ Stem/Progenitor Cells in the Adult Mouse Pituitary Support Organ Homeostasis and Have Tumor-Inducing Potential. Cell stem cell *13*, 433-445.

Arnold, K., Sarkar, A., Yram, M.A., Polo, J.M., Bronson, R., Sengupta, S., Seandel, M., Geijsen, N., and Hochedlinger, K. (2011). Sox2(+) adult stem and progenitor cells are important for tissue regeneration and survival of mice. Cell stem cell *9*, 317-329.

612 Azzolin, L., Panciera, T., Soligo, S., Enzo, E., Bicciato, S., Dupont, S., Bresolin, S.,
613 Frasson, C., Basso, G., Guzzardo, V., *et al.* (2014). YAP/TAZ Incorporation in the
614 beta-Catenin Destruction Complex Orchestrates the Wnt Response. Cell *158*, 157-
615 170.
616 Basham, K.J., Rodriguez, S., Turcu, A.F., Lerario, A.M., Logan, C.Y., Rysztak, M.R.,
617 Gomez-Sanchez, C.E., Breault, D.T., Koo, B.K., Clevers, H., *et al.* (2019). A ZNRF3-
618 dependent Wnt/beta-catenin signaling gradient is required for adrenal homeostasis.
619 Genes & development *33*, 209-220.
620 Bilodeau, S., Roussel-Gervais, A., and Drouin, J. (2009). Distinct developmental roles
621 of cell cycle inhibitors p57Kip2 and p27Kip1 distinguish pituitary progenitor cell
622 cycle exit from cell cycle reentry of differentiated cells. Molecular and cellular
623 biology *29*, 1895-1908.
624 Carbajo-Perez, E., and Watanabe, Y.G. (1990). Cellular proliferation in the anterior
625 pituitary of the rat during the postnatal period. Cell Tissue Res *261*, 333-338.
626 Carpenter, A.C., Rao, S., Wells, J.M., Campbell, K., and Lang, R.A. (2010).
627 Generation of mice with a conditional null allele for Wntless. Genesis *48*, 554-558.
628 Castinetti, F., Davis, S.W., Brue, T., and Camper, S.A. (2011). Pituitary stem cell
629 update and potential implications for treating hypopituitarism. Endocr Rev *32*, 453-
630 471.
631 Clevers, H., and Watt, F.M. (2018). Defining Adult Stem Cells by Function, not by
632 Phenotype. Annu Rev Biochem *87*, 1015-1027.
633 Cox, B., Laporte, E., Vennekens, A., Kobayashi, H., Nys, C., Van Zundert, I., Uji,
634 I.H., Vercauteren Drubbel, A., Beck, B., Roose, H., *et al.* (2019). Organoids from
635 pituitary as a novel research model toward pituitary stem cell exploration. The Journal
636 of endocrinology *240*, 287-308.
637 Davis, S.W., Mortensen, A.H., and Camper, S.A. (2011). Birthdating studies reshape
638 models for pituitary gland cell specification. Developmental biology *352*, 215-227.
639 Deschene, E.R., Myung, P., Rompolas, P., Zito, G., Sun, T.Y., Taketo, M.M.,
640 Saotome, I., and Greco, V. (2014). beta-Catenin activation regulates tissue growth
641 non-cell autonomously in the hair stem cell niche. Science (New York, NY) *343*,
642 1353-1356.
643 Doupe, D.P., Marshall, O.J., Dayton, H., Brand, A.H., and Perrimon, N. (2018).
644 Drosophila intestinal stem and progenitor cells are major sources and regulators of

645 homeostatic niche signals. Proceedings of the National Academy of Sciences of the
646 United States of America *115*, 12218-12223.
647 Fauquier, T., Rizzoti, K., Dattani, M., Lovell-Badge, R., and Robinson, I.C. (2008).
648 SOX2-expressing progenitor cells generate all of the major cell types in the adult
649 mouse pituitary gland. Proc Natl Acad Sci U S A *105*, 2907-2912.
650 Ferrer-Vaquer, A., Piliszek, A., Tian, G., Aho, R.J., Dufort, D., and Hadjantonakis,
651 A.K. (2010). A sensitive and bright single-cell resolution live imaging reporter of
652 Wnt/ss-catenin signaling in the mouse. BMC Dev Biol *10*, 121.
653 Gaston-Massuet, C., Andoniadou, C.L., Signore, M., Jayakody, S.A., Charolidi, N.,
654 Kyeyune, R., Vernay, B., Jacques, T.S., Taketo, M.M., Le Tissier, P., *et al.* (2011).
655 Increased Wingless (Wnt) signaling in pituitary progenitor/stem cells gives rise to
656 pituitary tumors in mice and humans. Proceedings of the National Academy of
657 Sciences of the United States of America *108*, 11482-11487.
658 Gonzalez-Meljem, J.M., Haston, S., Carreno, G., Apps, J.R., Pozzi, S., Stache, C.,
659 Kaushal, G., Virasami, A., Panousopoulos, L., Mousavy-Gharavy, S.N., *et al.* (2017).
660 Stem cell senescence drives age-attenuated induction of pituitary tumours in mouse
661 models of paediatric craniopharyngioma. Nature communications *8*, 1819.
662 Gregorieff, A., Liu, Y., Inanlou, M.R., Khomchuk, Y., and Wrana, J.L. (2015). Yap-
663 dependent reprogramming of Lgr5+ stem cells drives intestinal regeneration and
664 cancer. Nature *advance online publication*.
665 Gremeaux, L., Fu, Q., Chen, J., and Vankelecom, H. (2012). Activated phenotype of
666 the pituitary stem/progenitor cell compartment during the early-postnatal maturation
667 phase of the gland. Stem Cells Dev *21*, 801-813.
668 Haston, S., Pozzi, S., Carreno, G., Manshaei, S., Panousopoulos, L., Gonzalez-
669 Meljem, J.M., Apps, J.R., Virasami, A., Thavaraj, S., Gutteridge, A., *et al.* (2017).
670 MAPK pathway control of stem cell proliferation and differentiation in the embryonic
671 pituitary provides insights into the pathogenesis of papillary craniopharyngioma.
672 Development (Cambridge, England) *144*, 2141-2152.
673 Higuchi, M., Yoshida, S., Kanno, N., Mitsuishi, H., Ueharu, H., Chen, M., Nishimura,
674 N., Kato, T., and Kato, Y. (2017). Clump formation in mouse pituitary-derived non-
675 endocrine cell line Tpit/F1 promotes differentiation into growth-hormone-producing
676 cells. Cell Tissue Res *369*, 353-368.
677 Iwai-Liao, Y., Kumabe, S., Takeuchi, M., and Higashi, Y. (2000).
678 Immunohistochemical localisation of epidermal growth factor, transforming growth

679 factor alpha and EGF receptor during organogenesis of the murine hypophysis in
680 vivo. Okajimas Folia Anat Jpn *76*, 291-301.
681 Kelberman, D., de Castro, S.C., Huang, S., Crolla, J.A., Palmer, R., Gregory, J.W.,
682 Taylor, D., Cavallo, L., Faienza, M.F., Fischetto, R., *et al.* (2008). SOX2 plays a
683 critical role in the pituitary, forebrain, and eye during human embryonic development.
684 J Clin Endocrinol Metab *93*, 1865-1873.
685 Kim, D., Langmead, B., and Salzberg, S.L. (2015). HISAT: a fast spliced aligner with
686 low memory requirements. Nat Methods *12*, 357-360.
687 Levy, A. (2002). Physiological implications of pituitary trophic activity. The Journal
688 of endocrinology *174*, 147-155.
689 Liao, Y., Smyth, G.K., and Shi, W. (2014). featureCounts: an efficient general
690 purpose program for assigning sequence reads to genomic features. Bioinformatics
691 *30*, 923-930.
692 Lim, X., Tan, S.H., Koh, W.L., Chau, R.M., Yan, K.S., Kuo, C.J., van Amerongen,
693 R., Klein, A.M., and Nusse, R. (2013). Interfollicular epidermal stem cells self-renew
694 via autocrine Wnt signaling. Science (New York, NY) *342*, 1226-1230.
695 Lodge, E.J., Russell, J.P., Patist, A.L., Francis-West, P., and Andoniadou, C.L.
696 (2016). Expression Analysis of the Hippo Cascade Indicates a Role in Pituitary Stem
697 Cell Development. Frontiers in physiology *7*, 114.
698 Lodge, E.J., Santambrogio, A., Russell, J.P., Xekouki, P., Jacques, T.S., Johnson,
699 R.L., Thavaraj, S., Bornstein, S.R., and Andoniadou, C.L. (2019). Homeostatic and
700 tumourigenic activity of SOX2+ pituitary stem cells is controlled by the
701 LATS/YAP/TAZ cascade. eLife *8*.
702 Love, M.I., Huber, W., and Anders, S. (2014). Moderated estimation of fold change
703 and dispersion for RNA-seq data with DESeq2. Genome Biol *15*, 550.
704 Moiseenko, A., Kheirollahi, V., Chao, C.M., Ahmadvand, N., Quantius, J., Wilhelm,
705 J., Herold, S., Ahlbrecht, K., Morty, R.E., Rizvanov, A.A., *et al.* (2017). Origin and
706 characterization of alpha smooth muscle actin-positive cells during murine lung
707 development. Stem cells (Dayton, Ohio) *35*, 1566-1578.
708 Nabhan, A.N., Brownfield, D.G., Harbury, P.B., Krasnow, M.A., and Desai, T.J.
709 (2018). Single-cell Wnt signaling niches maintain stemness of alveolar type 2 cells.
710 Science (New York, NY) *359*, 1118-1123.

Nolan, L.A., Kavanagh, E., Lightman, S.L., and Levy, A. (1998). Anterior pituitary cell population control: basal cell turnover and the effects of adrenalectomy and dexamethasone treatment. J Neuroendocrinol *10*, 207-215.

Ohlstein, B., and Spradling, A. (2007). Multipotent Drosophila intestinal stem cells specify daughter cell fates by differential notch signaling. Science (New York, NY) *315*, 988-992.

Osmundsen, A.M., Keisler, J.L., Taketo, M.M., and Davis, S.W. (2017). Canonical WNT Signaling Regulates the Pituitary Organizer and Pituitary Gland Formation. Endocrinology *158*, 3339-3353.

Palma, V., Lim, D.A., Dahmane, N., Sanchez, P., Brionne, T.C., Herzberg, C.D., Gitton, Y., Carleton, A., Alvarez-Buylla, A., and Ruiz i Altaba, A. (2005). Sonic hedgehog controls stem cell behavior in the postnatal and adult brain. Development (Cambridge, England) *132*, 335-344.

Pardo-Saganta, A., Tata, P.R., Law, B.M., Saez, B., Chow, R.D., Prabhu, M., Gridley, T., and Rajagopal, J. (2015). Parent stem cells can serve as niches for their daughter cells. Nature *523*, 597-601.

Perez Millan, M.I., Brinkmeier, M.L., Mortensen, A.H., and Camper, S.A. (2016). PROP1 triggers epithelial-mesenchymal transition-like process in pituitary stem cells. eLife *5*.

Pevny, L., and Rao, M.S. (2003). The stem-cell menagerie. Trends Neurosci *26*, 351-359.

Potok, M.A., Cha, K.B., Hunt, A., Brinkmeier, M.L., Leitges, M., Kispert, A., and Camper, S.A. (2008). WNT signaling affects gene expression in the ventral diencephalon and pituitary gland growth. Developmental dynamics : an official publication of the American Association of Anatomists *237*, 1006-1020.

Rizzoti, K., Akiyama, H., and Lovell-Badge, R. (2013). Mobilized adult pituitary stem cells contribute to endocrine regeneration in response to physiological demand. Cell stem cell *13*, 419-432.

Roose, H., Cox, B., Boretto, M., Gysemans, C., Vennekens, A., and Vankelecom, H. (2017). Major depletion of SOX2(+) stem cells in the adult pituitary is not restored which does not affect hormonal cell homeostasis and remodelling. Sci Rep *7*, 16940.

Sarkar, A., Huebner, A.J., Sulahian, R., Anselmo, A., Xu, X., Flattery, K., Desai, N., Sebastian, C., Yram, M.A., Arnold, K., *et al.* (2016). Sox2 Suppresses Gastric Tumorigenesis in Mice. Cell reports *16*, 1929-1941.

Schindelin, J., Arganda-Carreras, I., Frise, E., Kaynig, V., Longair, M., Pietzsch, T., Preibisch, S., Rueden, C., Saalfeld, S., Schmid, B., *et al.* (2012). Fiji: an open-source platform for biological-image analysis. Nat Methods *9*, 676-682.

Schofield, R. (1978). The relationship between the spleen colony-forming cell and the haemopoietic stem cell. Blood Cells *4*, 7-25.

Subramanian, A., Tamayo, P., Mootha, V.K., Mukherjee, S., Ebert, B.L., Gillette, M.A., Paulovich, A., Pomeroy, S.L., Golub, T.R., Lander, E.S., *et al.* (2005). Gene set enrichment analysis: a knowledge-based approach for interpreting genome-wide expression profiles. Proceedings of the National Academy of Sciences of the United States of America *102*, 15545-15550.

Syed, S.M., Kumar, M., Ghosh, A., Tomasetig, F., Ali, A., Whan, R.M., Alterman, D., and Tanwar, P.S. (2020). Endometrial Axin2(+) Cells Drive Epithelial Homeostasis, Regeneration, and Cancer following Oncogenic Transformation. Cell stem cell *26*, 64-80 e13.

Takase, H.M., and Nusse, R. (2016). Paracrine Wnt/beta-catenin signaling mediates proliferation of undifferentiated spermatogonia in the adult mouse testis. Proceedings of the National Academy of Sciences of the United States of America *113*, E1489-1497.

Takeo, M., Chou, W.C., Sun, Q., Lee, W., Rabbani, P., Loomis, C., Taketo, M.M., and Ito, M. (2013). Wnt activation in nail epithelium couples nail growth to digit regeneration. Nature *499*, 228-232.

Tan, D.W., and Barker, N. (2014). Intestinal stem cells and their defining niche. Current topics in developmental biology *107*, 77-107.

Taniguchi, Y., Yasutaka, S., Kominami, R., and Shinohara, H. (2002). Mitoses of thyrotrophs contribute to the proliferation of the rat pituitary gland during the early postnatal period. Anat Embryol (Berl) *206*, 67-72.

Tata, P.R., and Rajagopal, J. (2016). Regulatory Circuits and Bi-directional Signaling between Stem Cells and Their Progeny. Cell stem cell *19*, 686-689.

Trapnell, C., Roberts, A., Goff, L., Pertea, G., Kim, D., Kelley, D.R., Pimentel, H., Salzberg, S.L., Rinn, J.L., and Pachter, L. (2012). Differential gene and transcript expression analysis of RNA-seq experiments with TopHat and Cufflinks. Nat Protoc *7*, 562-578.

van Amerongen, R., Bowman, A.N., and Nusse, R. (2012). Developmental stage and time dictate the fate of Wnt/beta-catenin-responsive stem cells in the mammary gland. Cell stem cell *11*, 387-400.

Vidal, V., Sacco, S., Rocha, A.S., da Silva, F., Panzolini, C., Dumontet, T., Doan, T.M., Shan, J., Rak-Raszewska, A., Bird, T., *et al.* (2016). The adrenal capsule is a signaling center controlling cell renewal and zonation through Rspo3. Genes & development *30*, 1389-1394.

Wang, B., Zhao, L., Fish, M., Logan, C.Y., and Nusse, R. (2015). Self-renewing diploid Axin2(+) cells fuel homeostatic renewal of the liver. Nature *524*, 180-185.

Wang, L., Wang, S., and Li, W. (2012). RSeQC: quality control of RNA-seq experiments. Bioinformatics *28*, 2184-2185.

Willems, C., Fu, Q., Roose, H., Mertens, F., Cox, B., Chen, J., and Vankelecom, H. (2016). Regeneration in the Pituitary After Cell-Ablation Injury: Time-Related Aspects and Molecular Analysis. Endocrinology *157*, 705-721.

Xekouki, P., Lodge, E.J., Matschke, J., Santambrogio, A., Apps, J.R., Sharif, A., Jacques, T.S., Aylwin, S., Prevot, V., Li, R., *et al.* (2018). Non-secreting pituitary tumours characterised by enhanced expression of YAP/TAZ. Endocrine-related cancer.

Xekouki, P., Lodge, E.J., Matschke, J., Santambrogio, A., Apps, J.R., Sharif, A., Jacques, T.S., Aylwin, S., Prevot, V., Li, R., *et al.* (2019). Non-secreting pituitary tumours characterised by enhanced expression of YAP/TAZ. Endocrine-related cancer *26*, 215-225.

Yan, K.S., Janda, C.Y., Chang, J., Zheng, G.X.Y., Larkin, K.A., Luca, V.C., Chia, L.A., Mah, A.T., Han, A., Terry, J.M., *et al.* (2017). Non-equivalence of Wnt and R-spondin ligands during Lgr5(+) intestinal stem-cell self-renewal. Nature *545*, 238-242.

Yoshida, S., Kato, T., Higuchi, M., Chen, M., Ueharu, H., Nishimura, N., and Kato, Y. (2015). Localization of juxtacrine factor ephrin-B2 in pituitary stem/progenitor cell niches throughout life. Cell Tissue Res *359*, 755-766.

Yoshida, S., Kato, T., Kanno, N., Nishimura, N., Nishihara, H., Horiguchi, K., and Kato, Y. (2017). Cell type-specific localization of Ephs pairing with ephrin-B2 in the rat postnatal pituitary gland. Cell Tissue Res *370*, 99-112.

Zhu, X., Tollkuhn, J., Taylor, H., and Rosenfeld, M.G. (2015). Notch-Dependent Pituitary SOX2(+) Stem Cells Exhibit a Timed Functional Extinction in Regulation of the Postnatal Gland. Stem Cell Reports *5*, 1196-1209.

FIGURES

Figure 1. *Axin2* expressing cells contribute to pituitary growth and expansion of all lineages

A. Immunofluorescence staining against GFP (green) with markers of PSCs or lineage commitment (magenta) in *Axin2*$^{CreERT2/+}$*; ROSA26*$^{mTmG/+}$ pituitaries harvested from mice induced at P14 and lineage traced for 2 days (top panel) and 14 days (bottom panel). Scale bar 10μm.

B. Quantification of lineage expansion between 2 and 14 days following induction at P14. Graph shows that the proportion of lineage committed cells (either PIT1^{+}, TPIT^{+} or SF1^{+}) and PSCs (SOX2^{+}), i.e. that are transcription factor (TF)$^{+}$ cells that are GFP^{+} increases between 2 days (black bars) and 14 days (grey bars) post induction. PIT1 P=0.000004, TPIT P=0.008 multiple t-tests. n=4 animals per time point.

C. Immunofluorescence staining against GFP (green) in pituitaries harvested from *Axin2*$^{CreERT2/+}$*;ROSA26*$^{mTmG/+}$ mice induced at P14 and lineage traced for 2 days, 2 weeks and 8 weeks. Bottom panel shows magnified fields of view of regions of interest indicated by white boxes in panels above. Scale bars 50μm.

D. Top panel showing the quantification of the proportion of all cells in *Axin2*$^{CreERT2/+}$*;ROSA26*$^{mTmG/+}$ pituitaries that are GFP^{+} at 2, 7, 14, 28 and 56 days

post induction as analysed by flow cytometry. Day 2 to 7 $P<0.0001$ unpaired *t*-test. Data points show individual measurements from biological replicates, $n=4$-8 pituitaries per time point. (Bottom) Graph of the absolute number of GFP+ cells (green) and as a proportion of total cells (blue) at the time points indicated.

E. X-gal staining in $Axin2^{CreERT2/+};ROSA26^{LacZ/+}$ pituitaries harvested from mice induced at P14 and lineage traced for 8 weeks (left) and 1 year (right). Scale bars 500μm.

F. Model summarising the major contribution of WNT-responsive progenitors of all lineages to pituitary growth, in addition to that of $SOX2^{+}$ PSCs.

Figure 2. Activation of WNT signalling in SOX2^{+} PSCs and their descendants is necessary for long-term growth

A. Schematic of the experimental timeline used in panels A and B. Endogenous expression of tdTomato (magenta, *Axin2* targeted cells) and EGFP (green, *Sox2* expressing cells) in *Axin2*$^{CreERT2/+}$;*Sox2*$^{Egfp/+}$;*ROSA26*$^{tdTomato/+}$ pituitaries harvested at P24 sectioned in the frontal plane. Nuclei are counterstained with Hoechst in the merged panel. Scale bar 50μm.

B. A representative culture plate showing colonies derived from Tomato^{+}, EGFP^{+} or Tomato^{+};EGFP^{+} cells that were isolated from *Axin2*$^{CreERT2/+}$;*Sox2*$^{Egfp/+}$;*ROSA26*$^{tdTomato/+}$ pituitaries by FACS plated in stem cell promoting media at clonogenic densities and stained with crystal violet (left panel). The proportion of colony-forming cells in each subpopulation were quantified by counting the number of colonies per well (right panel). Each data point indicates individual wells, n=5 separate pituitaries. P=0.0226, Mann-Whitney U test (two-tailed). Scale bar 10mm.

C. Immunofluorescence staining against SOX2 (green) and Ki-67 (magenta) in *Sox2*$^{+/+}$*Ctnnb1*$^{LOF/LOF}$ (control) and *Sox2*$^{CreERT2/+}$*Ctnnb1*$^{LOF/LOF}$ (mutant) pituitaries from mice induced at P14 and analysed 22 weeks after induction (at P168) (bottom panel). Scale bar 50μm.

D. Dorsal view of whole mount pituitaries of *Sox2*$^{+/+}$;*Ctnnb1*$^{LOF/LOF}$ (control) and *Sox2*$^{CreERT2/+}$;*Ctnnb1*$^{LOF/LOF}$ (mutant), 22 weeks after induction (i.e. P168). Scale bars 1mm.

E. Model summarising the effect of *Ctnnb1* deletion in SOX2^{+} PSCs.

PL, posterior lobe; IL, intermediate lobe; AL, anterior lobe.

Figure 3. SOX2^{+} PSCs are as a source of WNT ligands in the pituitary

A. Immunofluorescence staining against GFP (green) and SOX2 (magenta) in *Axin2$^{CreERT2/+}$; ROSA26$^{mTmG/+}$* pituitaries 48 hours post induction. Graph representing a quantification of the proximity of individual GFP^{+} cells to the nearest SOX2^{+} cell as quantified by the number of nuclei separating them. Plotted data represents the proportion of GFP+ cells that fall in to each category of the total GFP+ cells, taken from *n*=3 separate pituitaries. Scale bars 50μm.

B. Experimental paradigm for RNA Seq analysis of *Sox2* positive and negative cells.

C. Graphs representing the FPKM values of *Wls* and *Porcupine* in *Sox2* positive and negative cells (black and grey bars, respectively). mRNA in situ hybridisation for *Sox2* and for *Wls* on wild type sagittal pituitaries at P14, demonstrating strong *Wls* expression in the marginal zone epithelium. Scale bars 250μm.

D. Bar chart showing the FPKM values of *Wnt* genes in the *Sox2+* and *Sox2-* fractions. Double mRNA in situ hybridisation against *Wnt2*, *Wnt5a* and *Wnt9a* (blue) together with *Sox2* (red) validating expression in the *Sox2+* population. Boxed regions through the marginal zone epithelium are magnified. Scale bars 100μm and 50μm in boxed inserts.

Figure 4. Paracrine secretion of WNTs from SOX2$^+$ PSCs is necessary for expansion of committed cells

A. Immunofluorescence staining against SOX2 (green) and Ki-67 (magenta) in *Sox2*$^{+/+}$;*Wls*$^{fl/fl}$ (control) and *Sox2*$^{CreERT2/+}$;*Wls*$^{fl/fl}$ (mutant) pituitaries induced from P14 and analysed after one week. Nuclei were counterstained with Hoechst. (i) and (ii) represent magnified fields of view of regions indicated by white boxes in top panels. Scale bars 50μm. Graph of quantification of cycling cells marked by Ki-67 among cells negative for SOX2. Values represent mean +/- SEM, *P*=0.0008, unpaired *t*-test. Graph of quantification of cycling cells marked by Ki-67 among SOX2-positive cells. Values represent mean +/- SEM, *P*=0.0121, unpaired *t*-test. Each data point shows the mean of one biological replicate, *n*=4 pituitaries from controls and 5 pituitaries from mutants.

B. Double mRNA in situ hybridisation using specific probes against *Lef1* (blue) and *Sox2* (red) in control and mutant pituitaries following tamoxifen induction from P14 and tracing for 7 days. Scale bars 250μm and 50μm in boxed regions.

C. Model summarising paracrine WNT secretion from SOX2$^+$ PSCs to lineage-committed progenitors and the effects of abolishing WNT secretion from SOX2$^+$ PSCs through the deletion of *Wls*.

SUPPLEMENTARY INFORMATION

Supplementary File 1. Gene lists of Gene Set Enrichment Analyses

Gene lists generated from Gene Set Enrichment Analyses of bulk RNA-sequencing data comparing *Sox2*$^{+}$ and *Sox2*$^{-}$ cells. Associated with Figure 3 – figure supplement 1.

SUPPLEMENARY FIGURES

Figure 1 – figure supplement 1. *Axin2* expressing cells contribute to pituitary growth and expansion of all lineages

A. Schematic of the combined experimental timeline used in panels A, B and C. Immunofluorescence staining against GFP (green) and markers of hormone-secreting endocrine cells (GH (somatotrophs), ACTH (corticotrophs), PRL (lactotrophs), TSH (thyrotrophs), FSH/LH (gonadotrophs)) in *Axin2*$^{CreERT2/+}$*;Rosa26*$^{mTmG/+}$ pituitaries induced at P14 and lineage traced for 48 hours. Scale bar 10μm.

B. Graph of quantification of expansion of the WNT-responsive SF1^{+} population in *Axin2*$^{CreERT2/+}$*;ROSA26*$^{mTmG/+}$ pituitaries induced at P14 and lineage traced for 2 or 28 days. There is a significant increase of GFP^{+};SF1^{+} cells as a proportion of the total SF1^{+} cells at P28. P=0.0048, unpaired t-test (n=2 at 2 days, 3 at 28 days).

C. Immunofluorescence staining against GFP (green) and markers of hormone-secreting endocrine cells of the PIT1 lineage (GH (somatotrophs), PRL (lactotrophs), TSH (thyrotrophs)) in *Axin2*$^{CreERT2/+}$*;ROSA26*$^{mTmG/+}$ pituitaries induced at P14 and lineage traced for 14 days. Scale bars 50μm. Graph showing expansion of each of the Hormone^{+} cell types (Hormone^{+};GFP^{+}) as a percentage of the total Hormone^{+} population between 2 and 14 days post-induction. There is

a significant increase in GH^+ somatotrophs (P=0.000548), and TSH^+ thyrotrophs (P=0.0016), whilst there is no significance (ns) between PRL^+ lactotroph populations between the two time points. multiple *t*-test (n=3 at 48 h, n=4 at 14 days post-induction).

D. Clonal analysis of individual cells targeted in *Sox2*$^{CreERT2/+}$;*ROSA26*$^{Confetti/+}$ (left panel) and *Axin2*$^{CreERT2/+}$;*ROSA26*$^{Confetti/+}$ pituitaries (right panel), induced at P14 and harvested after 4 weeks (P42). Arrows point to individual clones, numbered for the number of cells in the clone. Scale bar 100µm.

Figure 1 – figure supplement 2. *Axin2* expressing cells contribute to pituitary growth and expansion of all lineages

A. Dorsal wholemount view of *Axin2*$^{CreERT2/+}$; *Ctnnb1*$^{LOF/+}$;*ROSA26*$^{mTmG/+}$and *Axin2*$^{CreERT2/+}$; *Ctnnb1*$^{LOF/LOF}$;*ROSA26*$^{mTmG/+}$ pituitaries induced at P14 and lineage traced for 5 days. Scale bars 500µm. Immunofluorescence staining against GFP (green) and pH-H3 (magenta) in *Axin2*$^{CreERT2/+}$; *Ctnnb1*$^{LOF/+}$;*ROSA26*$^{mTmG/+}$and *Axin2*$^{CreERT2/+}$; *Ctnnb1*$^{LOF/LOF}$;*ROSA26*$^{mTmG/+}$ pituitaries. Scale bar 50µm. Quantification of the contribution of lineage traced cells in control and mutants. Each data point represents the mean from one individual. P=0.0313, unpaired *t*-test (n=3).

B. Immunofluorescence staining against GFP (green) and PIT1, SF1 and ACTH (magenta) in *Axin2*$^{CreERT2/+}$; *Ctnnb1*$^{LOF/+}$;*ROSA26*$^{mTmG/+}$and *Axin2*$^{CreERT2/+}$;*Ctnnb1*$^{LOF/LOF}$;*ROSA26*$^{mTmG/+}$ pituitaries induced at P14 and lineage traced for 5 days. Quantification of the percentage of GFP^+ cells, double-positive for each of the lineage markers, showing no significant changes for each lineage

between controls and mutants (Unpaired *t*-test, PIT1 P=0.1729, SF1 P=0.9488, ACTH P=0.6186. n=4 controls, 2 mutants). Scale bars 50μm.

C. Immunofluorescence against GFP (green) and SOX2 (magenta) in $Axin2^{CreERT2/+}$; $Ctnnb1^{LOF/+}$;$ROSA26^{mTmG/+}$ and $Axin2^{CreERT2/+}$;$Ctnnb1^{LOF/LOF}$;$ROSA26^{mTmG/+}$ induced at P14 and lineage traced for 5 days (n=4 controls, 2 mutants). Scale bars 50μm.

D. Immunofluorescence against GFP (green) and Cleaved Caspase-3 (magenta) in $Axin2^{CreERT2/+}$; $Ctnnb1^{LOF/+}$;$ROSA26^{mTmG/+}$ and $Axin2^{CreERT2/+}$;$Ctnnb1^{LOF/LOF}$;$ROSA26^{mTmG/+}$ induced at P14 and lineage traced for 5 days (n=4 controls, 2 mutants). Scale bars 50μm.

Figure 2 – figure supplement 1. Activation of WNT signalling in SOX2$^+$ PSCs and their descendants is necessary for long-term growth

A-E Step-wise gating strategy to isolate WNT-responsive, SOX2-EGFP$^+$ cells by flow sorting.

A – B Single pituitary cells dissociated from *Axin2$^{CreERT2/+}$;ROSA26$^{tdTomato/+}$;Sox2$^{eGFP/+}$* mice were gated to exclude debris (A) and gated for single cells according to SSC-A and SSC-W (B).

C. Dead cells were excluded according to incorporation of DAPI.

D. Three populations of fluorescent cells were identified and sorted according to the following profiles: GFP$^-$;tdTomato$^+$, GFP$^+$;tdTomato$^+$ or GFP$^+$;tdTomato$^-$.

E. Quantification of the number of GFP$^+$ cells out of all gated cells (left, *n*=5 biological repeats), the proportion of all GFP$^+$ cells that were found to be tdTomato$^+$ (right, *n*=5 biological repeats) and a representation of the gating used for quantification (bottom).

Figure 2 – figure supplement 2. Activation of WNT signalling in SOX2$^+$ PSCs and their descendants is necessary for long-term growth

A. Confocal images of native GFP fluorescence in frontal sections from TCF/Lef:H2B-EGFP pituitaries at P21. Scale bar 50μm.

B. mRNA *in situ* hybridisation in TCF/Lef:H2B-EGFP pituitaries at P21, detecting *Egfp* transcripts (red). Double mRNA *in situ* hybridisation showing overlap between *Sox2* (red) and *Egfp* (blue) transcripts in pituitaries at P21. White arrowheads indicate double-positive staining. Scale bars 50μm.

C. Immunofluorescence staining against SOX2 (magenta) and GFP (green) in TCF/Lef:H2B-EGFP pituitaries harvested from P21 mice. White arrows indicate

994 double positive cells. Graph of quantification of the *in vitro* colony forming
995 potential of GFP cells isolated from P21 TCF/Lef:H2B-EGFP pituitaries by flow
996 sorting. Each data point represents single well replicates. Error bars show SEM,
997 $P<0.001$ (One-way ANOVA, $n=3$ individual pituitaries). Scale bar 50μm.
998 Representative scatter plot showing gating used for fluorescence activated cell
999 sorting and population percentages in each gate.
1000 D. Immunofluorescence staining against PIT1, TPIT and SF1 (magenta) in
1001 $Sox2^{CreERT2/+};Ctnnb1^{LOF/+};ROSA26^{mTmG/+}$ and
1002 $Sox2^{CreERT2/+};Ctnnb1^{LOF/LOF};ROSA26^{mTmG/+}$ pituitaries 22 weeks post-induction at
1003 P14 (age P24). Arrows indicate double positive cells. Scale bar 50μm.
1004 E. Immunofluorescence staining against β-catenin (magenta) and GFP (green) in
1005 $Sox2^{CreERT2/+}$; $Ctnnb1^{LOF/+};ROSA26^{mTmG/+}$ and $Sox2^{CreERT2/+}$;
1006 $Ctnnb1^{LOF/LOF};ROSA26^{mTmG/+}$ pituitaries 22 weeks post-induction. Arrowheads
1007 indicate double positive cells, arrows indicate GFP^+ cells that have lost β-catenin
1008 expression in mutants. Scale bar 50μm.
1009 PL, posterior lobe; IL, Intermediate lobe; AL, anterior lobe; Inf, infundibulum; RP,
1010 Rathke's pouch; Sph, sphenoid bone.
1011

Figure 3 – figure supplement 1. SOX2^{+} PSCs are as a source of WNT ligands in the pituitary

A. Native EGFP protein expression in frontal cryosection of a P14 *Sox2$^{Egfp/+}$* pituitary. Schematic of the workflow used for bulk RNA-sequencing analysis of *Sox2^{+}* and *Sox2^{-}* cells. Genome browser views of reads aligning to the *Sox2* and *Pit1* loci in the positive and negative fractions indicating good separation of the EGFP^{+} population. Scale bar 50µm.

B. *Sox2^{+}* cells express a significant enrichment in markers associated with epithelial-to-mesenchymal transition (EMT), adherens and tight junctions, consistent with their epithelial nature. GSEA plots and immunofluorescence staining against E-Cadherin (adherens junction marker) and ZO1 (tight junction marker) in the marginal zone epithelium at P14. Scale bar 50µm. See Supplementary File 1 for full GSEA gene lists.

C. *Sox2^{+}* cells express a significant enrichment in several signalling pathways, shown with respective GSEA plots. See Supplementary File 1 for full GSEA gene lists.

D. Bar charts showing the FPKM values of components of the LGR/RNF43/ZNRF3/RSPONDIN module in the *Sox2+* and *Sox2-* fractions and the distribution of the Frizzled receptors. GSEA plot for components of the WNT pathway. Validation of sequencing: (i) mRNA *in situ* hybridisation with specific probes against *Lgr4* (blue) and *Sox2* (red) in P14 pituitaries showing co-expression. (ii) Double mRNA in situ hybridisation against *Fzd4* (blue) and *Sox2* (red) indicating co-expression in both the marginal zone epithelium and parenchymal *Sox2^{+}* cells. Boxed regions are magnified. Scale bars 250µm and 50µm in boxed inserts. (iii) mRNA in situ hybridisation against *Rspo1, Rspo2, Rspo3* and *Rspo4* in sagittal sections of wild type pituitaries at P14. Boxed regions

1037 are magnified, only *Rspo4* is detected. Scale bars 250μm and 100μm in boxed

1038 inserts.

1039

Figure 4 – figure supplement 1. Paracrine secretion of WNTs from SOX2^{+} PSCs is necessary for expansion of committed cells

A. Schematic of time points for induction by tamoxifen induction and tissue harvesting of control *Sox2*$^{+/+}$*;Wls*$^{fl/fl}$ and mutant *Sox2*$^{CreERT2/+}$*;Wls*$^{fl/fl}$ pituitaries.

B. Whole mount, dorsal views of control *Sox2*$^{+/+}$*;Wls*$^{fl/fl}$ (top panel) and mutant *Sox2*$^{CreERT2/+}$*;Wls*$^{fl/fl}$ (bottom panel) pituitaries at P21, representative of *n*=4 controls and *n*=5 mutants. Scale bars 500μm.

Key Resources Table				
Reagent type (species) or resource	**Designation**	**Source or reference**	**Identifiers**	**Additional information**
genetic reagent (*Mus musculus*)	*Axin2*$^{CreERT2/+}$	Roel Nusse, Stanford University The Jackson Laboratory	JAX:018867, RRID:IMSR_JAX:018867	
genetic reagent (*Mus musculus*)	*Sox2*$^{CreERT2/+}$	(Andoniadou et al. 2013) PMID: 24094324 DOI: 10.1016/j.stem.2013.07.004	MGI:5512893	
genetic reagent (*Mus musculus*)	*ROSA26*$^{mTmG/mTmG}$	The Jackson Laboratory	JAX:007676, RRID:IMSR_JAX:007676	
genetic reagent (*Mus musculus*)	*ROSA26*$^{Confetti/Confetti}$	The Jackson Laboratory	JAX:017492, RRID:IMSR_JAX:017492	
genetic reagent (*Mus musculus*)	*ROSA26*$^{tdTomato/tdTomato}$	The Jackson Laboratory	JAX:007909, RRID:IMSR_JAX:007909	
genetic reagent (*Mus musculus*)	*Ctnnb1*$^{fl(ex2-6)/fl(ex2-6)}$ (*Ctnnb*$^{LOF/LOF}$)	The Jackson Laboratory	JAX:004152, RRID:IMSR_JAX:004152	
genetic reagent (*Mus musculus*)	*Wls*$^{fl/fl}$	The Jackson Laboratory	JAX:012888, RRID:IMSR_JAX:012888	
genetic reagent (*Mus musculus*)	*Sox2*$^{eGFP/+}$	(Ellis et al., 2004) PMID:	MGI:3589809	

		15711057 DOI: 10.1159/000082134		
genetic reagent (*Mus musculus*)	TCF/Lef:H2B-GFP	The Jackson Laboratory	JAX:013752, RRID:IMSR_JAX:013752	
cell line (*Mus musculus*)	Primary anterior pituitary cells	This paper	N/A	Freshly isolated from *Mus musculus*.
antibody	Anti-GFP, (Chicken Polyclonal)	Abcam	ab13970, RRID:AB_300798	IF(1:400)
antibody	Anti-SOX2, (Goat Polyclonal)	Immune Systems Ltd	GT15098, RRID:AB_2195800	IF(1:200)
antibody	Anti-SOX2, (Rabbit Monoclonal)	Abcam	ab92494, RRID:AB_10585428	IF(1:100)
antibody	Anti-SOX9, (Rabbit Monoclonal)	Abcam	ab185230, RRID:AB_2715497	IF(1:500)
antibody	Anti-POU1F1 (PIT1), (Rabbit Monoclonal)	Gifted by Dr S. J. Rhodes (IUPUI, USA)	422_Rhodes, RRID:AB_2722652	IF(1:500)
antibody	Anti-SF1 (NR5A1, clone N1665), (Mouse Monoclonal)	Thermo Fisher Scientific	434200, RRID:AB_2532209	IF(1:300)
antibody	Anti-TBX19 (TPIT), (Rabbit Polyclonal)	Gifted by Dr J. Drouin (Montreal Clinical Research Institute, Canada)	Ac1250 #71, RRID:AB_2728662	IF(1:200)

antibody	Anti-Ki67, (Rabbit Monoclonal)	Abcam	ab15580, RRID:AB_443209	IF(1:100)
antibody	Anti-pH-H3, (Rabbit Polyclonal)	Abcam	ab5176, RRID:AB_304763	IF(1:500)
antibody	Anti-GH, (Rabbit Polyclonal)	National Hormone and Peptide Program (NHPP)	AFP-5641801	IF(1:1000)
antibody	Anti-TSH, (Rabbit Polyclonal)	National Hormone and Peptide Program (NHPP)	AFP-1274789	IF(1:1000)
antibody	Anti-PRL, (Rabbit Polyclonal)	National Hormone and Peptide Program (NHPP)	AFP-4251091	IF(1:1000)
antibody	Anti-ACTH, (Mouse Monoclonal)	Fitzgerald	10C-CR1096M1, RRID:AB_1282437	IF(1:400)
antibody	Anti-LH, (Rabbit Polyclonal)	National Hormone and Peptide Program (NHPP)	AFP-697071P	IF(1:300)
antibody	Anti-FSH, (Rabbit Polyclonal)	National Hormone and Peptide Program (NHPP)	AFP-HFS6	IF(1:300)
antibody	Anti-ZO-1, (Rat Monoclonal)	Santa Cruz	SC33725, RRID:AB_628459	IF(1:300)

antibody	Anti-E-CADHERIN, (Rabbit Monoclonal)	Cell Signaling	3195S, RRID:AB_2291471	IF(1:300)
antibody	Anti-Rabbit 488, (Goat Polyclonal)	Life Technologies	A11008, RRID:AB_143165	IF(1:400)
antibody	Anti-Rabbit 555, (Goat Polyclonal)	Life Technologies	A21426, RRID:AB_1500929	IF(1:400)
antibody	Anti-Rabbit 633, (Goat Polyclonal)	Life Technologies	A21050, RRID:AB_141431	IF(1:400)
antibody	Anti-Goat 488, (Donkey Polyclonal)	Abcam	ab150133, RRID:AB_2832252	IF(1:400)
antibody	Anti-Chicken 488, (Goat Polyclonal)	Life Technologies	A11039, RRID:AB_142924	IF(1:400)
antibody	Anti-Chicken 647, (Goat Polyclonal)	Life Technologies	A21449, RRID:AB_1500594	IF(1:400)
antibody	Anti-Rat 555, (Goat Polyclonal)	Life Technologies	A21434, RRID:AB_141733	IF(1:400)
antibody	Anti-Mouse 555, (Goat Polyclonal)	Life Technologies	A21426, RRID:AB_1500929	IF(1:400)
antibody	Anti-Rabbit Biotinylated, (Donkey Polyclonal)	Abcam	ab6801, RRID:AB_954900	IF(1:400)

antibody	Anti-Rabbit Biotinylated, (Goat Polyclonal)	Abcam	ab207995	IF(1:400)
antibody	Anti-Mouse Biotinylated, (Goat Biotinylated)	Abcam	ab6788, RRID:AB_954885	IF(1:400)
sequence-based reagent	RNAscope probe *M.musculus Axin2*	Advanced Cell Diagnostics	400331	
sequence-based reagent	RNAscope probe *M.musculus Lef1*	Advanced Cell Diagnostics	441861	
sequence-based reagent	RNAscope probe *M.musculus Wls*	Advanced Cell Diagnostics	405011	
sequence-based reagent	RNAscope probe *M.musculus Rspo1*	Advanced Cell Diagnostics	401991	
sequence-based reagent	RNAscope probe *M.musculus Rspo2*	Advanced Cell Diagnostics	402001	
sequence-based reagent	RNAscope probe *M.musculus Rspo3*	Advanced Cell Diagnostics	402011	
sequence-based reagent	RNAscope probe *M.musculus Rspo4*	Advanced Cell Diagnostics	402021	
sequence-based reagent	RNAscope probe *M.musculus Lgr4*	Advanced Cell Diagnostics	318321	

sequence-based reagent	RNAscope probe *M.musculus Wnt9a*	Advanced Cell Diagnostics	405081	
sequence-based reagent	RNAscope probe *M.musculus Wnt2*	Advanced Cell Diagnostics	313601	
sequence-based reagent	RNAscope probe *M.musculus Wnt5a*	Advanced Cell Diagnostics	316791	
sequence-based reagent	RNAscope probe *eGFP*	Advanced Cell Diagnostics	400281	
sequence-based reagent	RNAscope probe *M.musculus Jun*	Advanced Cell Diagnostics	453561	
sequence-based reagent	RNAscope probe *M.musculus Axin2* (Channel 2)	Advanced Cell Diagnostics	400331-C2	
sequence-based reagent	RNAscope probe *M.musculus Sox2* (Channel 2)	Advanced Cell Diagnostics	401041-C2	
sequence-based reagent	RNAscope probe *eGFP* (Channel 2)	Advanced Cell Diagnostics	400281-C2	
sequence-based reagent	RNAscope probe *M.musculus Sox2*	Advanced Cell Diagnostics	401041	
sequence-based reagent	RNAscope probe *M.musculus Pou1f1*	Advanced Cell Diagnostics	486441	

sequence-based reagent	RNAscope probe Duplex Positive Control *Ppib-C1, Polr2a-C2*	Advanced Cell Diagnostics	321641	
sequence-based reagent	RNAscope probe Duplex Negative Control *DapB* (both channels)	Advanced Cell Diagnostics	320751	
sequence-based reagent	RNAscope probe Singleplex Positive Control *Ppib*	Advanced Cell Diagnostics	313911	
sequence-based reagent	RNAscope probe: Singleplex Negative Control *DapB*	Advanced Cell Diagnostics	310043	
peptide, recombinant protein	Streptavidin 488	Life Technologies	S11223	IF(1:400)
peptide, recombinant protein	Streptavidin 555	Life Technologies	S32355	IF(1:400)
peptide, recombinant protein	Streptavidin 633	Life Technologies	S21375	IF(1:400)
commercial assay or kit	RNAScope 2.5 HD Assay -RED	Advanced Cell Diagnostics	322350	
commercial assay or kit	RNAScope 2.5 HD Duplex Assay	Advanced Cell Diagnostics	322430	
commercial assay or kit	LIVE/DEAD Fixable Near IR-Dead Cell	Life Technologies	L34975	

	Stain Kit			
commercial assay or kit	FIX and PERM Cell Permeabilization Kit	Life Technologies	GAS003	
chemical compound, drug	Tamoxifen	Sigma	T5648	
chemical compound, drug	Corn Oil	Sigma	C8267	
chemical compound, drug	Collagenase Type 2	Worthington	4178	
chemical compound, drug	10X Trypsin	Sigma	59418C	
chemical compound, drug	Deoxyribonuclease I	Worthington	LS002172	
chemical compound, drug	Fungizone	Gibco	15290	
chemical compound, drug	Hank’s Balanced Salt Solution (HBSS)	Gibco	14170	
chemical compound, drug	Fetal Bovine Serum	Sigma	F2442	
chemical compound, drug	HEPES	Thermo Fisher	15630	

chemical compound, drug	bFGF	R&D Systems	233-FB-025	
chemical compound, drug	Cholera Toxin	Sigma	C8052	
chemical compound, drug	DMEM-F12	Thermo Fisher	31330	
chemical compound, drug	Penicillin/Streptomycin	Gibco	15070-063	
chemical compound, drug	Neutral Buffered Formalin	Sigma	HT501128	
chemical compound, drug	Hoechst 33342	Thermo Fisher	H3570	1:1000
chemical compound, drug	Declere	Sigma	D3565	
chemical compound, drug	Neo-Clear	Sigma	65351-M	
software, algorithm	FlowJo	FlowJo, LLC	https://www.flowjo.com/ RRID:SCR_008520	
software, algorithm	Prism 7	GraphPad Software	https://www.graphpad.com/	

software, algorithm	Image Lab	Bio-Rad Laboratories	http://www.bio-rad.com/	
software, algorithm	NDP View	Hamamatsu Photonics	https://www.hamamatsu.com/	
software, algorithm	HISAT v2.0.3	(Kim, Langmead, & Salzberg, 2015)	https://github.com/infphilo/hisat2 RRID:SCR_015530	
software, algorithm	DESeq2 v2.11.38	(Love, Huber, & Anders, 2014)	https://github.com/Bioconductor-mirror/DESeq2 RRID:SCR_015687	
software, algorithm	featureCounts v1.4.6p5	(Liao, Smyth, & Shi, 2014)	http://subread.sourceforge.net/ RRID:SCR_012919	
software, algorithm	The Galaxy Platform	(Afgan et al., 2016; Blankenberg et al., 2010; Goecks, Nekrutenko, & Taylor, 2010)	https://usegalaxu.org RRID:SCR_006281	
software, algorithm	Gene Set Enrichment Analysis (GSEA)	(Subramanian et al, 2005)	software.broadinstitute.org/gsea/index.jsp RRID:SCR_003199	

software, algorithm	Cufflinks	(Trapnell et al., 2012)	https://github.com/cole-trapnell-lab/cufflinks RRID:SCR_014597	
other	Deposited Data, RNA-Seq	BioProject (NCBI)	PRJNA421806	

1

A

P14 + 2 days

α-GFP/α-SOX2 | α-GFP/α-PIT1 | α-GFP/α-TPIT | α-GFP/α-SF1

P14 + 14 days

α-GFP/α-SOX2 | α-GFP/α-PIT1 | α-GFP/α-TPIT | α-GFP/α-SF1

Axin2$^{CreERT2/+}$;*ROSA26*$^{mTmG/+}$

B

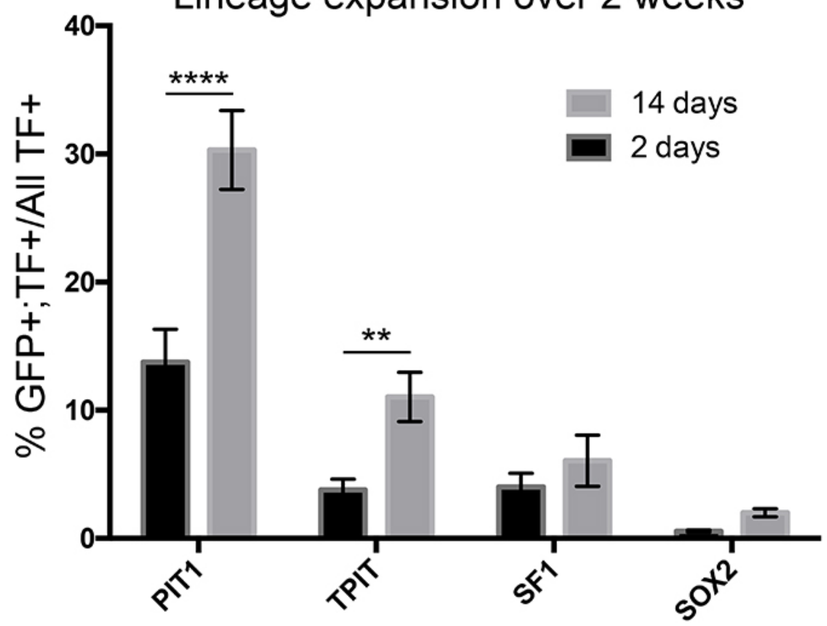

C

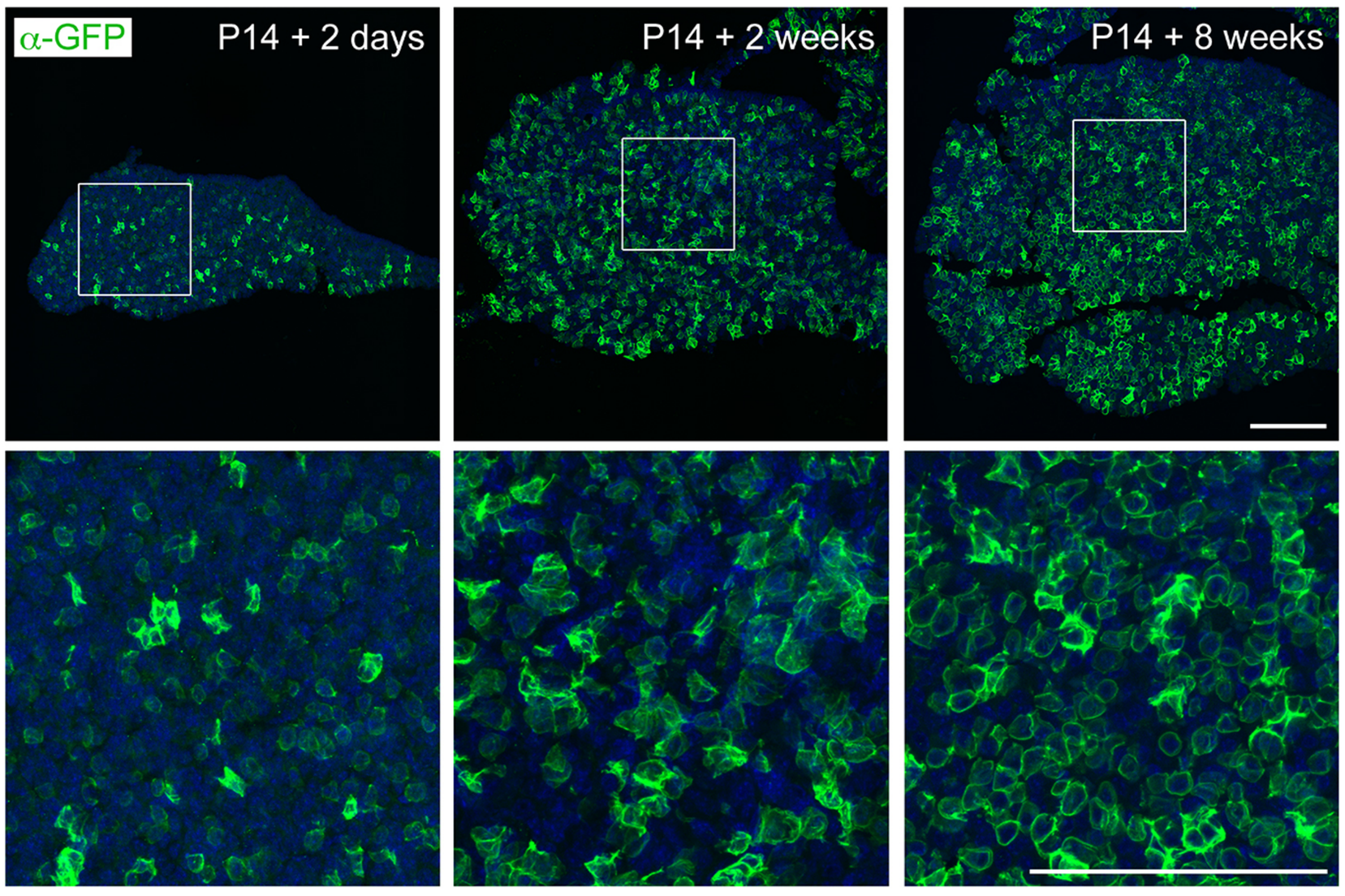

Axin2$^{CreERT2/+}$;*ROSA26*$^{mTmG/+}$

D

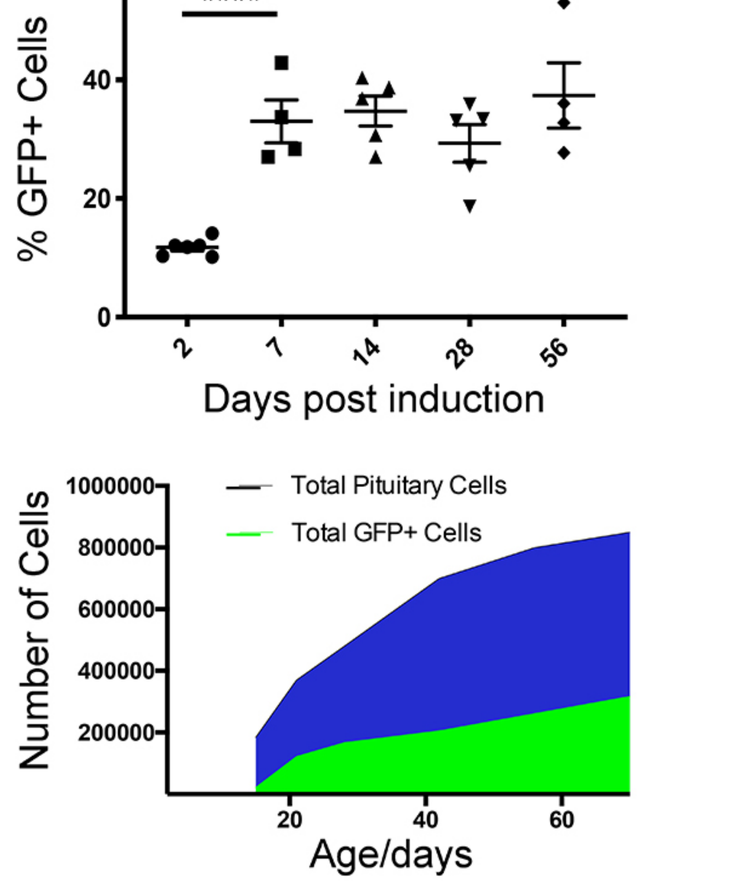

E

P14 +8 weeks

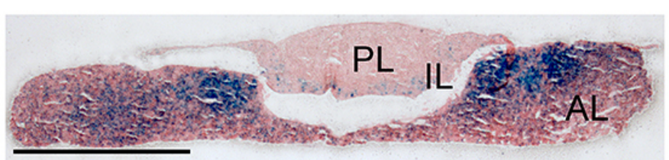

P14 +1 year

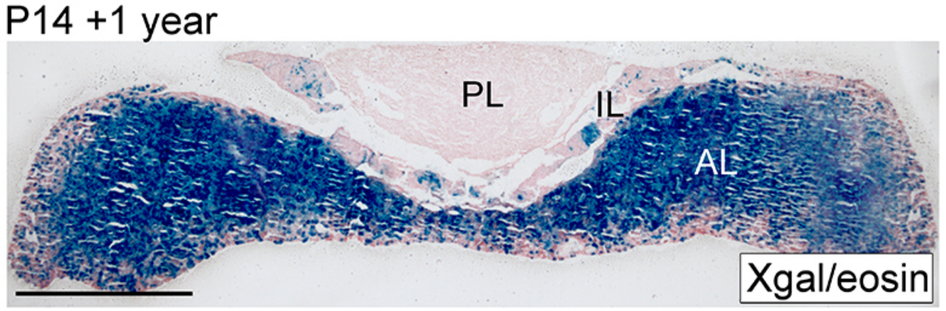

Axin2$^{CreERT2/+}$;*ROSA26*$^{LacZ/+}$

F

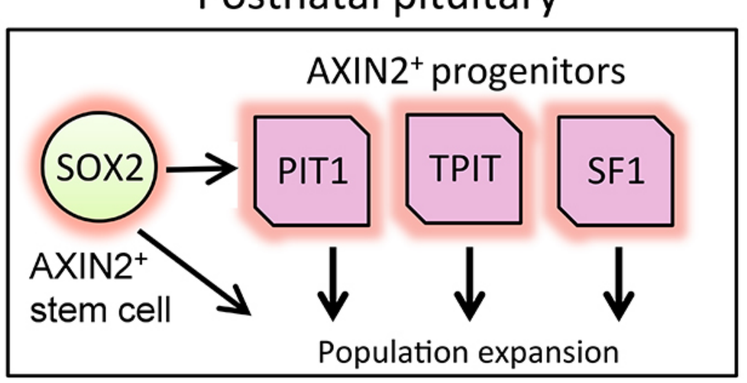

A

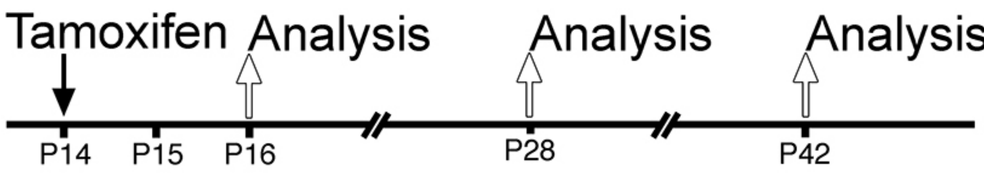

Axin2CreERT2/+;ROSA26mTmG/+ P14 + 2

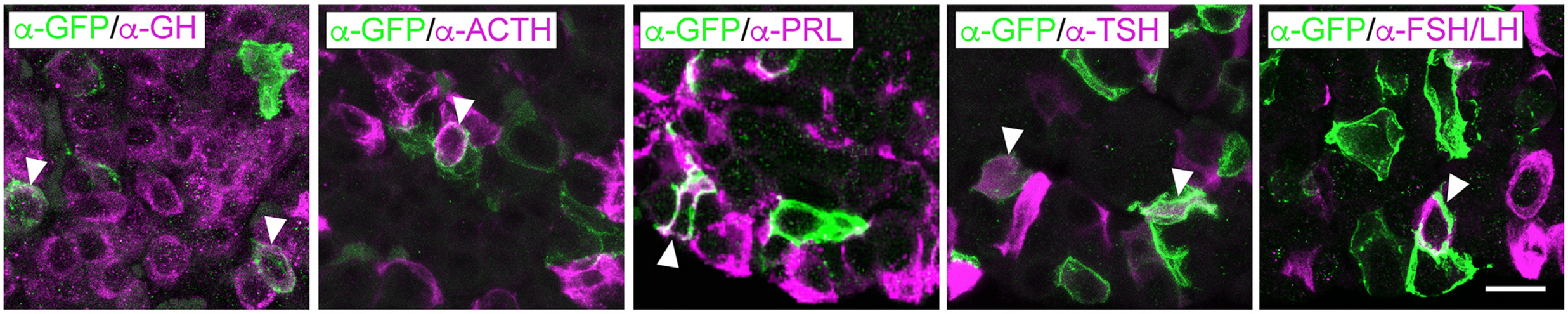

B

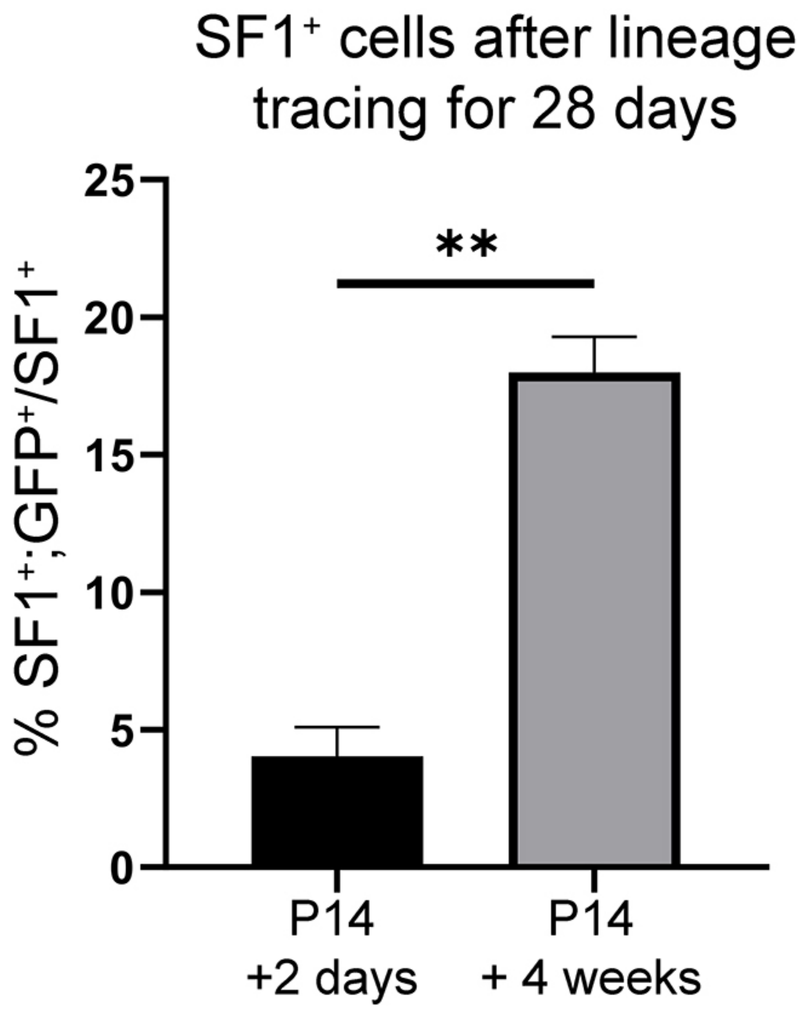

C

Axin2CreERT2/+;ROSA26mTmG/+

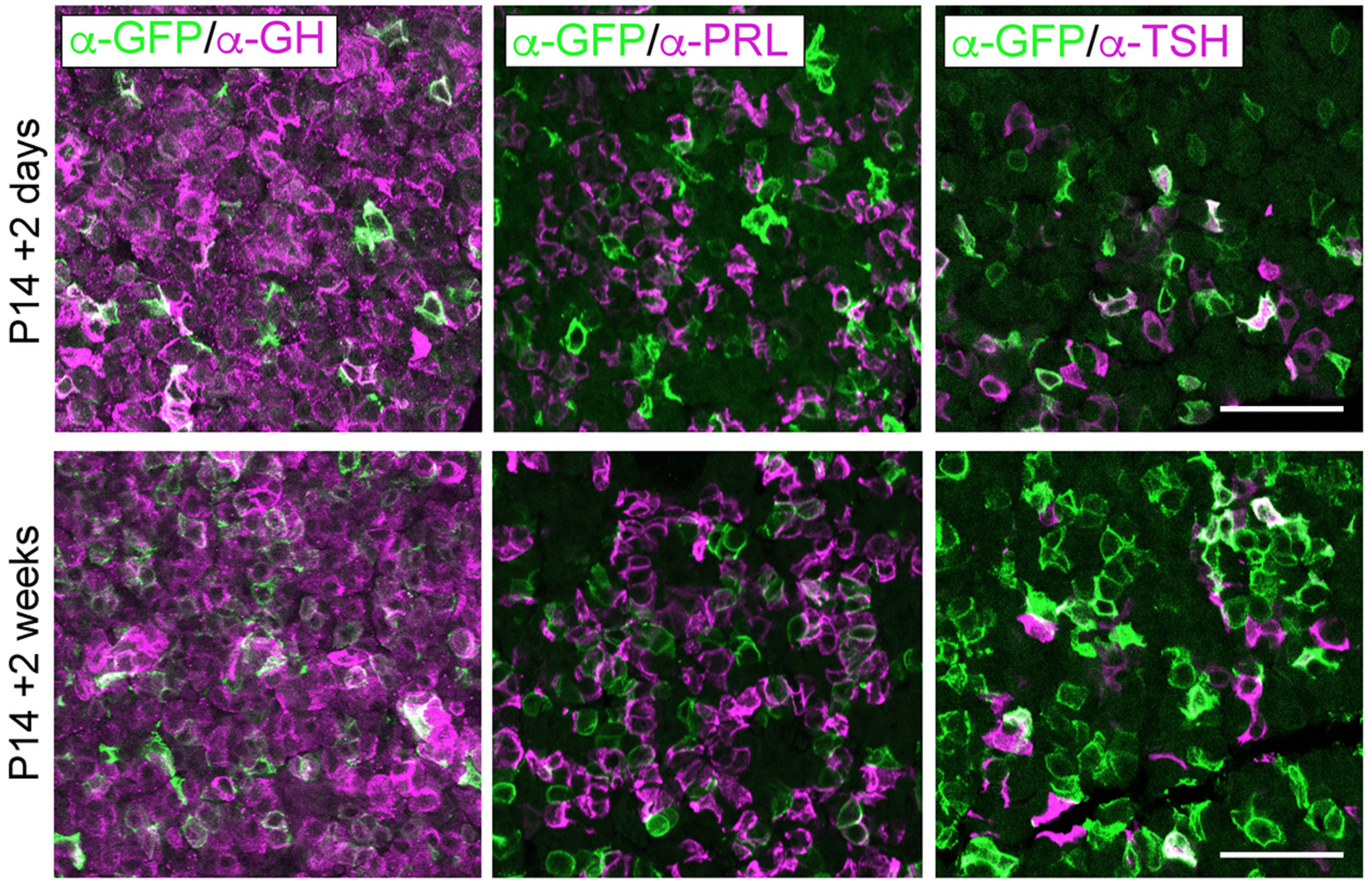

D

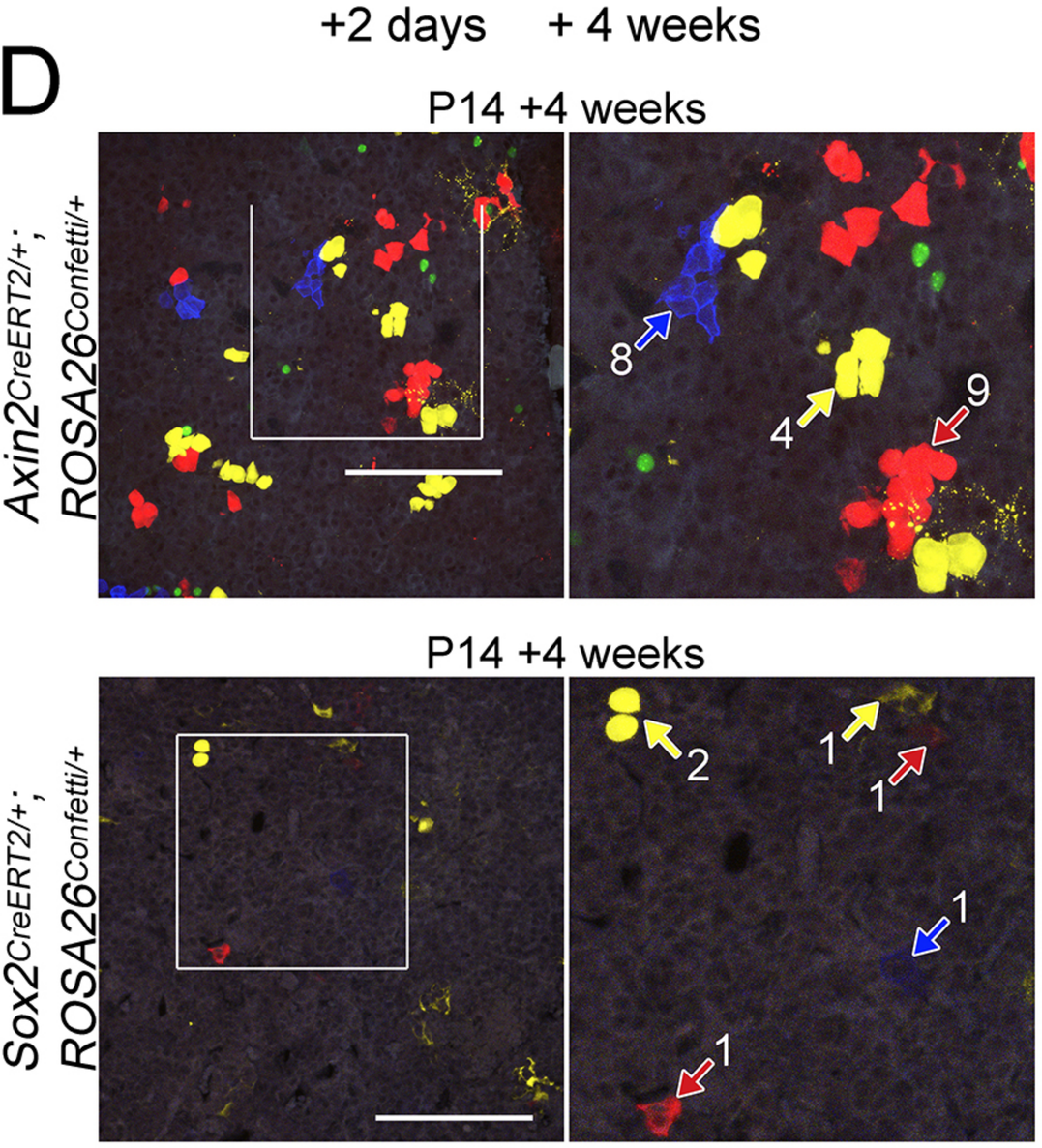

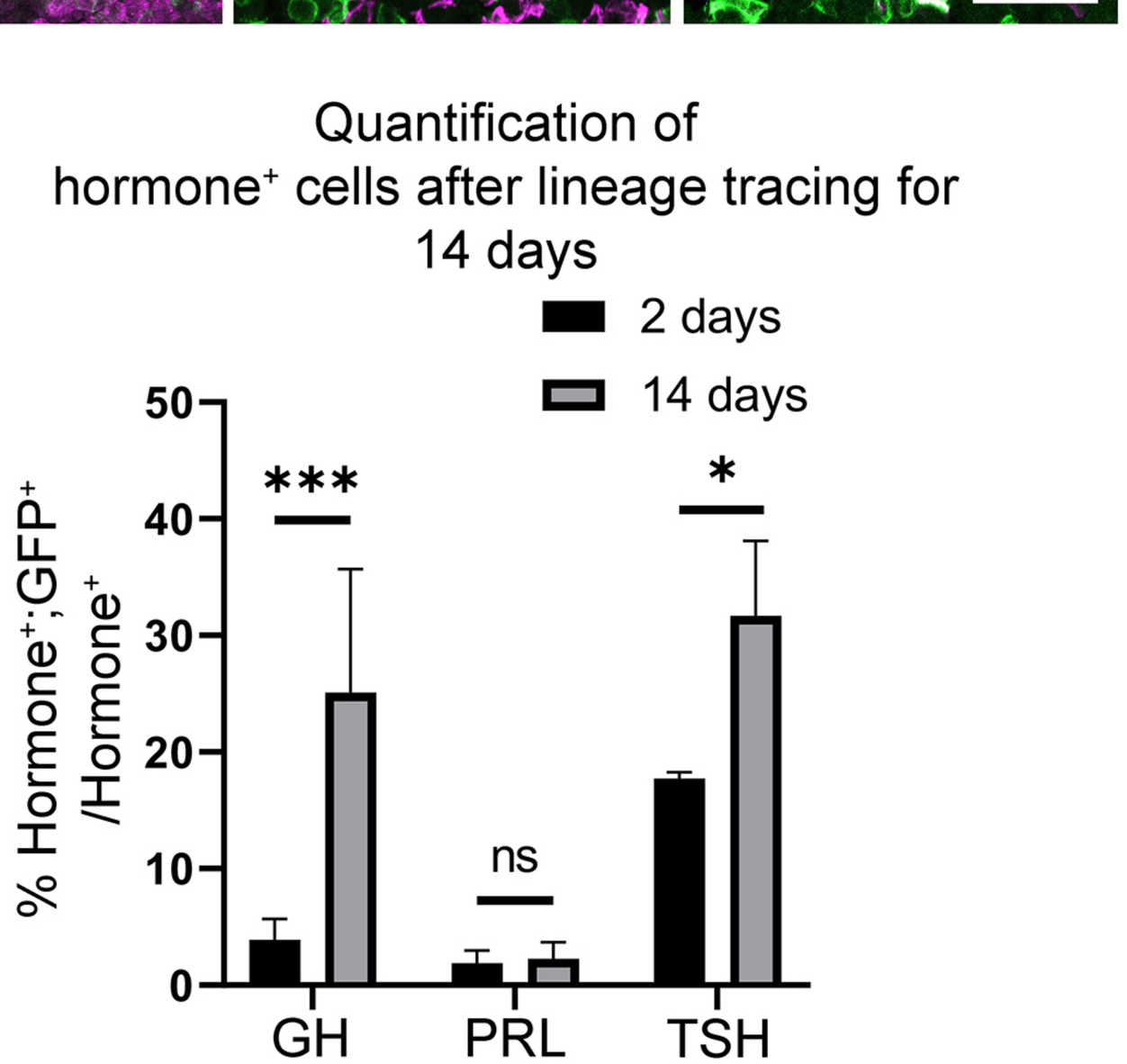

A

P14 +5 days

Axin2CreERT2/+;Ctnnb1LOF/+

Axin2CreERT2/+;Ctnnb1LOF/LOF

Axin2CreERT2/+;Ctnnb1LOF/+;ROSA26mTmG/+

α-GFP/α-pH-H3

Axin2CreERT2/+;Ctnnb1LOF/LOF;ROSA26mTmG/+

P14 +5 days

Quantification of dividing cells

% GFP+;pH-H3+/pH-H3+

50
40
30
20
10
0

*

LOF/+

LOF/LOF

B

Axin2CreERT2/+;Ctnnb1LOF/+;ROSA26mTmG/+

α-GFP/α-PIT1

α-GFP/α-SF1

α-GFP/α-ACTH

Axin2CreERT2/+;Ctnnb1LOF/LOF;ROSA26mTmG/+

P14 +5 days

Quantification of lineage-committed cells

% of GFP+ Cells

80
60
40
20
0

n.s.

n.s.

n.s.

LOF/+

LOF/LOF

PIT1

SF1

ACTH

C

Axin2CreERT2/+;Ctnnb1LOF/+;ROSA26mTmG/+

α-GFP/α-SOX2

Axin2CreERT2/+;Ctnnb1LOF/LOF;ROSA26mTmG/+

D

Axin2CreERT2/+;Ctnnb1LOF/+;ROSA26mTmG/+

α-GFP/α-Cl.Casp3

Axin2CreERT2/+;Ctnnb1LOF/LOF;ROSA26mTmG/+

A

Tamoxifen

In vitro assay

P21 P22 P23 P24

Axin2$^{CreERT2/+}$;*Sox2*$^{Egfp/+}$;*ROSA26*$^{tdTomato/+}$

Axin2$^{CreERT2/+}$;*Sox2*$^{Egfp/+}$;*ROSA26*$^{tdTomato/+}$

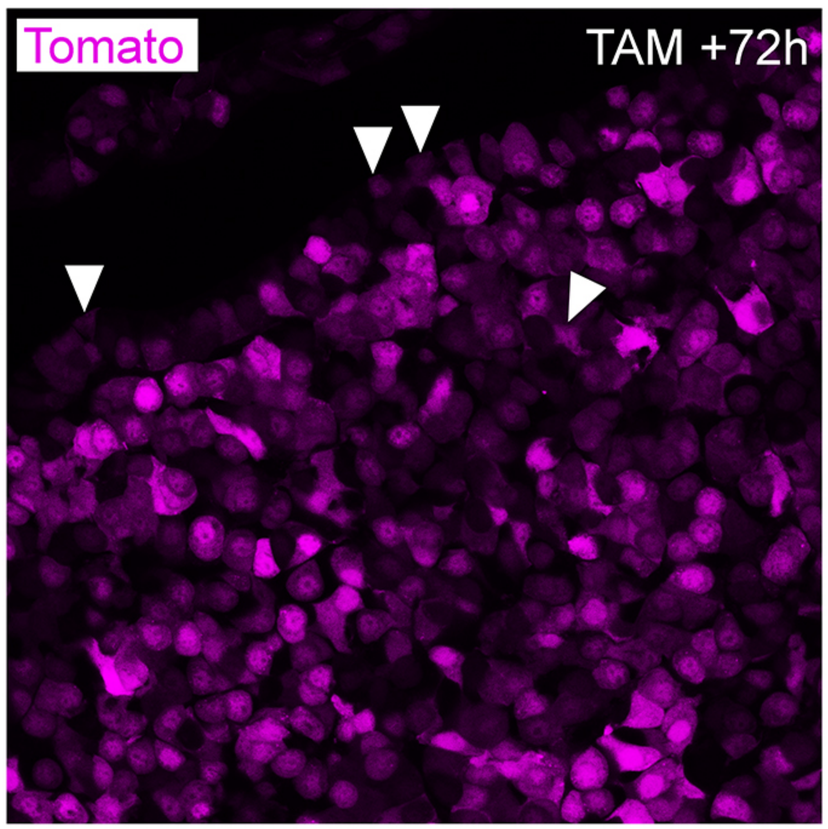

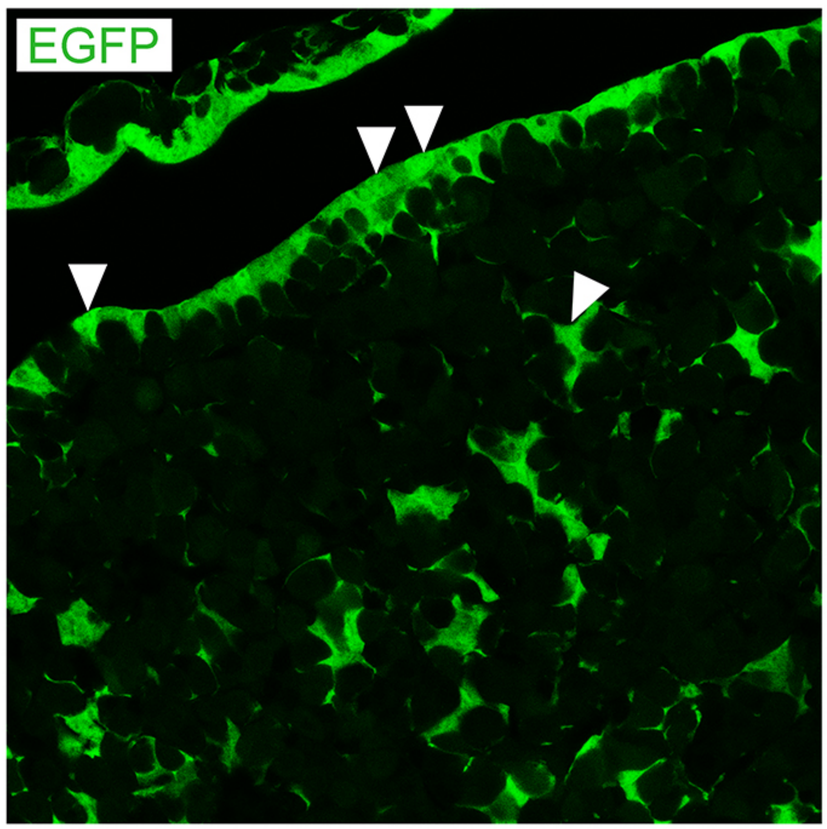

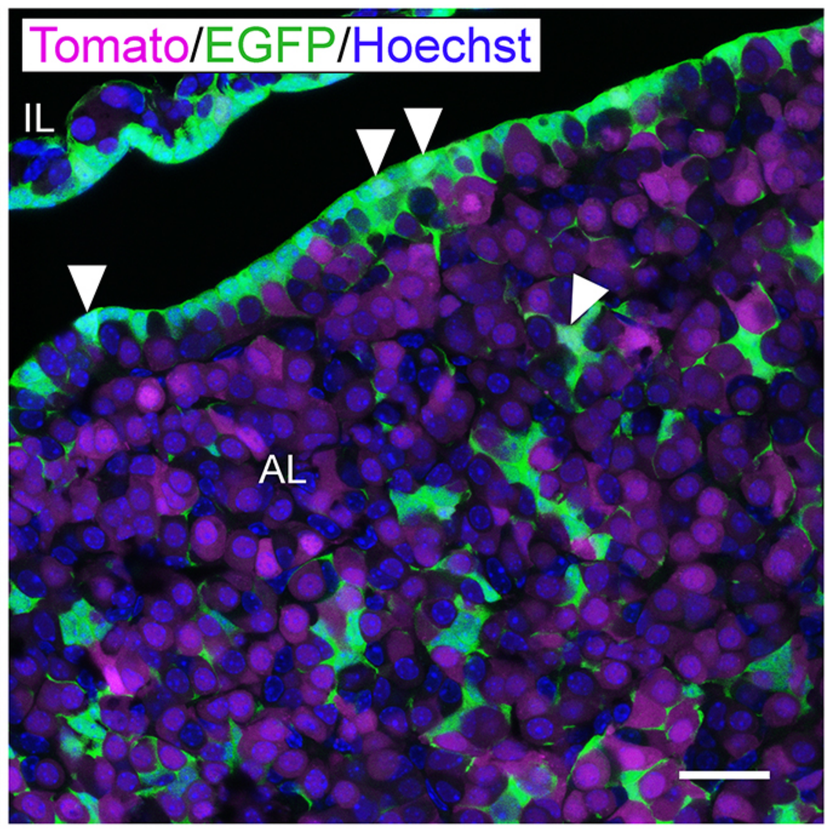

B

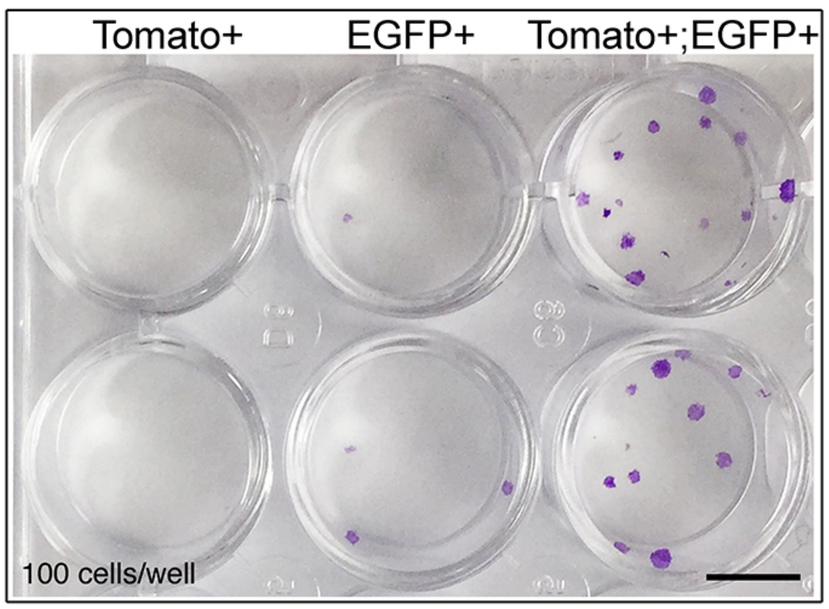

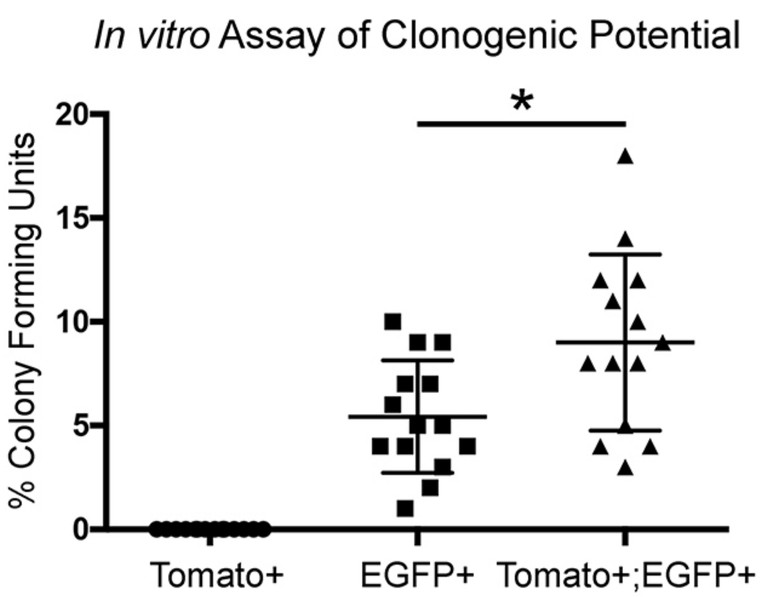

E

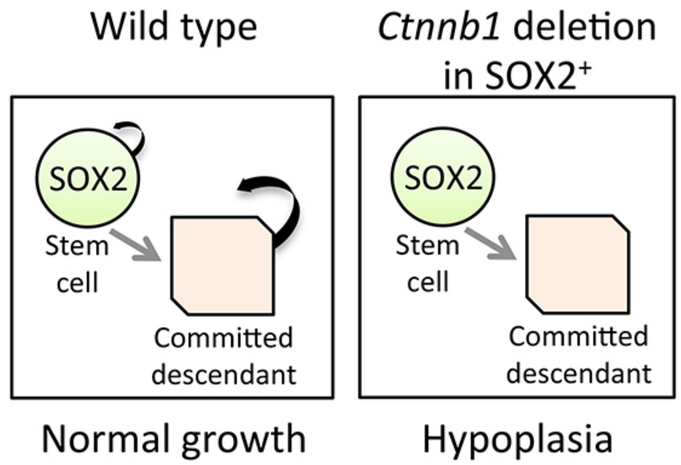

C

Sox2$^{+/+}$;*Ctnnb1*$^{LOF/LOF}$

Sox2$^{CreERT2/+}$;*Ctnnb1*$^{LOF/LOF}$

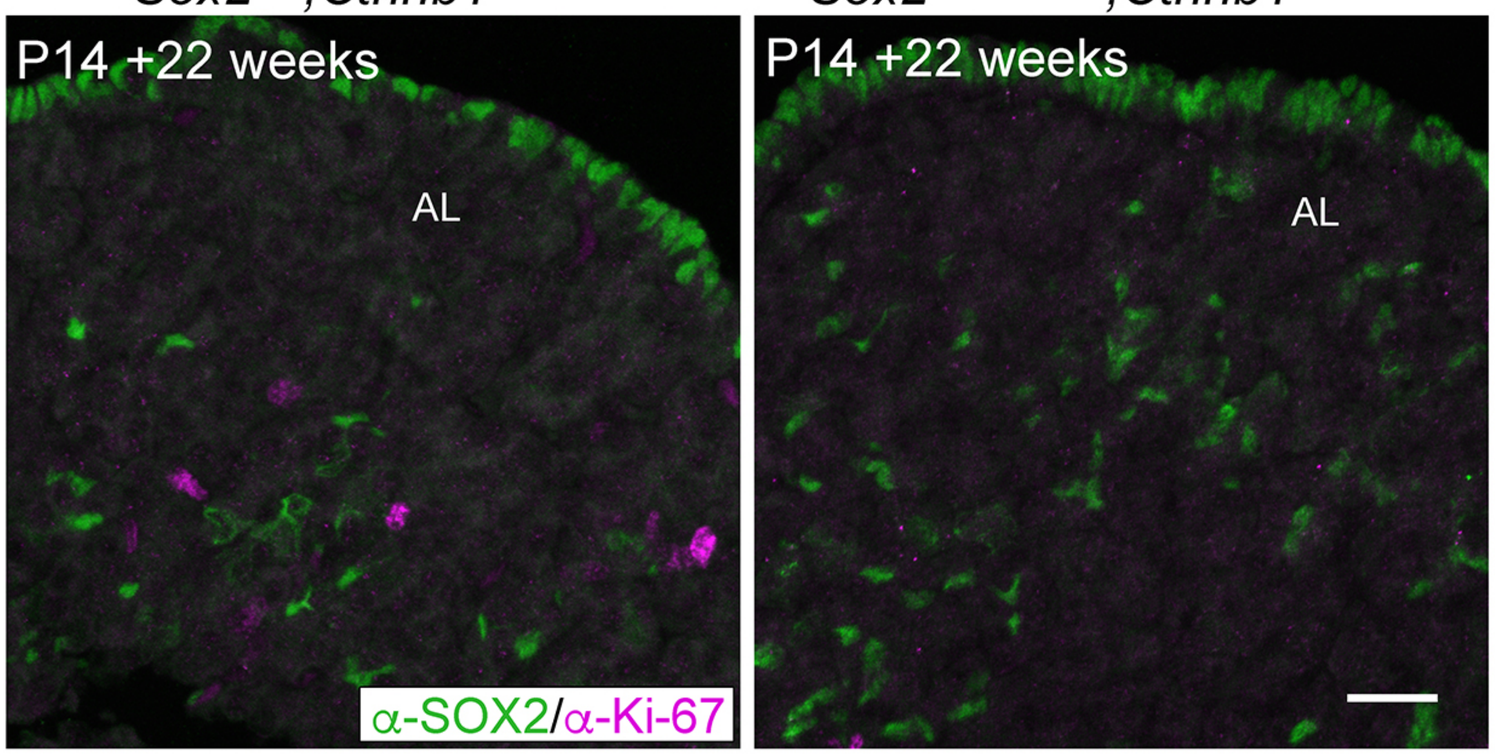

D

Sox2$^{+/+}$;*Ctnnb1*$^{LOF/LOF}$

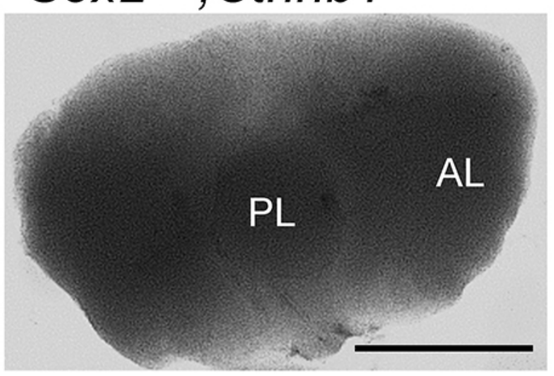

Sox2$^{CreERT2/+}$;*Ctnnb1*$^{LOF/LOF}$

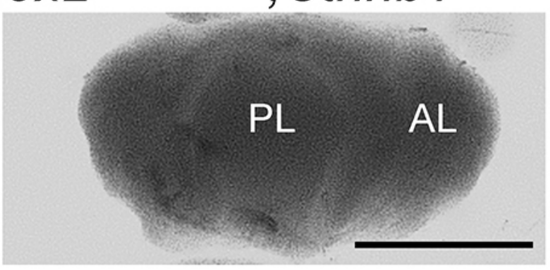

A

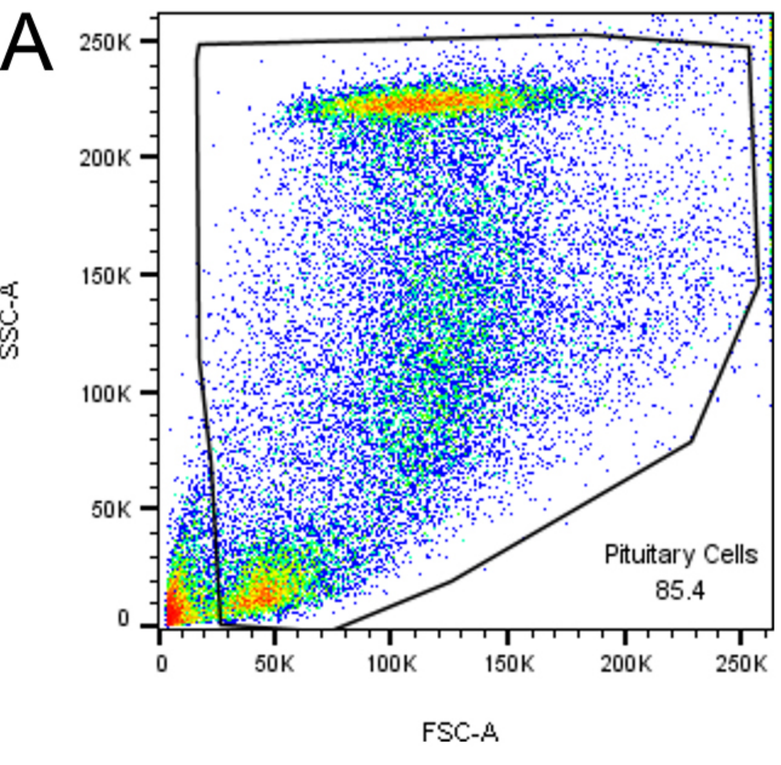
250K
200K
150K
100K
50K
0
SSC-A
0
50K
100K
150K
200K
250K
FSC-A
Pituitary Cells
85.4

B

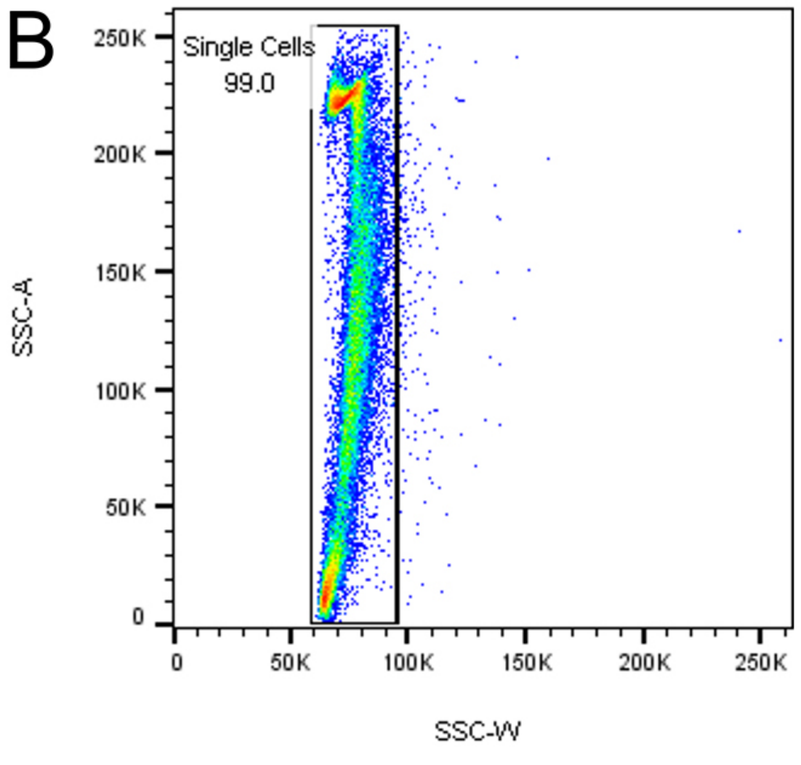
250K
200K
150K
100K
50K
0
SSC-A
Single Cells
99.0
0
50K
100K
150K
200K
250K
SSC-W

C

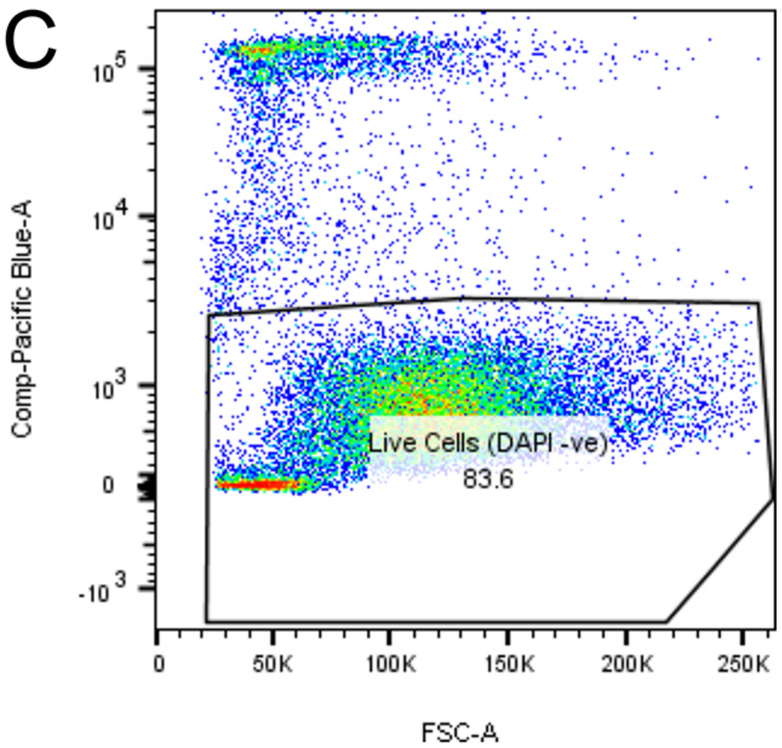
10^5
10^4
10^3
0
-10^3
Comp-Pacific Blue-A
Live Cells (DAPI -ve)
83.6
0
50K
100K
150K
200K
250K
FSC-A

D

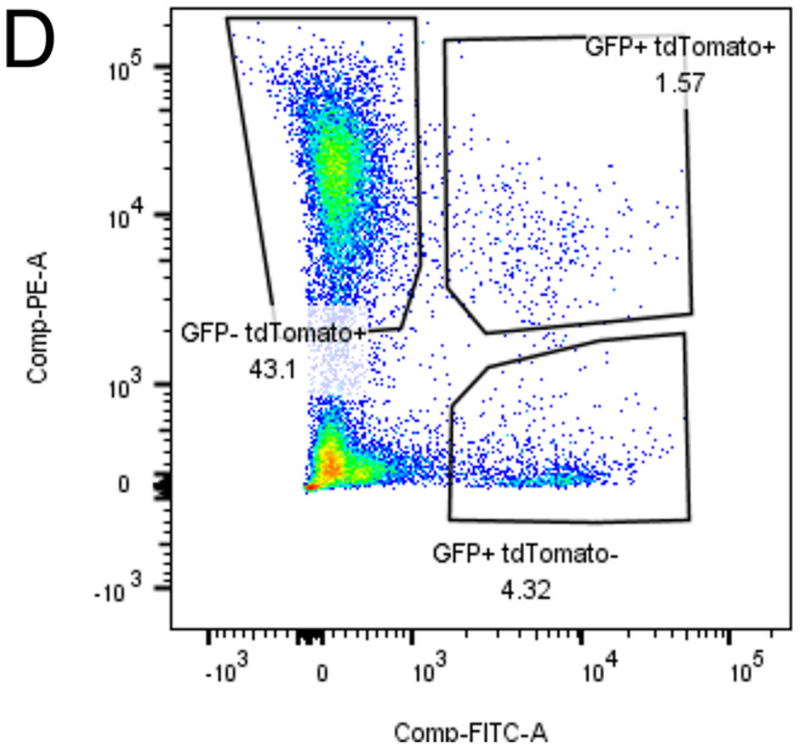
10^5
10^4
10^3
0
-10^3
Comp-PE-A
GFP+ tdTomato+
1.57
GFP- tdTomato+
43.1
GFP+ tdTomato-
4.32
-10^3
0
10^3
10^4
10^5
Comp-FITC-A

E

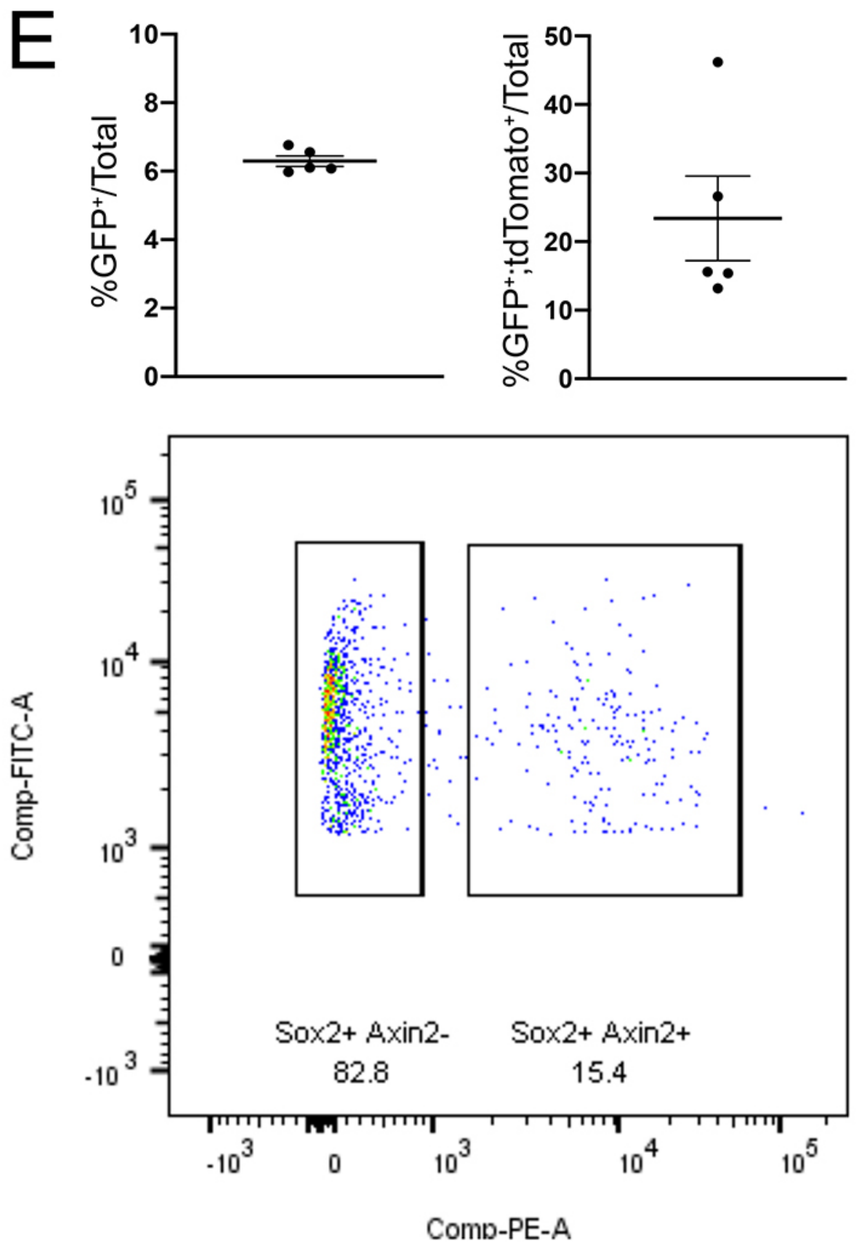
%GFP+/Total
10
8
6
4
2
0
%GFP+;tdTomato+/Total
50
40
30
20
10
0
Comp-FITC-A
10^5
10^4
10^3
0
-10^3
Sox2+ Axin2-
82.8
Sox2+ Axin2+
15.4
-10^3
0
10^3
10^4
10^5
Comp-PE-A

A

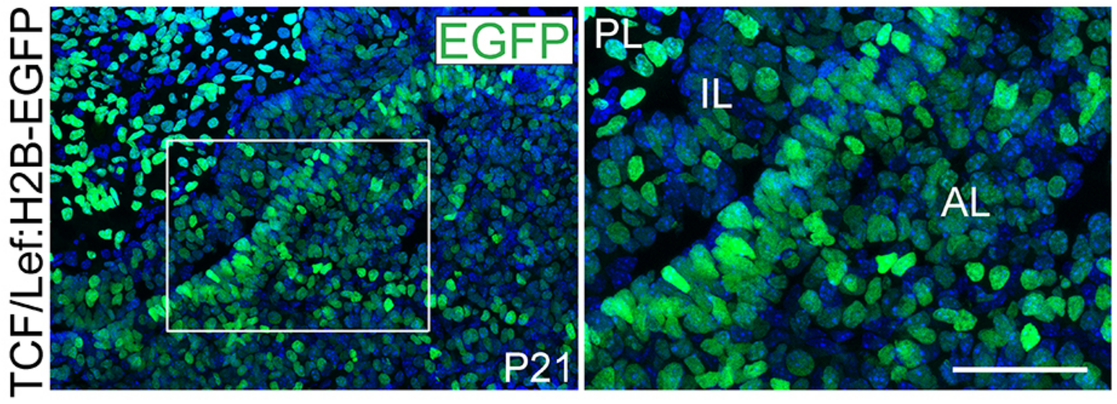
TCF/Lef:H2B-EGFP
EGFP
P21
PL
IL
AL

B

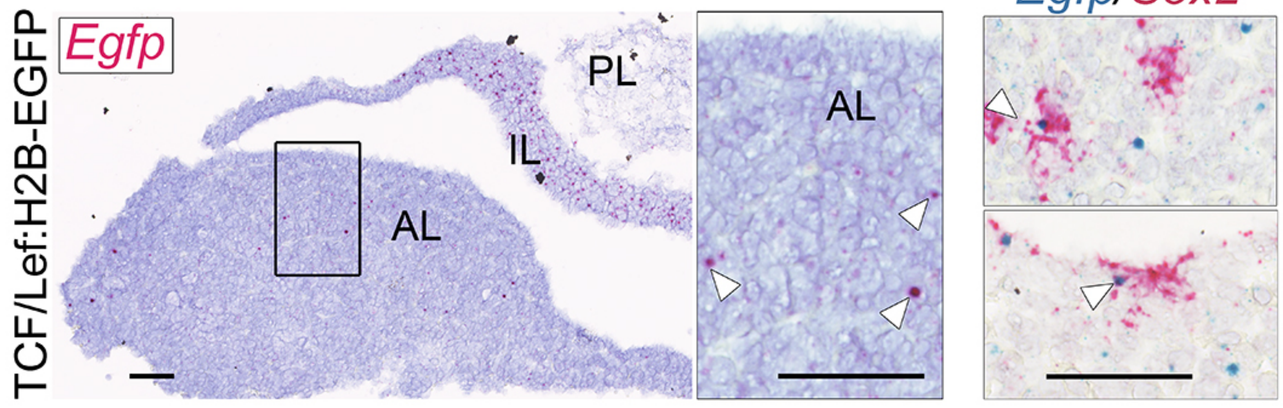
TCF/Lef:H2B-EGFP
Egfp
PL
IL
AL
AL
Egfp/Sox2

C

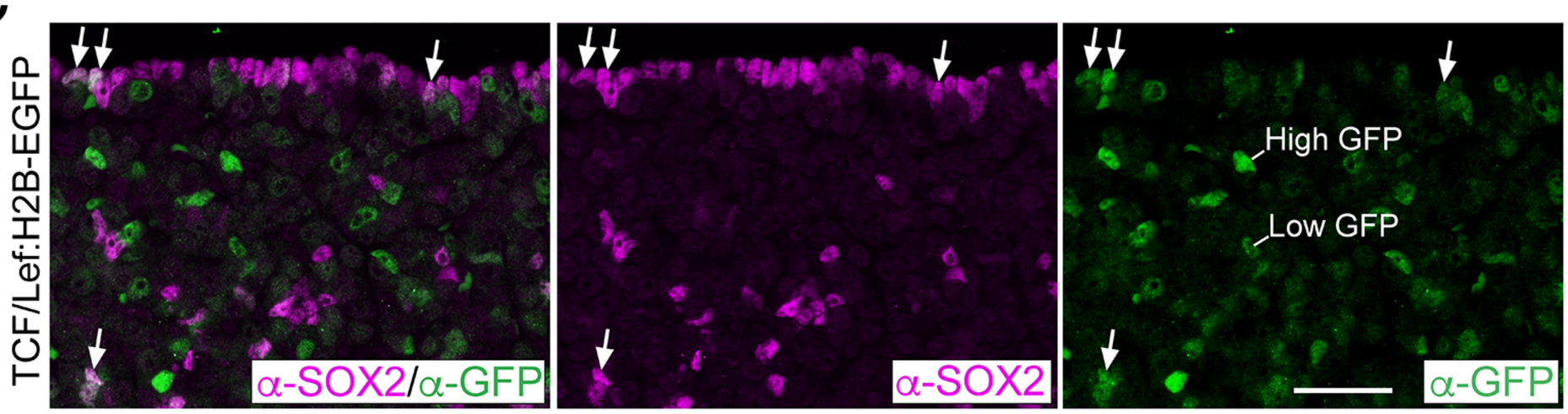
TCF/Lef:H2B-EGFP
α-SOX2/α-GFP
α-SOX2
High GFP
Low GFP
α-GFP

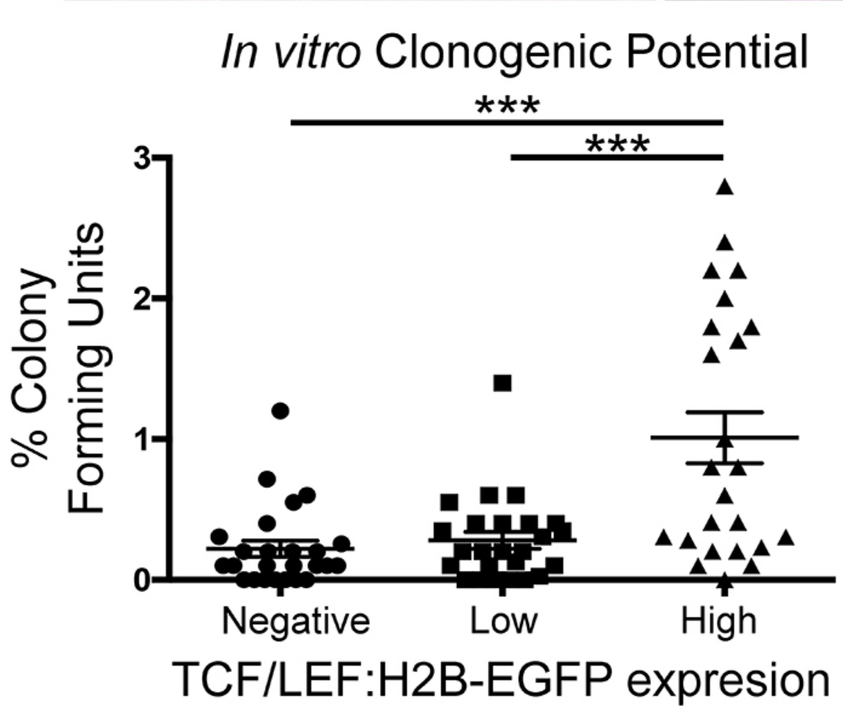
In vitro Clonogenic Potential
***
***
% Colony Forming Units
3
2
1
0
Negative
Low
High
TCF/LEF:H2B-EGFP expresion

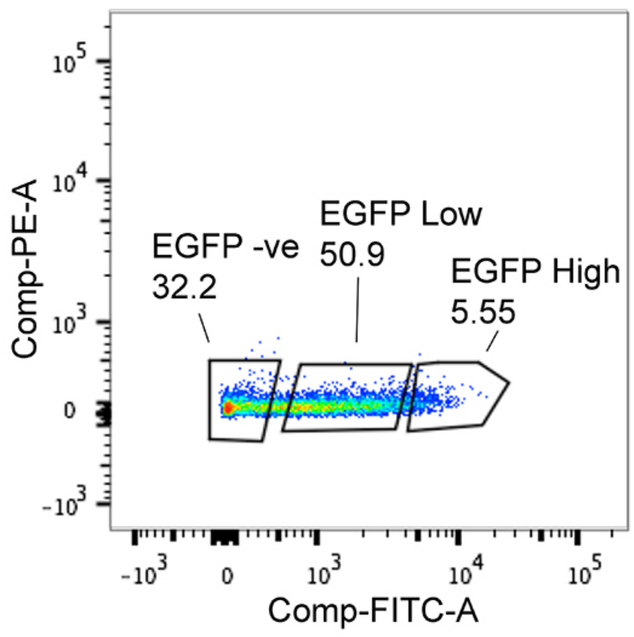
Comp-PE-A
Comp-FITC-A
EGFP -ve
32.2
EGFP Low
50.9
EGFP High
5.55

D

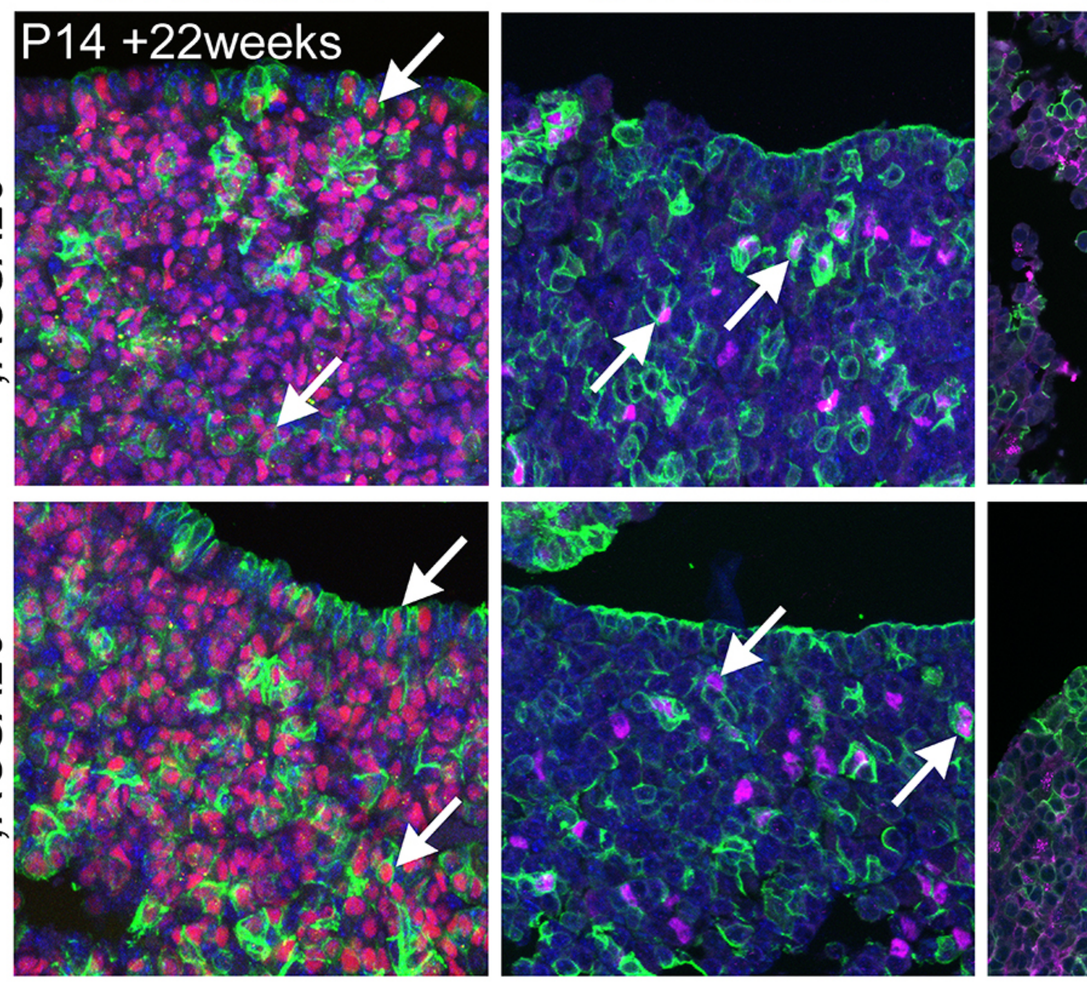
α-PIT1/α-GFP
α-TPIT/α-GFP
α-SF1/α-GFP
P14 +22weeks
Sox2CreERT2/+;Ctnnb1 LOF/+;ROSA26mTmG/+
Sox2CreERT2/+;Ctnnb1 LOF/LOF;ROSA26mTmG/+

E

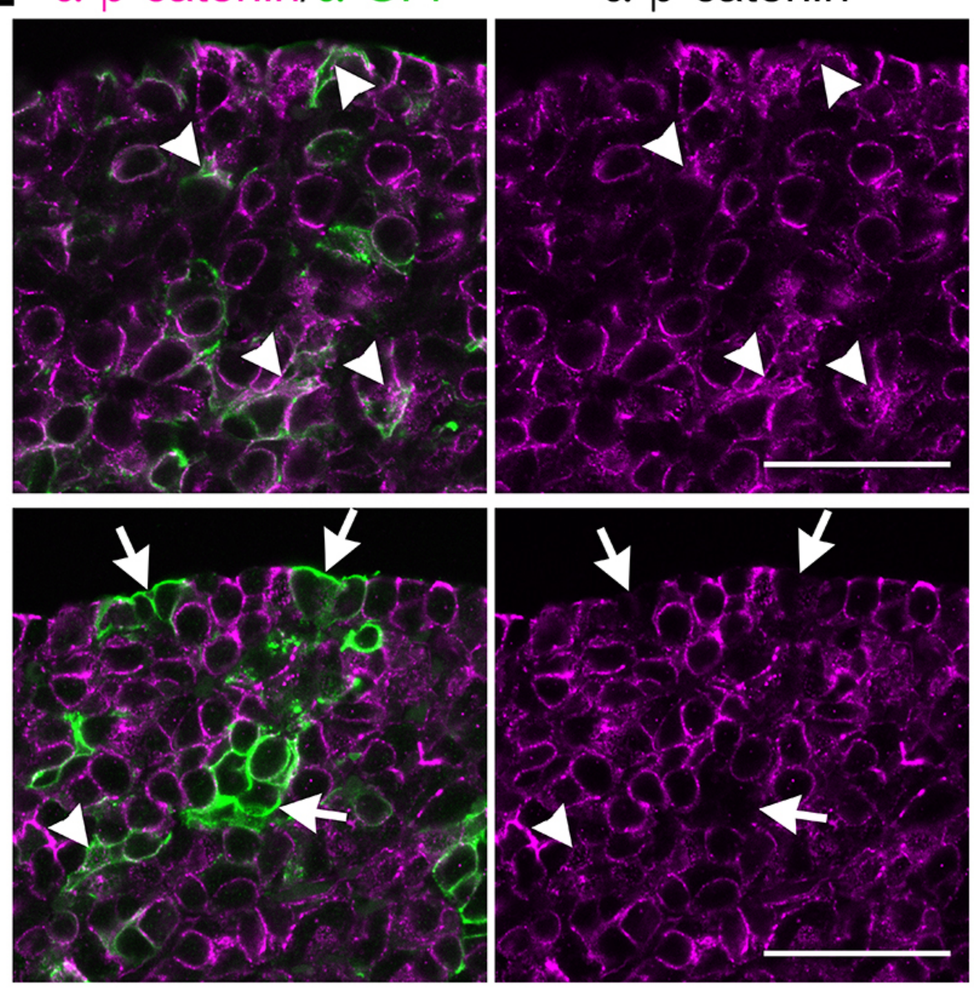
α-β-catenin/α-GFP
α-β-catenin

A

Axin2$^{CreERT2/+}$;*ROSA26*$^{mTmG/+}$

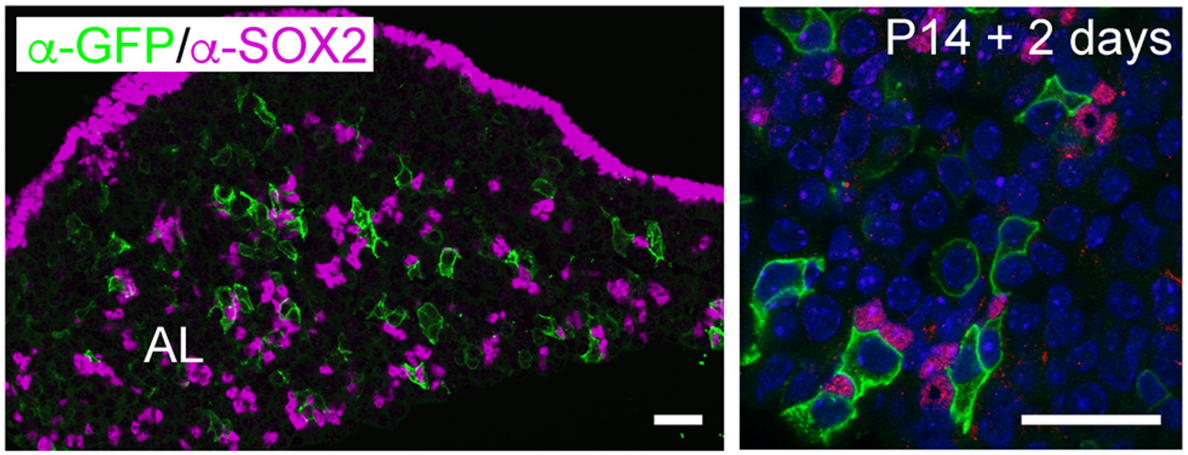

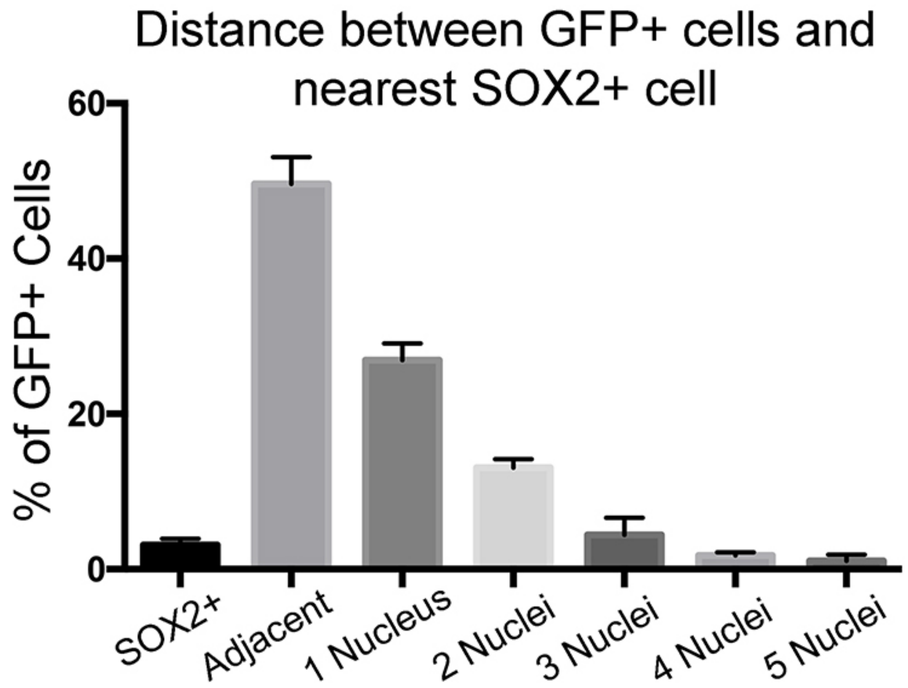

B

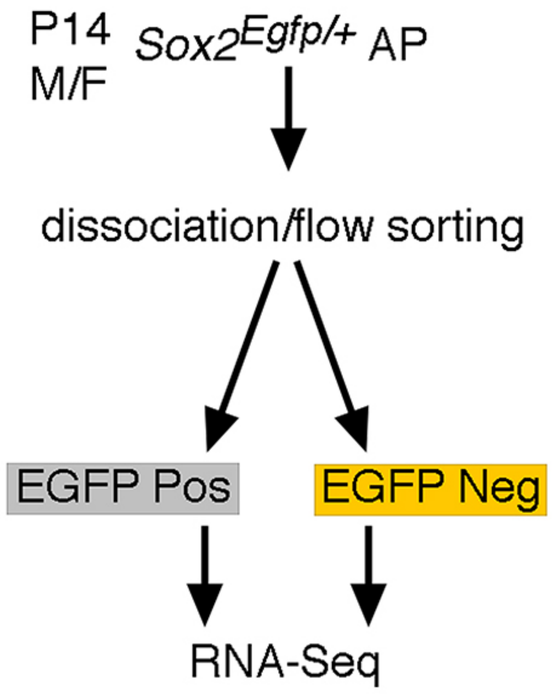

C

Expression of *Wls* and *Porcn* in the pituitary at P14

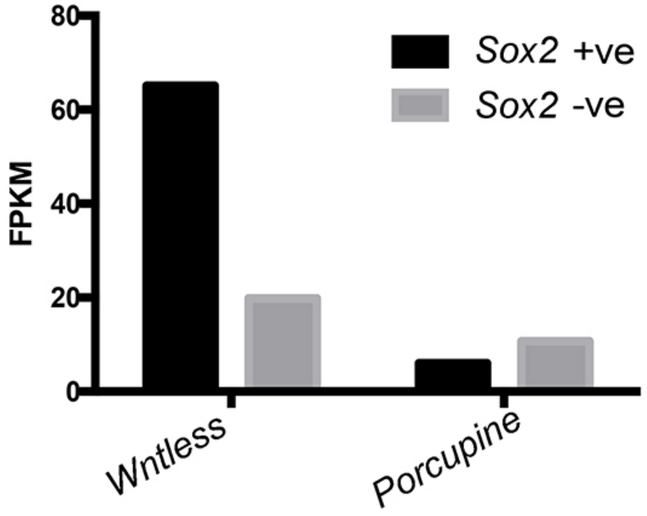

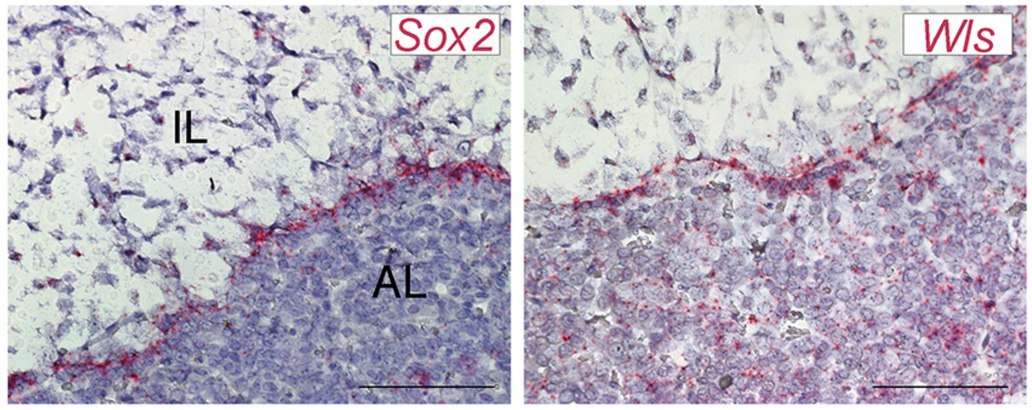

D

Expression of *Wnt* genes in the pituitary at P14

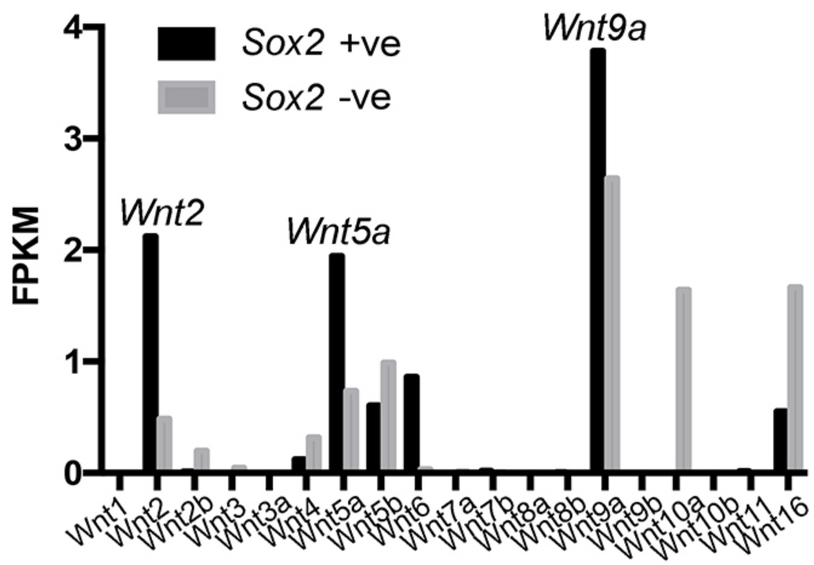

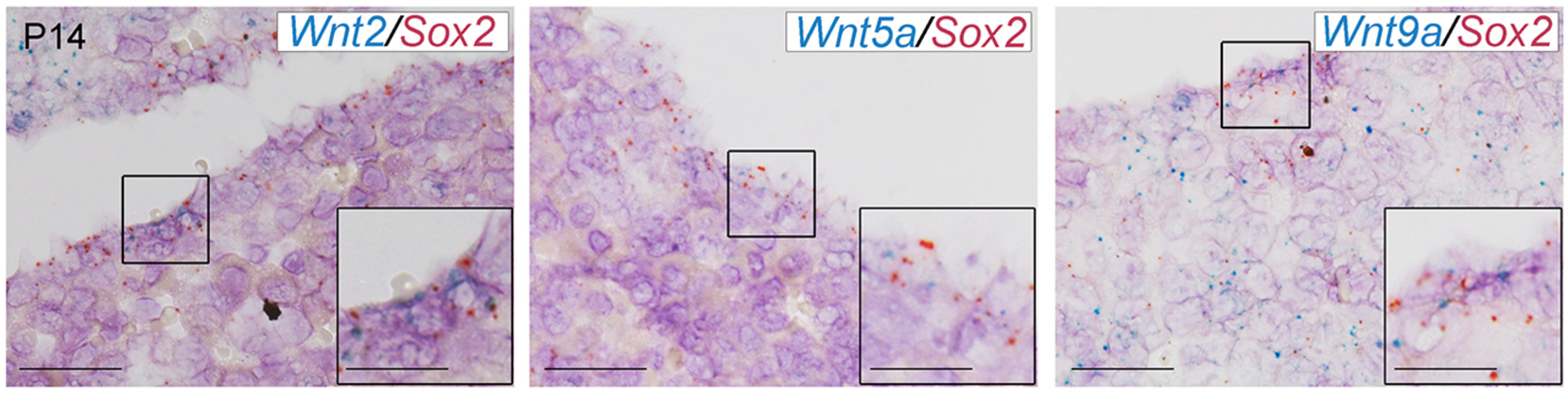

A

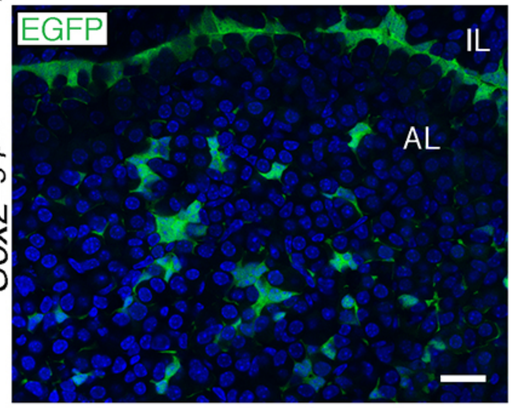

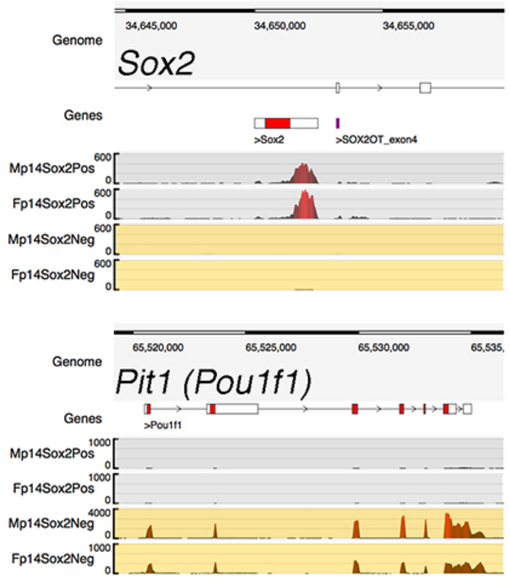

RNA-Seq Workflow

Quality Check & Filtering of reads (Galaxy)

↓

Mapping to mouse GRCm38/mm10 Genome (HISAT2)

↓

Transcript assembly & Quantification (Cufflinks)

↓

Merging of assembled transcripts (Cuffmerge)

↓

Transcript Differential expression testing (CuffDiff)

↓

Differential expression results

↓

Expression Plots (R/ CummerBand)

B

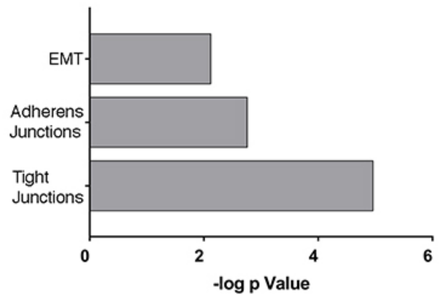

C

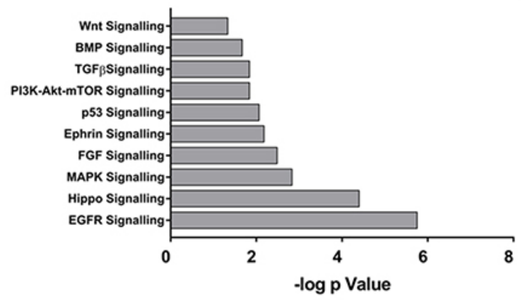

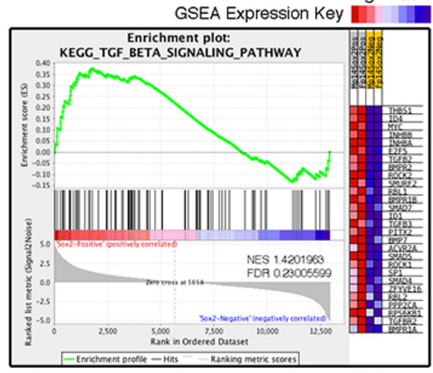

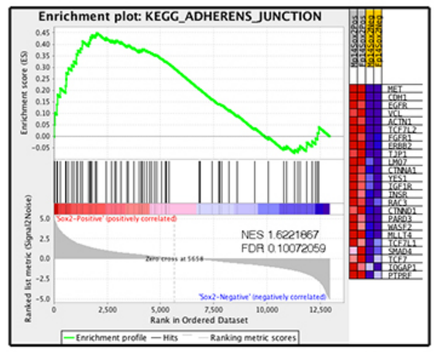

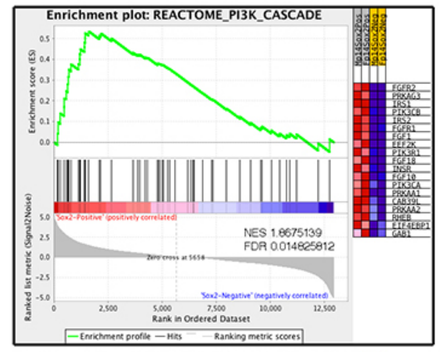

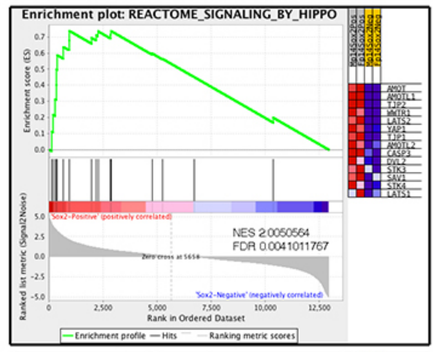

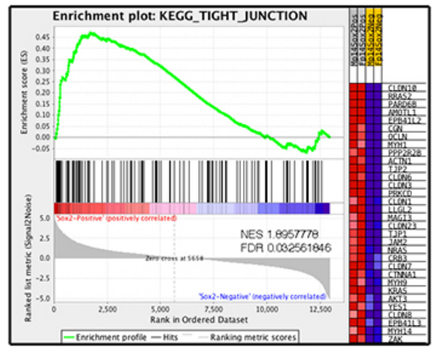

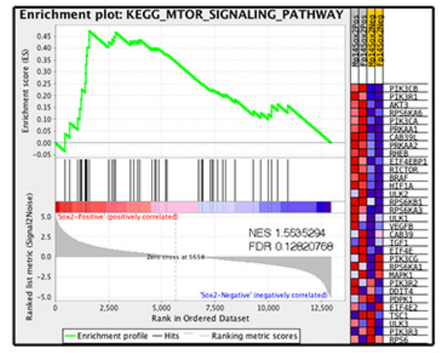

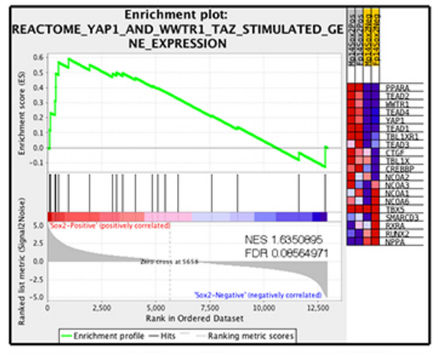

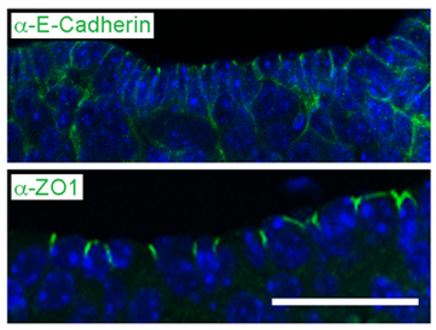

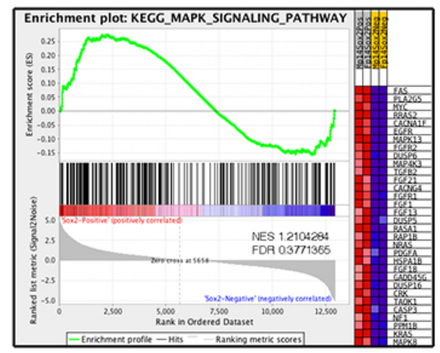

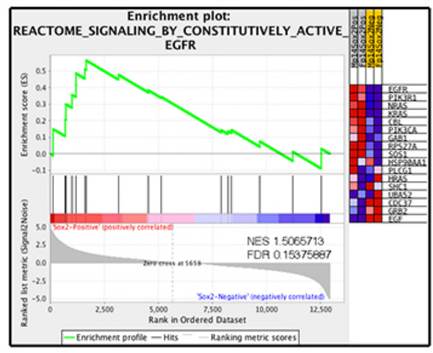

D

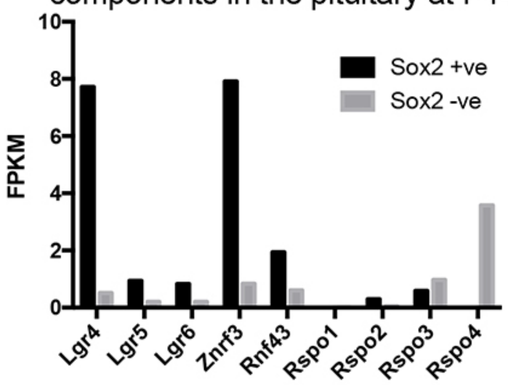

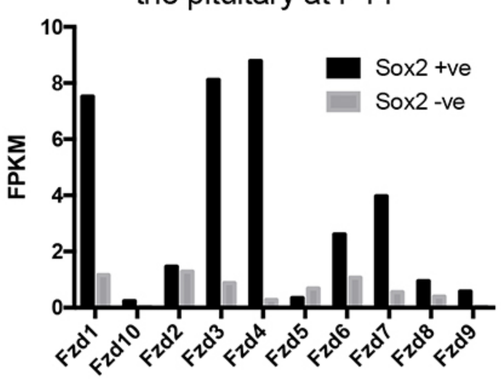

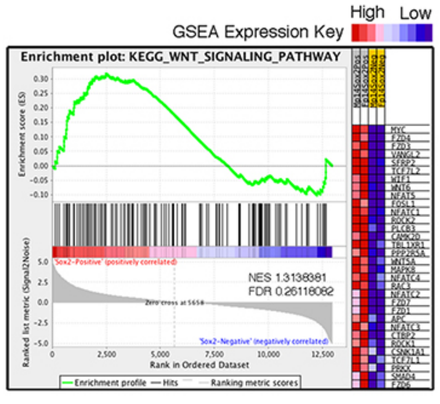

(i)

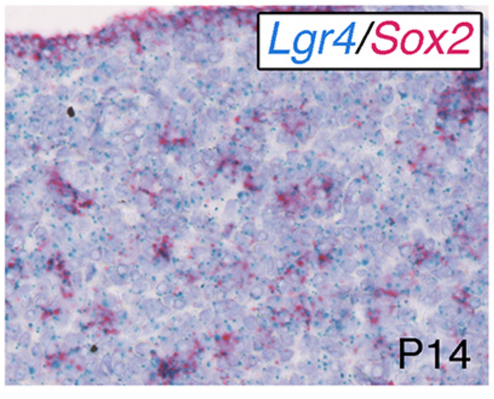

(ii)

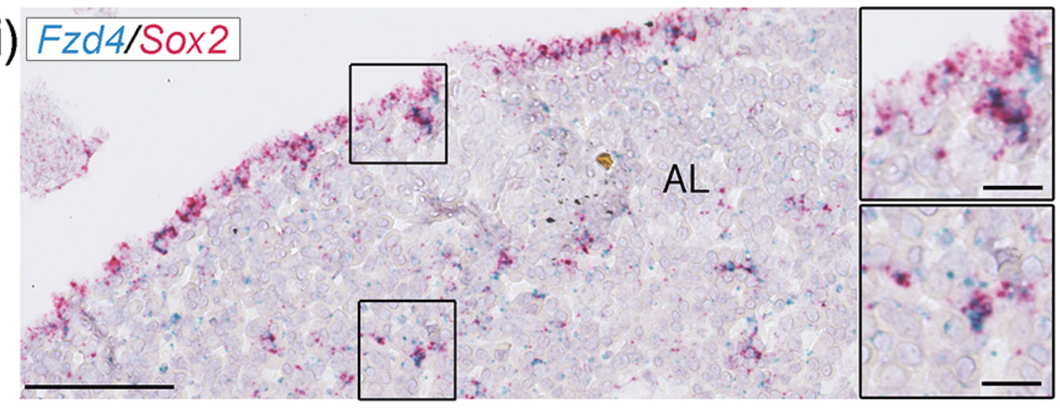

(iii)

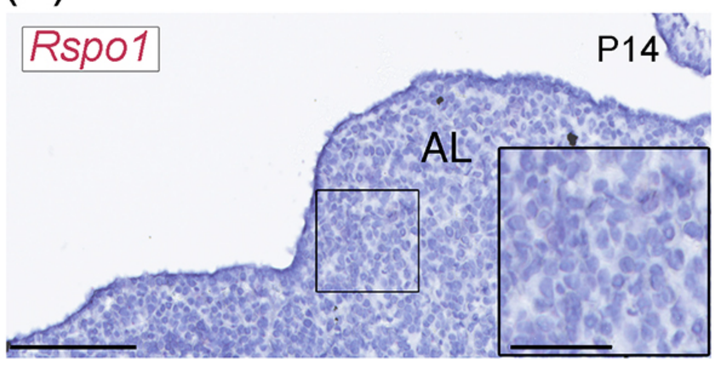

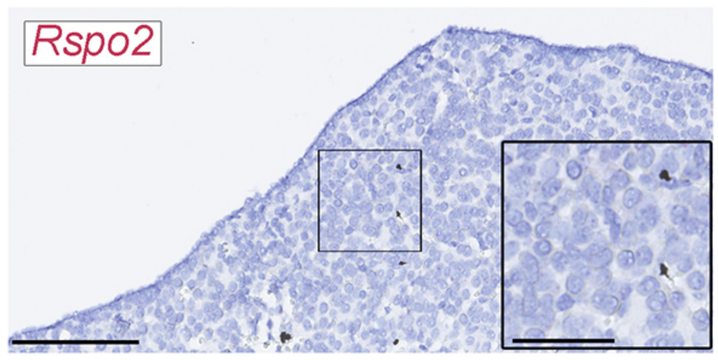

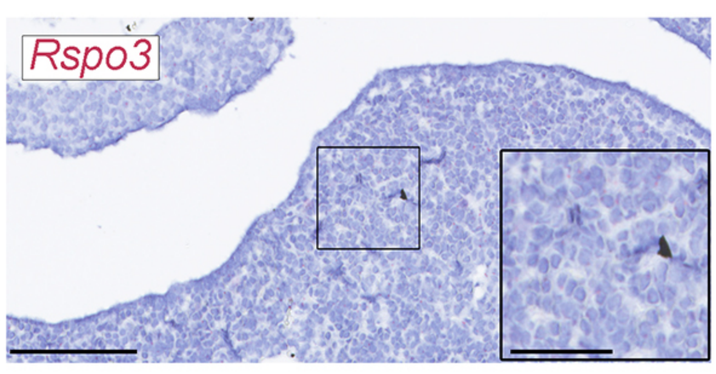

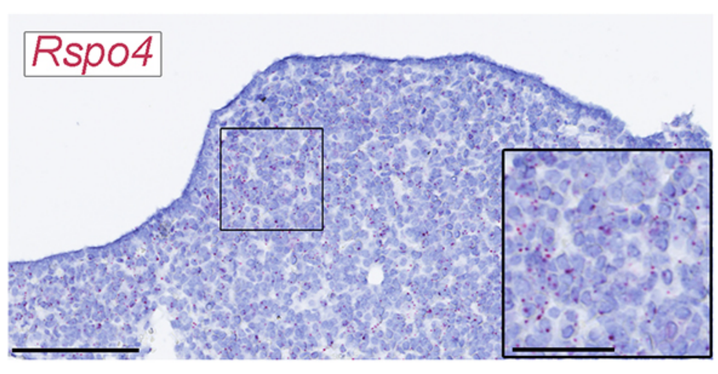

A

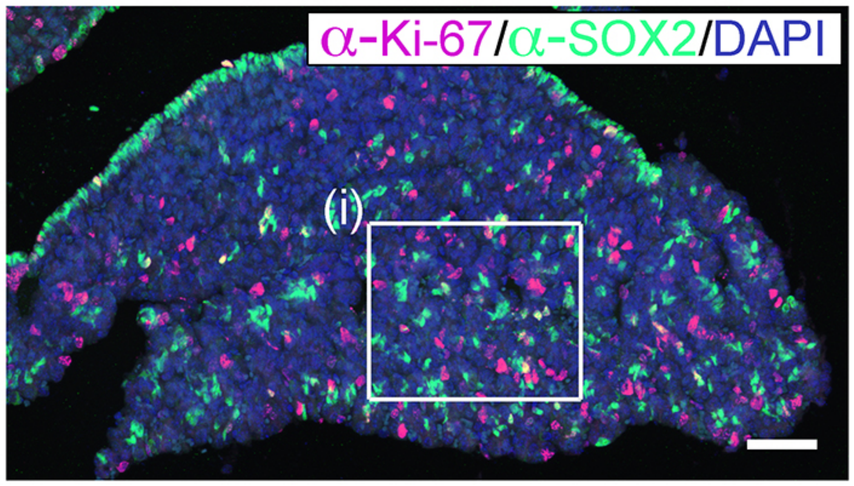
Sox2+/+;Wlsfl/fl
α-Ki-67/α-SOX2/DAPI
(i)

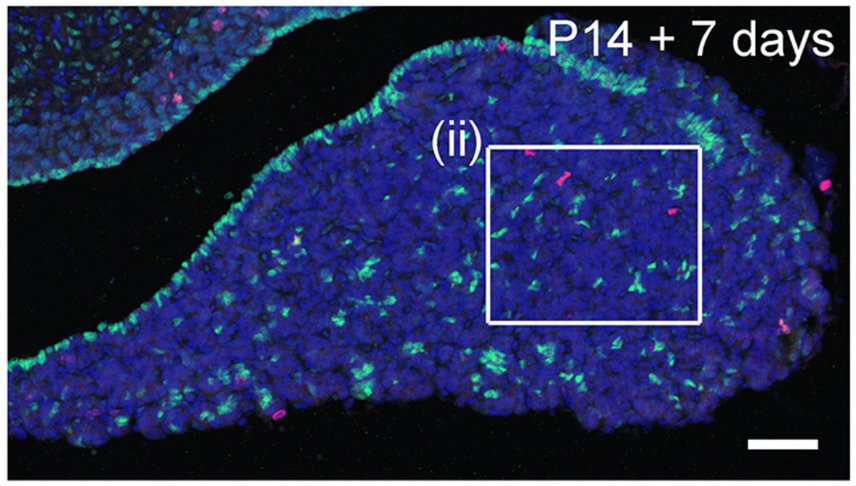
Sox2CreERT2/+;Wlsfl/fl
P14 + 7 days
(ii)

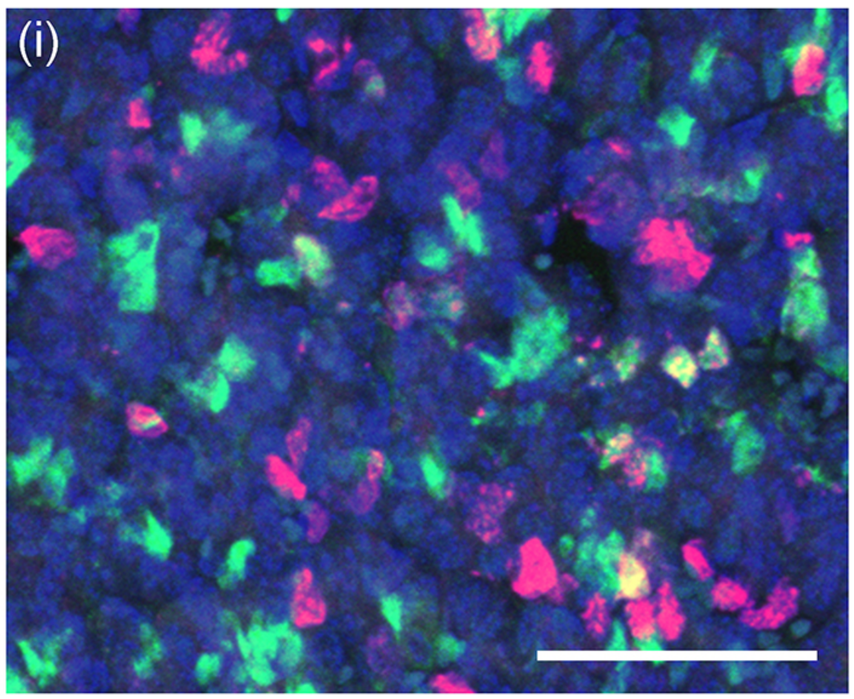
(i)

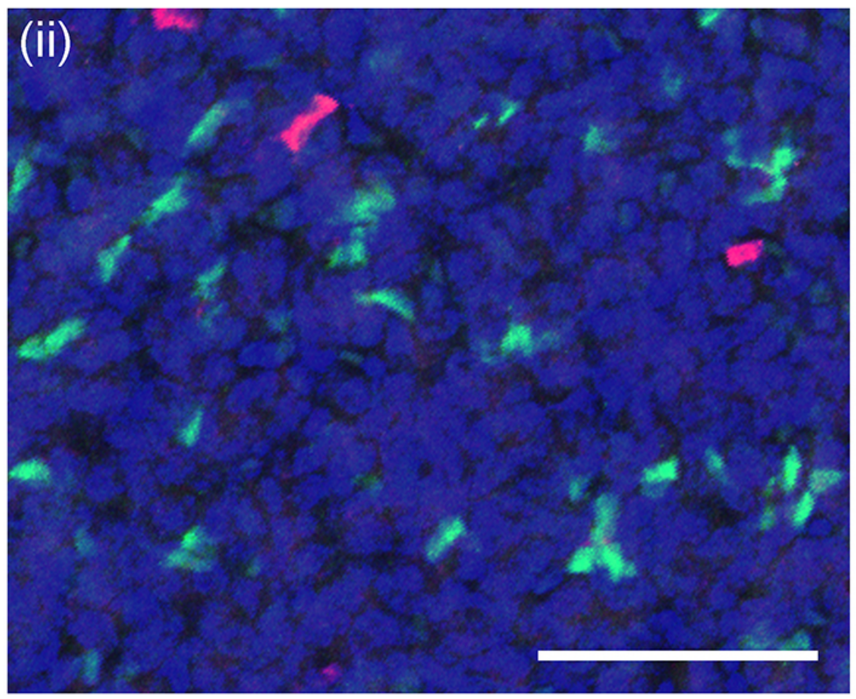
(ii)

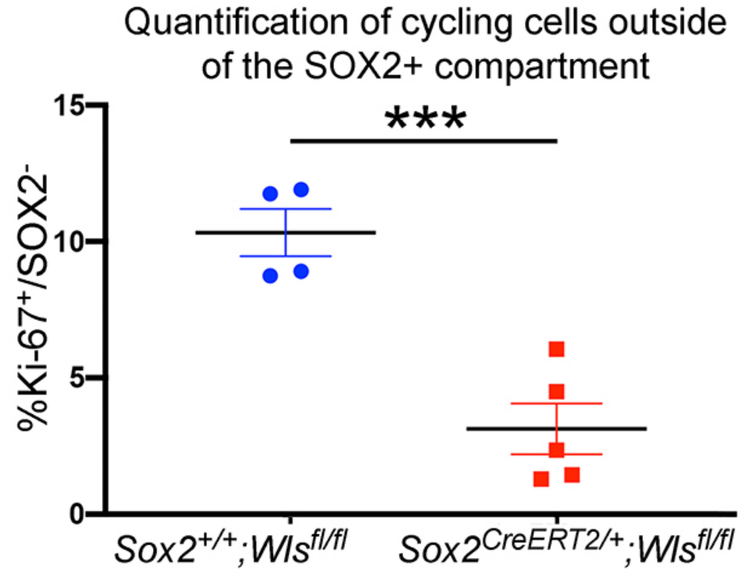
Quantification of cycling cells outside of the SOX2+ compartment
***
%Ki-67+/SOX2-
15
10
5
0
Sox2+/+;Wlsfl/fl
Sox2CreERT2/+;Wlsfl/fl

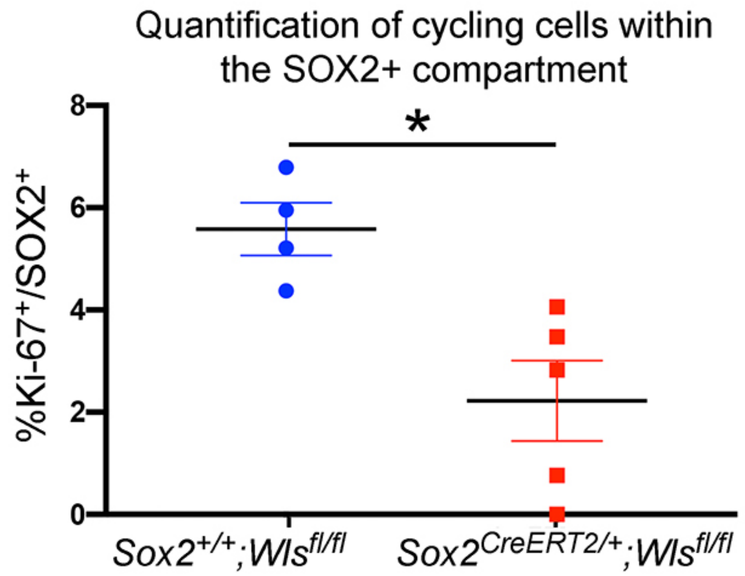
Quantification of cycling cells within the SOX2+ compartment
*
%Ki-67+/SOX2+
8
6
4
2
0
Sox2+/+;Wlsfl/fl
Sox2CreERT2/+;Wlsfl/fl

B

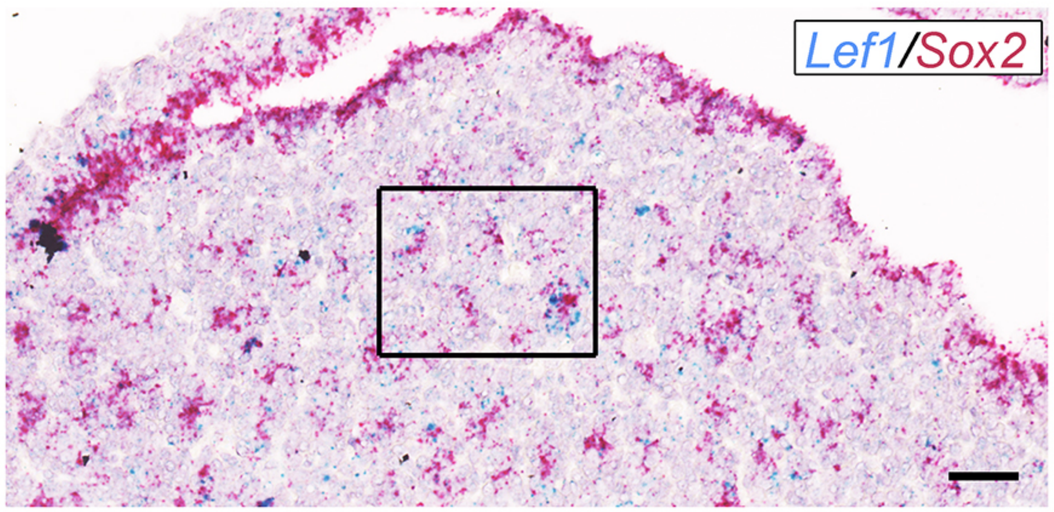
Lef1/Sox2
Sox2+/+;Wlsfl/fl

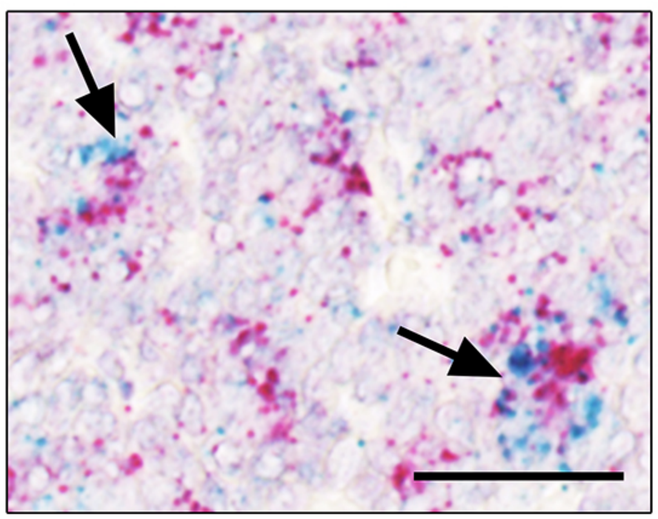

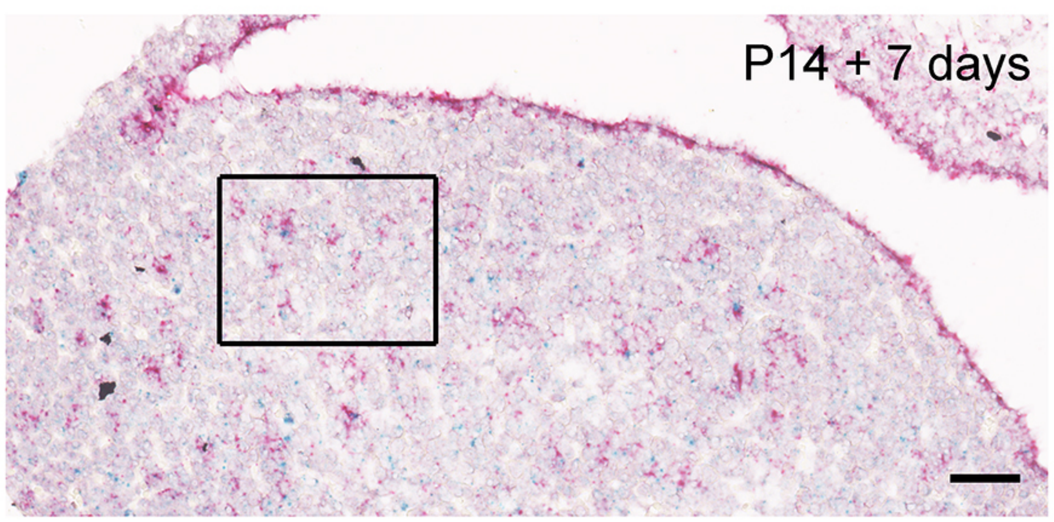
P14 + 7 days
Sox2CreERT2/+;Wlsfl/fl

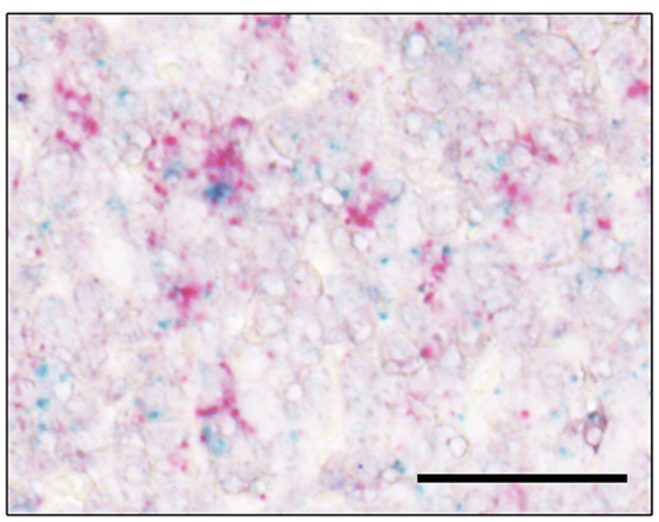

C

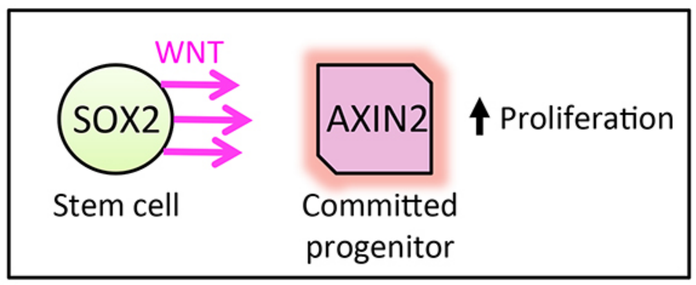
Wild type
WNT
SOX2
AXIN2
Proliferation
Stem cell
Committed progenitor

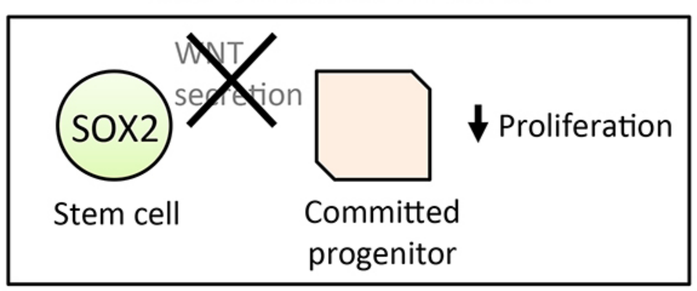
Wls deletion in SOX2+
WNT secretion
SOX2
Proliferation
Stem cell
Committed progenitor

A

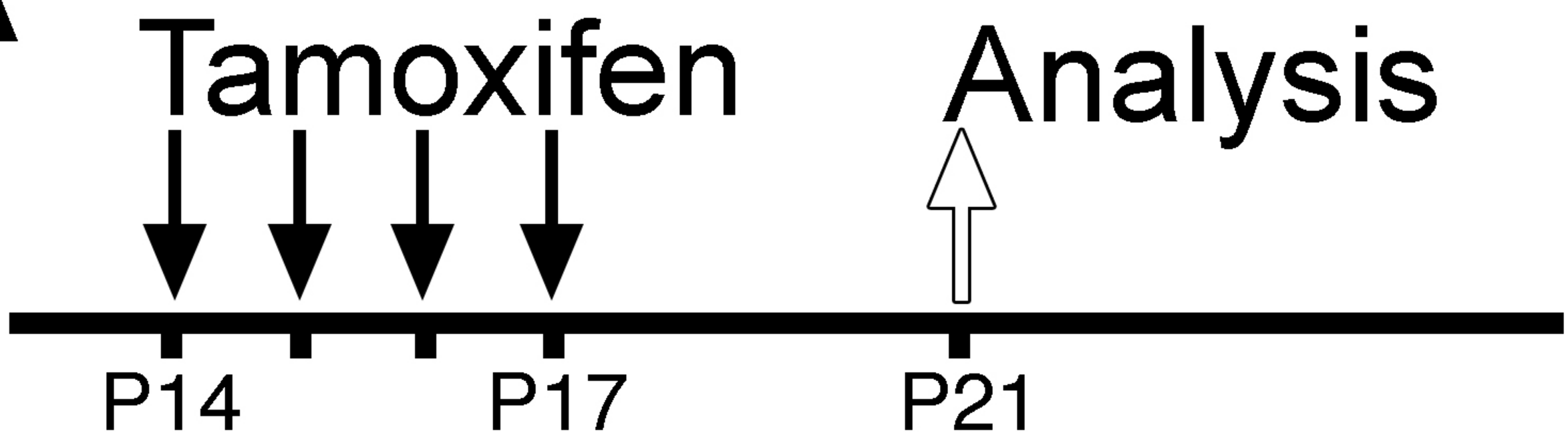
Tamoxifen
Analysis
P14
P17
P21

B

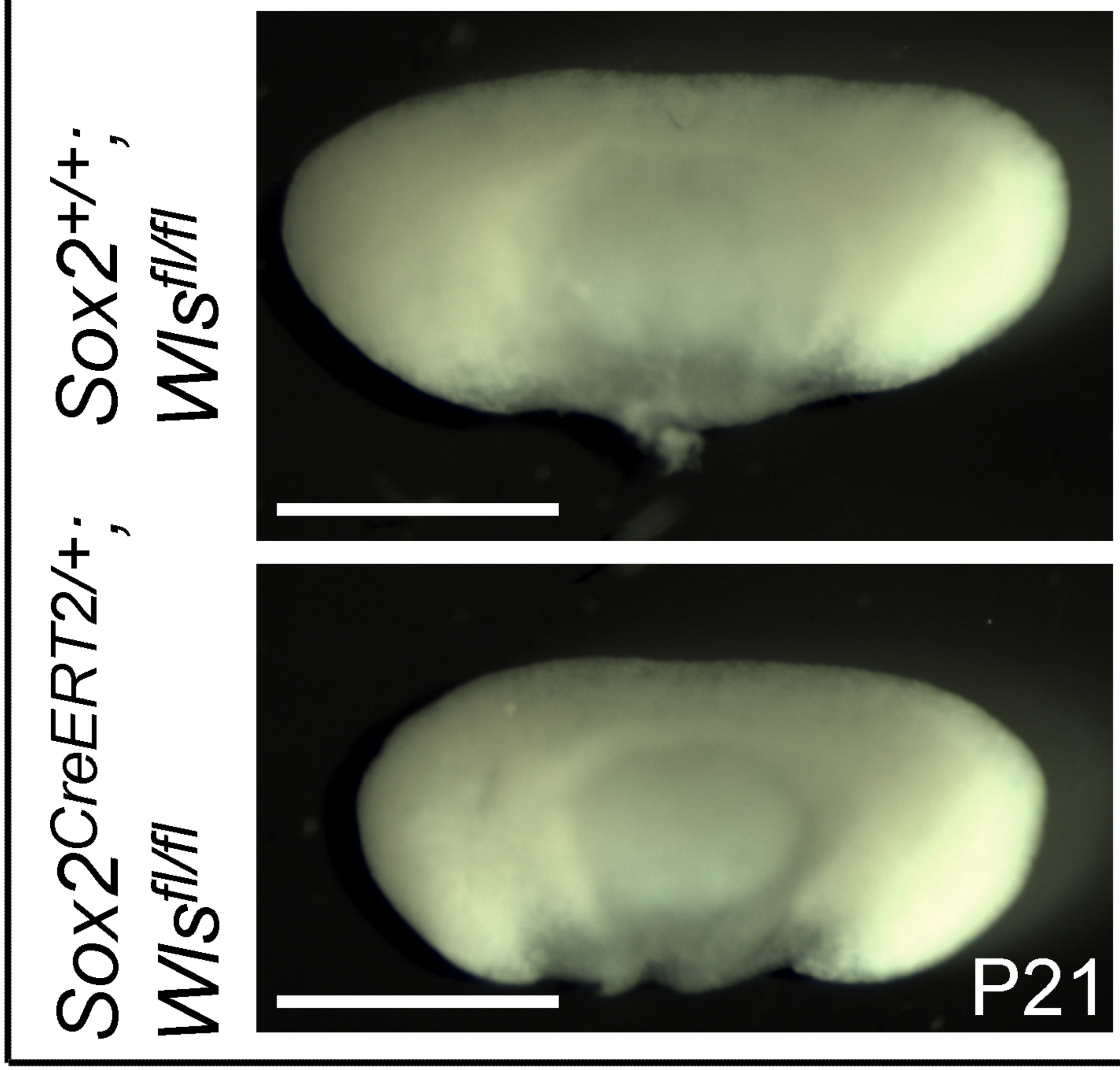
Sox2CreERT2/+; Sox2+/+; Wls fl/fl
Sox2CreERT2/+; Wls fl/fl
P21